The Pennsylvania State University

The Graduate School

IMMUNE-MEDIATED ANTIVIRAL DEFENSE AGAINST POLYOMAVIRUS INFECTION OF THE BRAIN

A Dissertation in

Neuroscience

by

Taryn E. Mockus

Submitted in Partial Fulfillment
of the requirements
for the Degree of

Doctor of Philosophy

May 2019

The dissertation of Taryn E. Mockus was reviewed by the following:

Aron E. Lukacher
Professor of Microbiology and Immunology
Chair of the Department of Microbiology and Immunology
Chair of Committee
Dissertation Adviser

Ziaur S. M. Rahman
Associate Professor of Microbiology and Immunology

Todd Schell
Professor of Microbiology and Immunology

James D. Connor
Distinguished professor of Neuroscience and Anatomy
Vice Chair for Research, Department of Neurosurgery
Professor of Neural and Behavioral Sciences and Pediatrics

Mark D. Meadowcroft
Assistant professor, Department of Neurosurgery

Alistair Barber, PhD
Associate professor, Department of Ophthalmology
Chair of Graduate Program

*Signatures are on file in the Graduate School

Abstract

Progressive multifocal leukoencephalopathy (PML) is an often-fatal demyelinating disease of the brain caused by JC polyomavirus (JCPyV) in immunocompromised individuals. Initially rare, PML has increased in prevalence with the rise of immunomodulatory therapies used for the treatment of autoimmune diseases, many of which impede the movement or function of immune cells. Despite increased incidence, PML pathogenesis remains poorly understood; the only treatment available for PML is to reconstitute the immune response, which can cause immune reconstitution inflammatory syndrome. Most studies of PML to date have utilized post mortem brains of PML patients or immunocompromised humanized mouse models, leaving many unresolved questions regarding the mechanisms of demyelination and the content and contribution of anti-polyomavirus (PyV) immunity. The aim of our work is to provide insight into PyV pathogenesis and defense in the brain using intracerebral (i.c.) infection of immunocompetent mice with mouse polyomavirus (MuPyV), a naturally occurring mouse pathogen, as a novel brain PyV infection model.

To this end, we first investigated the contribution of CD4 T cells to the development of antiviral brain-resident CD8 T cells (bT_{RM}). We found that CD4 T cells are required for MuPyV-specific CD8 bT_{RM} development, as demonstrated by decreased expression of canonical tissue-resident memory surface markers, continued dependence on CD8 T cells in the circulation, and decreased ability to control reinfection in CD8 T cells that develop in the absence of CD4 T cells. Furthermore, acquired CD4 T cell deficiency, modeled by delaying systemic CD4 T cell depletion until after the infiltration of MuPyV-specific CD8 T cells into the brain, also impacted the differentiation of CD8 bT_{RM} and decreased the ability of these cells to control reinfection. Together, these findings reveal an intimate association between CD4 T cells and homeostasis of functional CD8 bT_{RM} to brain polyomavirus infection. In conjunction with investigating the nature of the adaptive immune response to MuPyV, we also documented the role of type I, II,

and III interferons (IFNs) in anti-PyV defense in the brain. Previous work has shown that IFNs induce an antiviral state in the infected cell and modulate the immune response. We found that type I IFNs mediated viral control during acute brain infection, but no single IFN contributed substantially to PyV control during persistent MuPyV infection. However, mice deficient in signal transducer and activator of transcription 1 (STAT1), the common downstream effector of the IFN family, developed severe hydrocephalus, likely resulting from a loss of intrinsic viral control and a prolonged immune response consisting of inflammatory myeloid cells and polyfunctional CD8 T cells. These findings show that STAT1 is a critical component of the antiviral defense against MuPyV infection. Furthermore, we characterized the infection of brain resident cells and damage following MuPyV infection in the mouse brain. Histological and imaging analysis of MuPyV-infected mouse brains demonstrated histopathological abnormalities similar to those found in PML patients, such as demyelination and infection of glial cells, and a critical role of T cells in preventing PyV encephalitis. Together, our work documents the components of host defense against brain PyV infection and provides insight into the mechanisms of immunological control of PML progression and PyV infection in the brain. A better understanding of polyomavirus infection in the brain is necessary to alleviate the morbidity and mortality that result from polyomavirus-associated diseases.

Table of Contents

List of Figures

List of Tables

Abbreviation List

Antigen presenting cell - APC
Basepairs - bp
BK polyomavirus - BKPyV
Blood brain barrier - BBB
Brain-derived neurotrophic factor - BDNF
Brain tissue-resident memory T cells - bT_{RM}
Cell-division cycle 42 – Cdc42
Central memory T cells - T_{CM}
Central nervous system - CNS
Cerebral spinal fluid - CSF
Cytotoxic T cells – CTLs
Diffusion tensor imaging - DTI
DNA-dependent activatory of IFN regulatory factors - DAI
Effector memory T cells - T_{EM}
Eomesodermin - Eomes
Experimental autoimmune encephalomyelitis - EAE
Extracellular signal regulated kinase 1/2 – Erk1/2
Formalin Fixed Paraffin Embedded - FFPE
Fractional anisotropy - FA
Gamma-activated sequences - GAS
Genomic RNA - gRNA
Glial fibrillary acidic protein - GFAP
Glial precursor cells - GPCs
Granule cell neuropathy - GCNHematoxylin and Eoson – H&E
Herpes simplex virus - HSV
Highly active antiretroviral therapy - HAART
Human immunodeficiency virus/ acquired immunodeficiency syndrome – HIV/AIDS
Immune reconstitution inflammatory syndrome - IRIS
IL-7Rα – CD127
Interferon – IFN
Interferon α receptor – IFNAR
Interferon γ receptor – IFNγR
Interferon λ receptor - IFNLR
Interferon-regulatory factor 9 – IRF9
Interferon-sensitive elements - ISRE
Interferon-stimulated gene factor 3 – ISGF3
Interferon-stimulated genes - ISG
Intracranial – i.c.
Intranasal – i.n.
Intraperitoneal – i.p.
Intravascular – i.v.
Janus kinase 1 – JAK1
JC polyomavirus - JCPyV
JHM strain of mouse hepatitis virus - JHMV
Kruppel-like factor 2 – Klf2
L-selectin – CD62L
Lmyphocyte-function associated antigen 1 – LFA-1
Lymphocytic choriomeningitis virus – LCMV
Luxol Fast Blue Periodic Acid Schiff – LFB-PAS

Magnetic resonance imaging - MRI
Major histocompatibility complex - MHC
Mean diffusivity - MD
Melanoma differentiation-associated protein 5 – MDA5
Merkel cell polyomavirus (MCPyV)
Mitochondrial antiviral signaling proteins - MAVS
Monoclonal antibodies - mAb
Mouse polyomavirus - MuPyV
Multiple sclerosis - MS
Natural killer - NK
Neutral buffered formalin - NBF
Oligodendrocyte precursor cells - OPCs
Pattern recognition receptors - PRRs
Polyomavirus - PyV
Post infection – p.i.
Progressive multifocal leukoencephalopathy - PML
Real-time PCR – RT-PCR
Relaxation rate – T_2R_2
Retinoic acid-inducible gene I – RIG-I
Rheumatoid arthritis - RA
Signal transducer and activator of transcription 1 – STAT1
Sphingosine-1 phosphate – S1P1
STAT1 Src 2 homology – SH2
Subventricular Zone - SVZ
Systemic lupus erythmatosis - SLE
T cell receptor - TCR
Theiler's murine encephalomyelitis virus - TMEV
Tissue resident memory cells - T_{RM}
Toll-like receptors - TLRs
Toxoplasma gondii – T. gondii
Trichodysplasia spinulosa-associated polyomavirus - TSPyV
Tumor necrosis factor α – TNFα
Tyrosine kinase 2 – TYK2
Vesicular stomatitis virus - VSV
Varicella zoster virus – VSV
West Nile Virus – WNV
Zonula occludens 1 – ZO-1

Acknowledgements

First, I would like to thank my mentor and thesis advisor, Dr. Aron Lukacher. Thank you for giving me the environment to grow into the scientist that I am today. Your constant support though the many presentation practices, paper drafts, and meetings has given me the confidence to move on and continue my career as a scientist. Thank you for all the advice, encouragement, and, of course, the extensive and careful editing of all my manuscripts. You have showed me that a whole document covered in red means that I have done a great job.

I would also like to thank my committee, Drs. Todd Schell, Ziaur Rahman, Mark Meadowcroft, and James Connor, for your support, insightful questions, and encouragement over the years.

My projects could not have been completed without the exceptional support from the Core Facilities at the Penn State College of Medicine, especially Comparative Medicine and Flow Cytometry. Nate Sheaffer and Joe Bednarczyk, thank you for providing a wonderful facility in which to complete my work and for the support during sorting. Jade Vogel, thank you for all our conversations and friendship. Running flow samples was the highlight of my day because I knew you would be there. Gretchen Snavely and Ellen Mulady, thank you for your careful attention when sectioning my nearly 400 brain samples over the years and for your assistance with all my staining concerns.

To my labmates, thank you for supporting me through the trials and tribulations of graduate school. Shwetank, Heather, Colleen, and Matt, thank you for helping me to finish my projects and for fostering a collaborative and fun space to work in. Ge Jin, thank you for the huge amount of technical knowledge that you have given me, both scientifically and non-scientifically, and for managing the many mouse strains that were part of these projects. I could not have finished this work without all your assistance, for which I am eternally grateful. I also thank all the other past lab members that have been part of this journey.

To my incredible circle of friends, both within and outside of graduate school, I thank you for making graduate school one of the best times of my life. Thank you for showing me that science can be fun and that there's a big, exciting life outside the laboratory. I could not have completed this journey without you.

To Brandon, thank you for the endless supply of chocolate, delicious Fancy Friday Feasts, and the enthusiastic encouragement from the moment I applied to graduate school till now. You have made the lows of graduate school more bearable and the highs more exciting. I would not be writing this thesis if you had not been cheering me on since day 1.

To my family, thank you for believing in me when I did not believe in myself. Everything that I have achieved has been because of you. Thank you for showing me the discipline, work ethic, and fortitude to see this project through and for teaching me the value of humility and compassion. This has all been possible because of your love and support of me throughout this scientific journey.

Dedicated to Dr. Robert Bonneau

Chapter 1

Introduction

1.1 The Not So Immune Privileged Brain

The immune system consists of a complex network of specialized cells, tissues, and molecules that act in a concerted effort to resist disease. Immune responses to pathogens are typically divided into two categories: innate and adaptive immunity. Upon infection, the innate immune response mediates initial, rapid, and broad-spectrum protection. Defense against infectious pathogens also employs the adaptive immune response, which develops slowly but provides more specialized and effective protection. The cells of the innate immune system recognize a limited number of microbial molecules and execute a stereotypic response, even after repeated encounter of the same pathogen. Conversely, the adaptive immune response targets a limitless array of pathogens through the development of antigen-specific antibodies and effector cells and generates a larger and faster response if restimulated with the same antigen due to the development of immunological memory.

The adaptive immune response consists of humoral and cell-mediated immunity. Humoral immunity involves B cell produced and secreted antibodies that bind to microbes and other foreign antigens. Cell-mediated immunity involves CD8 (also called cytotoxic lymphocytes, CTLs) and CD4 (also termed helper T cells) T cells, which work together to recognize and kill infected cells. The cytotoxicity and selectivity of the adaptive immune response is especially effective in the control of viral infections. However, T cell cytotoxicity must balance between viral control and tissue damage. The tissue destruction resulting from unchecked adaptive immune responses can be more detrimental and long lasting than damage from the pathogen itself, especially in organs populated by terminally differentiated cells like the brain.

Although the brain has long been considered an immune privileged organ, research has revealed standard lymphatic drainage, anatomical niches that harbor resident populations of macrophages and dendritic cells, and a population of innate immune cells (i.e., microglia and astrocytes) unique to the CNS [1-4]. These novel findings suggest that the brain may not be as immune privileged as previously thought. Microglia, especially, are an essential part of the

innate immune network of the brain, producing pro- and anti-inflammatory cytokines and chemokines, complement, neurotrophic factors, and free radicals upon inflammatory insult [3]. In addition, microglia actively survey the brain parenchyma during homeostatic conditions and release trophic factors that support synapses during brain development and adulthood [5, 6]. Similar to microglia, astrocytes have differing roles during homeostasis and infection. Astrocytes modulate synaptic activity and blood flow through their role in the tripartite synapse and the blood brain barrier (BBB) responses [7, 8]. The term tripartite synapse refers to the integration and proximity of an astrocyte, pre-synaptic neuron, and post-synaptic neuron during neurotransmitter release. During inflammatory insult, astrocytes are a principal source of innate immune cytokines and the predominant cell type in glial scars [9, 10]. Thus, although the homeostatic immunological landscape in the CNS does differ from other organs, the brain mounts vigorous immune responses after engagement of its unique innate immune cells and infiltration of peripheral immune cells.

The immune privileged hypothesis for the brain arose, in part, from the selective permeability of the BBB, which is formed by endothelial cells surrounding the brain. The permeability of endothelial barriers varies throughout the body, with the BBB recognized as the one of the least permeable endothelial barriers. The selective permeability of the BBB arises from tight junctions between adjacent endothelial cells and a continuous basement membrane connecting the endothelial cells to pericytes and astrocytic end feet [11, 12]. The permeability of the BBB is regulated by mediators, such as type I IFNs, released from neurons, astrocytes, pericytes, vascular endothelial cells, and immune cells during neurologic and systemic inflammation. Additionally, it acts as the first defense against invading pathogens by restricting movement into the brain of pathogens and immune cells alike.

In addition to a better understanding of the interactions between the immune system and the brain, research has indicated that many viruses exhibit neuro- and glio- tropism. Encephalitidies due to brain viral infections contribute to high mortality rates worldwide [13].

Preservation of virus-infected neurons and glial cells is more advantageous to the host, which leads to perpetual, non-lethal, detrimental consequences on brain function in patients who survive [13]. For many viral infections of the brain and other organs, viral control is mediated by CD8 T cells [14]. These cells secrete effector molecules including granzymes, perforin, and interferon (IFN) γ. IFNγ has been implicated in the control of many neurotropic infections including herpes simplex virus (HSV), varicella zoster virus (VZV), and toxoplasma gondii (*t. gondii*) [15-17]. However, IFNγ is also highly injurious to brain resident cells. T cells responding to infections in non-lymphoid organs can differentiate into tissue-resident memory (T_{RM}) cells, which remain in the brain and survey the tissue for reinfection [18]. T_{RM} will be discussed in more detail later in the chapter. Although it is well documented that T_{RM} cells are necessary for protecting non-lymphoid tissues from reinfection, understanding of the processes that influence the formation and maintenance of T_{RM} are poorly understood, especially in non-barrier organs such as the brain.

1.2 JC Polyomavirus and PML

Polyomaviruses (PyVs) are small non-enveloped viruses with a double stranded closed circular DNA genome of about 5K basepairs (bp) [19]. The viruses of the *polyomaviridae* family infect a wide range of host species, but all polyomaviruses are species-specific [20]. To date, 14 polyomaviruses have been identified that infect humans. Most infections are asymptomatic, but 4 polyomaviruses – BK polyomavirus (BKPyV), JC polyomavirus (JCPyV), Merkel cell polyomavirus (MCPyV), and trichodysplasia spinulosa-associated polyomavirus (TSPyV) – are associated with disease in immunocompromised individuals [21]. PyV infections, especially infections with BKPyV and JCPyV, are endemic in humans. Infection begins in childhood, with the seroprevalence of most polyomaviruses increasing with age [21, 22]. In most immunocompetent hosts, polyomavirus infection is asymptomatic and the virus establishes a lifelong, persistent infection.

After primary infection, JCPyV spreads to the kidneys, bone marrow, lymphoid tissues, and, potentially, the brain and remains in those organs asymptomatically in immunocompetent individuals [21]. However, in immunocompromised individuals, the virus can cause the disease progressive multifocal leukoencephalopathy (PML). PML was originally considered a rare complication of malignant lymphoma and leukemia [23]. However, studies documenting cytopathic changes in astrocytes and oligodendrocytes and isolation of viral particles from the brains of patients with PML identified JCPyV as the causative agent of PML [24, 25]. PML is a devastating demyelinating disease marked by demyelination in the subcortical white matter of the brain. 30-50% of patients die within the first few months of diagnosis. Unfortunately, there are large gaps in our knowledge of PML including the risk factors predisposing people to PML, pathogenesis of JCPyV, and importance of immune protection.

JCPyV is considered a gliotropic virus and predominately infects astrocytes, oligodendrocytes, and glial precursor cells (GPCs). Research with glial chimeric mice suggests that oligodendrocytes are infected later, less effectively, and non-productively [26]. The subcortical demyelination hallmarks of PML are thought to be secondary to oligodendrocyte infection and death. However, the rapid clinical deterioration of PML patients may more accurately reflect the loss of astrocytes, especially given their importance in the tripartite synapse, plasticity, and neural support, more than demyelination from oligodendrocyte death. Infected astrocytes appear bizarre with enlarged and multilobular nuclei. In addition to JCPyV infection of glial cells, three novel JCPyV-associated non-gliotropic diseases have been described [27]. JCV-granule cell neuropathy (GCN) is characterized by infection of granular cells of the cerebellum, cerebellar atrophy, and white matter changes only in the cerebellum [28]. Similarly, JCV encephalopathy is marked by productive infection of cortical pyramidal neurons and PML-like lesions in the gray matter [29]. JCPyV has also been detected in the cerebrospinal fluid (CSF) of patients presenting with classical meningitis symptoms (i.e., headache, nausea, and stiff neck) [27, 30]. Although research suggests that mutations in the

VP1 epitope predispose patients to developing JCV-GCN, the etiology of these non-PML JCPyV-associated diseases is largely unknown [31, 32]. The understanding of these novel JCPyV-associated brain diseases demonstrates that JCPyV has the ability to infect multiple cell types in the brain.

1.2.1 PML and the Immune System

PML remained an extremely rare disease until the HIV/AIDS (human immunodeficiency virus/ acquired immunodeficiency syndrome) epidemic. During the peak of the epidemic, the prevalence of PML in AIDS patients was 3-5%, overall compromising 87% of all diagnosed PML cases in 1993 [33, 34]. The implementation of highly active antiretroviral therapy (HAART) significantly reduced the incidence of PML in AIDS patients (from 14.8 cases/1000 patients pre-HAART to 0.8 cases/1000 patients post-HAART) [35, 36].

Currently, patients receiving monoclonal antibodies (mAb) for the treatment of autoimmune disease comprise the population most at risk of developing PML. Natalizumab – a mAb predominately used for the treatment of multiple sclerosis (MS) that targets the movement of lymphocytes into the brain by blocking the cell adhesion molecule α4 - treatment has the highest risk of PML development (28 cases out of 1,000 patients receiving Natalizumab) [37]. The risk of developing PML in patients receiving Natalizumab is based on three factors: JCPyV seropositivity, history of prior immunosuppressive therapies, and treatment duration [38]. Cases of PML have also been reported in patients receiving other immunomodulatory therapies such as efalizumab [mAb against lymphocyte function-associated antigen 1 (LFA1) for treatment of psoriasis], rituximab [CD20 mAb that triggers apoptosis pathways in B cells for treatment of cancers involving B cells and rheumatoid arthritis], alemtuzumab [mAb against mature CD52-bearing lymphocytes for treatment of MS], fingolimod [sphingosine-1 phosphate receptor agonist for treatment of MS], and dimethyl fumarate [cytokine production blocker for treatment of psoriasis], with nearly all immunosuppressive therapies coming with an FDA black box warning

of PML currently [39]. There is also evidence that autoimmune disease itself predisposes patients to PML. Although the incidence of PML is low, patients with systemic lupus erythmatosis (SLE), rheumatoid arthritis (RA), and other connective tissue diseases have a slightly elevated risk of PML development compared to the general population [40].

The incidence of PML in immunocompromised patients highlights the importance of the immune system in the control of JCPyV infection in the brain. Polyomavirus-specific CD8 T cells in peripheral blood correlate with improved survival in PML patients [41-43]. A recent case report documented that administration of BKPyV-specific CD8 T cells to PML patients alleviated clinical symptoms [44]. The presence of JCPyV-specific CD8 T cells early after PML diagnosis correlated with a better PML disease course, whereas their absence worsened PML progression [42]. CD4 T cells are also important in the immune response to JCPyV in the brain. A reduced population of L-selectin$^+$ (CD62L) CD4 T cells, also known as central memory CD4 T cells (T_{CM}, described in more detail later in the chapter), is associated with a higher risk of PML development in AIDS patients and patients receiving immunomodulatory therapies, suggesting that a reduction of CD4 T_{CM} could be a biomarker for PML risk stratification [45-47]. Mutations in the genes encoding the major capsid protein VP1, the CD4 T cell epitope, allowed viral persistence in the brains of MS patients and reduced the infiltration of immune cells [31]. Taken together, these studies suggest that JCPyV-specific CD4 and CD8 T cells are an integral part of the defense against JCPyV spread in the brain.

However, similar to many other viral infections, the infiltration of T cells into the brain is a double-edged sword. The only known therapy for PML is to reconstitute the immune system, which can result in PML-IRIS (PML-immune reconstitution inflammatory syndrome). Clinical features of PML-IRIS often manifest as an abrupt, sudden, and severe worsening of pre-existing deficits, which is inconsistent with the previous course of PML [48]. Upon immune reconstitution, the number of B cells and Granzyme-B$^+$ CD8 T cells significantly increased in lesions, but the number of inflammatory macrophages and microglia remained relatively unchanged [49, 50].

Histological analyses suggest that these Granzyme-B^{+} CD8 T cells attack infected cells at the periphery of lesions and induce them to undergo apoptosis, which is not often seen during PML [50]. The death of infected cells is amplified by bystander tissue damage [51]. Thus, CD8 T cells are instrumental in the control of JCPyV replication, but they do so at the cost of exacerbating lesions already present from PML itself.

Despite the high prevalence of PML in patients with adaptive immune system immunodeficiencies, the innate immune system also plays a role in the control of JCPyV. Recombinant IFNγ may prove to be a viable therapeutic for PML management. No HIV patients developed PML when receiving recombinant IFNγ, but the sample size was small and the observation is largely anecdotal [52]. Similarly, IFNγ and Type I IFNs inhibit JCPyV replication in cultured human fetal glial cells, and JCPyV transfection of cultured glial cells induced a strong antiviral response through the induction of several interferon-stimulated genes (ISG), including STAT1, the common signaling molecule of type I, II, and III IFNs [53-55]. Reports of PML in people with STAT1 mutations suggest that aberrations in STAT1 may be a risk factor for PML [56]. These findings demonstrate that the innate immune system also plays a role in restricting JCPyV proliferation in the brain.

1.2.2 Mouse Models of PML

Lack of a tractable animal model severely limits understanding of PML pathogenesis. Recently, Dr. Steven Goldman's group at the University of Rochester created a mouse model of PML by reconstituting Rag2$^{-/-}$/Mbp$^{shi/shi}$ mice (i.e. hypomyelinated immune deficient mice) with human fetal glial cells [57]. After 6 months, these glial precursor cells differentiated into astrocytes and oligodendrocytes and populated and myelinated the mouse brain. Infection of these chimeric mice showed a predominant infection of astrocytes and hallmark focal demyelination of PML [57]. Although studies in chimeric mice provide invaluable insights into JCPyV infection in human cells, they are unable to reveal the role of the immune system in PML

pathogenesis and they are technically challenging to create. Furthermore, the human-derived cells are the only cells capable of supporting JCPyV infection. Thus, an animal model with an intact immune system and a natural polyomavirus pathogen is needed to study virus and host interactions.

The 73 members of the polyomavirus family are structurally and genetically similar, including mouse polyomavirus (MuPyV) and JCPyV. Additionally, like JCPyV, MuPyV is a ubiquitous mouse pathogen that establishes a silent, persistent infection in multiple organs including the spleen, kidneys, brain, and bone marrow. Previous work has shown that CD8 T cells contribute a large part of the host defense against MuPyV infection in the periphery, similar to the control mediated by CD8 T cells to JCPyV [58, 59]. My work utilizes intracerebral (i.c.) inoculation of MuPyV into mouse brains to mimic brain JCPyV infection. This route of inoculation recruits a robust CD8 T cell population to the brain and reflects some hallmarks of PML including astrocytic-dependence of infection and subcortical demyelination. Additionally, the virus spreads systemically so I am able to ascertain differences in peripheral and CNS immune responses.

1.3 T cell-mediated immunity

T cells arise from multipotent hematopoetic cells in the bone marrow and the maturation of T cells occurs in the thymus. The development of T cells is marked by changes in T cell receptor (TCR) genes, the TCR itself, and cell-surface proteins such as CD3, CD4, and CD8. During the early stages of development, T cells become committed to either an α:β or γ:δ lineage. γ:δ T cell production is predominant early in development, and these cells will go on to seed tissues such as the skin and intestine. Different stages of α:β T cell development in the thymus, including α-chain rearrangement and CD4/CD8 expression, are stimulated by rearrangement of the β-chain and the resulting creation of the pre-TCR. Once a functional α:β

receptor is formed, the T cells are subjected to positive and negative selection, undergo final rearrangements to the TCR, and emigrate to the peripheral lymph nodes and spleen.

As the T cells move through the peripheral lymph nodes, they bind transiently to each antigen presenting cell (APC) they encounter in order to find their cognate antigen peptide. However, the recognition of a T cell's cognate peptide:MHC ligand alone is not sufficient to activate a T cell. The activation and differentiation of a naïve T cell, also called priming, requires three signals. The first is the interaction of the peptide:MHC complex on the APC. The second signal arises from the ligation of co-stimulatory receptors expressed on the T cell by ligands expressed on the APC, such as ligation of B7 molecules. The third signal includes cytokines that direct naïve T cells to differentiate into effector subsets. After activation, T cells proliferate rapidly and egress from the lymphoid organs to the site of infection. Additionally, the primed T cells no longer require the second and third signals to exert their effector functions.

CD4 T cell help is necessary in the majority of viral infections for the activation of CD8 T cells [60]. CD4 T cells that recognize related antigens amplify the co-stimulatory properties of APCs that present to CD8 T cells in a process called licensing. During licensing, B7 molecules on the APC stimulate CD4 T cells to express IL-2 and cell-surface CD40 ligand. CD40 ligand from CD4 T cell engagement with CD40 on the APC increases the expression of co-stimulatory molecules on the APC, surpassing the threshold for CD8 T cell activation. CD4 T cell derived IL-2 also promotes CD8 T cell proliferation. CD8 T cells primed in the absence of CD4 T cells are termed "unhelped" CD8 T cells. Unhelped CD8 T cells exhibit defective effector differentiation, memory formation, and viral control, regardless of whether CD4 T cell help was available during the initial priming phase [61-65].

1.3.1 Cytotoxic T cells

The overwhelming majority of CD8 T cells differentiate into cytotoxic T cells (CTLs), which are an important part of the defense against intracellular pathogens such as viruses. The

effector functions of CD8 T cells are elicited only when their TCR binds cognate peptide:MHC I complex on an infected target cell. The effector molecules produced by CD8 T cells fall into two broad categories: cytotoxic granules and cytokines. Cytotoxic granules are modified lysozymes that contain perforin, granzymes, and granulysin. These molecules work synergistically on the target cell to induce apoptosis. CD8 T cells also release cytokines such as tumor necrosis factor α (TNFα), IFNγ, and IL-2. These cytokines can work in concert with the cytotoxic granules to induce apoptosis in the target cell. They also have other roles, such as the activation of macrophages or the induction of MHC I on target cells, that contribute to host defense.

1.3.2 Immunological memory

The CD8 T cell response to infection can be divided into four parts: 1) priming, 2) contraction, 3) memory, and 4) reinfection [66]. Following priming, CD8 T cells undergo rapid proliferation, acquire effector function, and emigrate to infected tissue. About 90-95% of the newly generated CD8 T cells will die during the contraction phase. The remaining 5-10% of virus-specific CD8 T cells become long-lived memory cells [66]. Memory CD8 T cells have traditionally been divided into two subsets: T_{CM} and effector memory (T_{EM}) [67]. CD8 T cell memory subsets are defined by their trafficking, localization, and surface marker expression. T_{CM} circulate through the lymph nodes and lymph and are defined by their surface expression of $CD62L^{hi}CCR7^{+}$ [66]. Both CD62L and CCR7 are important for the function of T_{CM}. CD62L facilitates recirculation through blood and lymph whereas CCL19 and CCL21 binding to CCR7 recruits and retains T cells in secondary lymphoid organs. T_{EM} circulate through the blood, lymph, lymphoid organs, and non-lymphoid organs and adopt a $CD62L^{lo}$ $CCR7^{-}$ phenotype, which gives these cells the ability to circulate through lymphoid and non-lymphoid tissues [66]. However, recent research suggests that memory CD8 T cells are dynamic and shift between different types based on the infection and tissue [68]. Additionally, the rigid definition of only two subsets of memory CD8 T cells is incomplete. Many new subsets of memory T cells including

stem cell-like T cells, peripheral memory T cells, and long-lived effector T cells have been identified. These newly identified subsets and the differences between their trafficking, metabolism, epigenetic regulation, and longevity fail to fit into defined, classical memory T cell definitions, demonstrating that the properties of memory T cells may fall on a continuum with different CD8 T cells sharing similar functions, phenotypes, and migration pathways [68].

1.3.3 Tissue-resident memory

In addition to the multitude of effector memory subsets, CD8 T cells can also become tissue-resident memory cells (T_{RM}) [69]. This newly defined T cell subset is phenotypically, metabolically, and transcriptionally distinct from other T cells subsets [70-72]. T_{RM} are marked by their expression of CD69 and CD103, although not all T_{RM} will express these surface molecules to the same level [73]. For example, only 30-40% of brain T_{RM} (bT_{RM}) will become $CD103^{+}$ T cells during MuPyV and *T. gondii* infection, but close to 90% of CD8 T cells will express CD103 during brain VSV infection [74-76]. T_{RM} also adopt a $Ly6C^{lo}$, $CD122^{lo}$, $CD127^{-/int}$, $CD62L^{lo}$, and Granzyme-B^{+} expression profile, but this can vary with the tissue [71]. T_{RM} share a core gene signature of downregulated tissue egress genes, such as *Krüppel-like factor 2* (*Klf2*) and *S1pr1* (which encodes a receptor for sphingosine-1 phosphate, S1P1); downregulated cytokine responsiveness transcription factors, such as T-box transcription factors T-bet and Eomesodermin (Eomes); and upregulated transcription factors Hobit and Blimp1 [70]. Loss of Hobit and Blimp1 inhibits T_{RM} formation [77]. Like other memory T cell subsets, T_{RM} rely on a catabolic metabolism for their survival [78]. However, T_{RM} uniquely use exogenous free fatty acids from the tissue where they reside for their maintenance, highlighting the close relationship between the T_{RM} cell and its tissue of residence [72]. Similar to effector memory T cells, CD8 T_{RM} are heterogeneous, leading some to speculate that multiple T_{RM} subsets may exist [71]. These potential T_{RM} subsets may have different locations and cytotoxicity, which endow them

with unique and nonredundant roles upon reinfection. However, this is an area of active research and the constituents of these subsets may depend on the tissue infected and the chronicity of the viral infection.

T_{RM} seed infected and, potentially, uninfected non-lymphoid tissue during the effector phase of the T cell response and become permanently established in the tissue [69, 79]. The anatomical location of T_{RM} allows them to protect and rapidly clear reinfection in their tissue of residence. In the absence of infection, T_{RM} actively survey the tissue parenchyma [80-82]. It has been speculated that the expression of CD103 may dictate the degree of motility of a T_{RM} cell in the tissue, but this has not been shown in all non-lymphoid tissue [75, 83, 84]. In order to control reinfection, T_{RM} constitutively express Granzyme-B, thus ensuring rapid delivery of cytotoxic granules to infected cells [76, 85]. T_{RM} also produce IFNγ upon reinfection, which clears adjacent and neighboring infected cells, recruits circulating memory CD8 T cells and B cells, and promotes maturation of innate immune cells [71, 86, 87].The phenotype and effector capacity of T_{RM} provide efficient and crucial frontline defense against reinfection in many non-lymphoid tissues, such as the brain.

Similar to CD8 T cells, CD4 T cells also form T_{CM}, T_{EM}, and T_{RM} subsets. However, although there are similarities between CD4 and CD8 T_{RM}, clear differences exist between the two populations. For example, CD4 T cells express CD69, but few –if any- will express CD103 [88]. Recent research suggests that there may be two populations of CD4 T_{RM}: a static population that remains parked in the tissue; and another dynamic population that migrates between the tissue, draining lymph nodes, and blood [89]. The prevalence of either population may depend on the infection and location. During vaginal HSV infection, CD4 T_{RM} are maintained independently of the circulation and sustained by a network of macrophages, suggesting that reliance on antigen or environment may affect CD4 T_{RM} retention [90]. Conversely, CD4 T_{RM} to HSV infection in the skin equilibrate with the circulation during steady

state and rapidly accumulate upon reinfection [91]. These studies suggest that the CD4 T_{RM} population represents a heterogeneous population dependent on different factors for survival.

Similar to other non-lymphoid tissue, infection of the brain results in the infiltration and persistence of pathogen-specific CD8 T cells. CD8 bT_{RM} are maintained independently of the circulation and persist in the brain, presumably at sites of prior infection [18]. Comparison of $CD103^+$ and $CD103^-$ bT_{RM} to splenic $CD103^+$ and $CD103^-$ CD8 T cells revealed increased effector activity and differential regulation of chemokine and cytokine genes, such as CXCL10, CCL3, and S1P1 [76]. During chronic infection with *T. gondii*, the $CD103^+$ CD8 bT_{RM} subset provides rapid pro-inflammatory cytokine production, but CD103 does not determine location within the brain parenchyma [75]. Similarly, the high proliferative capacity and effector capabilities of CD8 bT_{RM} helped control lethal brain LCMV reinfection independently of the circulation [84]. In conclusion, the resident CD8 T cell population in the brain represents a bona fide CD8 T_{RM} population capable of rapid and efficient protection from infection.

1.4 Interferon-mediated Immunity

In response to infection, innate and adaptive immune cells secrete pro-inflammatory cytokines (IFNs, interleukins, and chemokines) that mediate immune reactions and communication. Viral infection, specifically, induces the production of IFNs; so named because they interfere with viral infection. There are three families of IFNs: Type I IFN, Type II IFN, and Type III IFN.

1.4.1 Type I IFN

The production of Type I IFNs is induced by signaling from infectious pathogens through various pattern-recognition receptors (PRRs) including toll-like receptors (TLRs), retinoic acid-inducible gene I (RIG-I), melanoma differentiation-associated protein 5 (MDA5), and DNA-

dependent activator of IFN regulatory factors (DAI) [92]. Nearly all cell types are capable of producing Type I IFNs. The Type I IFN family consists of a diverse group of signaling molecules including IFN –α, -β, -ε, -κ, and –ω, all of which signal through the heterodimeric interferon α receptor (IFNAR). Activation of the Type I IFN-antiviral pathway involves binding of the IFNAR subunits, IFNAR1 and IFNAR2, by Type I IFNs; recruitment of Janus kinase 1 (JAK1) and tyrosine kinase 2 (TYK2); phosphorylation of STAT1 and STAT2; and translocation of the STAT1, STAT2, and IFN-regulatory factor 9 (IRF9) complex to the nucleus (**Fig 1-1**). This interferon-stimulated gene factor 3 (ISGF3) complex binds interferon-sensitive elements (ISRE) upstream of ISGs [93].Transcription of ISGs results in cellular defense against viral, bacterial, and parasitic infections.

Nearly all brain resident cells can produce and respond to Type I IFNs, but the different cell types exhibit heterogeneity in their susceptibility to Type I IFNs [92, 94]. Microglia express numerous toll-like receptors (TLRs) that allow for rapid response to pathogens and, along with astrocytes, are one of the main producers of IFNβ in the CNS [95, 96]. Microglia express IFNAR and signaling through microglia-expressed IFNAR during neurodegenerative disease sustains phagocytosis of debris, creating a permissive environment for axon outgrowth [97]. In addition to IFNβ, astrocytes produce IFNα in response to viral infection [95, 96]. However, unlike the neuroprotective effects of microglia, astrocyte-derived Type I IFNs promoted demyelination in Theiler's murine encephalomyelitis virus (TMEV) infection and prolonged a neuroinflammatory state by increasing expression of MHC (major histocompability complex) I on astrocytes [98]. Neurons produce high levels of Type I IFNs in steady state and disease [99]. Neuronal production of Type I IFNs and expression of IFNAR is crucial for antiviral defense to neurotropic infections such as rabies, vesicular stomatitis virus (VSV), and reovirus [100-102]. Compared with other brain resident cells, the oligodendrocyte response to Type I IFNs is conflicting: oligodendrocytes express PRRs but fail to produce Type I IFNs when stimulated [103]. Finally, endothelial cells of the BBB are highly susceptible to Type I IFNS. Type I IFN signaling on

endothelial cells limits neuroinvasion by inducing an antiviral state in endothelial cells and, potentially, tightening the BBB [104, 105]. These studies show that Type I IFNs are an essential component of the brain's immune response to a viral infection.

Type I IFNs also have potent effects on the activation and function of T cells through both direct and indirect mechanisms. Indirectly, type I IFNs promote antigen presenting cell (APC) maturation, migration, and presentation; restrict viral replication; induce expression of cytokines that are necessary for the survival and differentiation of memory T cells; and stimulate MHC I expression thereby facilitating recognition and killing of virally infected cells [106]. Directly, type I IFN signaling is essential for the priming of T cells and protects them from natural killer (NK) cell-mediated killing immediately following priming [106]. However, a sustained IFN signature during persistent viral infections is detrimental to T cell function and survival [107, 108]. These studies highlight the implications of the timing and duration of type I IFN signaling on the function and maintenance of T cells.

1.4.2 Type II IFN

IFNγ is the sole Type II IFN. Unlike Type I IFNs, IFNγ is produced by T cells, NK cells, and NK T cells at high levels and microglia, macrophages, and B cells at low levels during infection [109]. IFNγ production in T cells is stimulated by antigen presented by MHC I or MHC II molecules [109]. The heterodimeric IFNγ receptor (IFNγR) is expressed on all nucleated cell types and signals through a homodimer of STAT1 (**Fig 1-1**, [93]). STAT1 homodimers translocate to the nucleus and bind to gamma-activated sequences (GAS). The genes transcribed combat viral infection in the cell [110].

In the brain, IFNγ production during neuroinflammatory events is responsible for the activation of and MHC I and II upregulation on microglia and, at a much lower level, astrocytes [111]. The pathogenicity of IFNγ and glial activation from IFNγ signaling drive chronic neuroinflammation and degeneration in neurodegenerative diseases such as Parkinson's

Disease and Alzheimer's Disease and in CNS infections including cerebral malaria, pneuomoccocal meningitis, prion disease, and arenavirus hemorrhagic fever [112-117]. In addition to its effects on glial cells, epithelial cells of the choroid plexus and endothelial cells of the BBB are susceptible to IFNγ produced by local T cells during neuroinflammation [118, 119]. IFNγ signaling results in increased permeability of the choroid plexus, thus increasing the transepithelial migration of leukocytes and pathogenesis of infection [118]. However, IFNγ is a pleiotropic cytokine and has some neuroprotective effects. Loss of IFNγ heightens acute manifestations of schizophrenic episodes and may be involved in the development of social deficits characteristic of people with autism [120, 121]. It is evident that IFNγ has multiple and contradictory effects on the brain.

1.4.3 Type III IFN

The Type III IFN family includes IFNλ1, IFNλ2, IFNλ3 [also known as IL-29, IL-28A, and IL-28B, respectively] and IFNλ4 [122]. The Type III receptor, ILNLR, is a heterodimeric receptor consisting of the receptor subunits IFNLR1 (also known as IL28Rα) and IL-10R2 [123]. IFNLR expression is mostly restricted to endothelial and epithelial cells at mucosal and other barriers, although recent research suggests that neutrophils and other immune cells are responsive to Type III signaling [124, 125]. Downstream signaling through IFNLR is nearly identical to the downstream signaling of Type I IFNs, but the kinetics of response differs between cell types (**Fig 1-1**, [126, 127]).

Although IFNλ has limited, if any, direct effects on brain resident cells, IFNλ potently induces antiviral defense in the BBB by inducing ISG expression in endothelial cells and increasing endothelial barrier properties [122]. Mice lacking IFNLR had elevated brain viral titers and barrier permeability during West Nile virus (WNV) infection [128]. Additionally, IFNλ modulates T cell activity, but virus-host interactions may impact its effect [129]. For example, IFNLR1$^{-/-}$ had increased CD8 T cell proliferation during acute lymphocytic choriomengitis virus

(LCMV) Armstrong infection, but CD8 T cells were reduced in number upon chronic LCMV Clone 13 infection [130]. Furthermore, IFNLR1$^{-/-}$ mice mounted a CD8 T cell response to brain WNV infection similarly to WT mice, suggesting that the tissue microenvironment also plays a role in the dependence of CD8 T cells on Type III IFNs [128]. Collectively, these studies demonstrate that IFNλ signaling is important for protection of the brain during viral infections.

1.4.4 STAT1

There are seven known STAT proteins: STAT1, STAT2, STAT3, STAT4, STAT5a, STAT5b, and STAT6 [93]. All members of the STAT family signal similarly. STATs are recruited to receptor signaling complexes by interactions between the STAT Src 2 homology (SH2) domain expressed on STAT proteins and phosphotyrosine sequences expressed on receptor-bound proteins, such as members of the Jak family [131]. The specificity of STAT activation is determined by the affinity of the SH2-phosphotyrosine interaction [132]. Once recruited, STATs are phosphorylated and then dimerize. This dimerization allows them to translocate to the nucleus, where they bind to gene promotors and activate transcription.

STAT1 is the common signaling molecule of the IFN family (**Fig 1-1**). STAT1 activation and translocation into the nucleus mediates the transcription of ISGs and GAS, which affect immune function, inflammation, and antiviral defense [93]. As expected from its central role in the IFN response, STAT1 deficiency results in increased susceptibility to viral infection, including many neurotropic infections [133]. However, STAT1 also mediates the transcription of some anti-inflammatory ISGs [131]. STAT1-deficient mice infected with an attenuated flu strain controlled virus efficiently, but ultimately died from an overactive immune response [134]. Thus, in conclusion, STAT1 maintains immune homeostasis by transcription of pro- and anti-inflammatory factors.

1.5 Specific Aims

Although PyV infection is initially asymptomatic, the lethality of PyV infection, particularly infection with JCPyV, in immunocompromised individuals necessitates a better understanding of host defense. The strict host specificity and rarity of PyV-associated diseases have impeded the understanding of immune and viral interactions. Here, we address several aspects of host PyV-defense in an MuPyV brain infection model.

1) An unknown in the field of CD8 T_{RM} is what signals and cells regulate the development and survival of CD8 T cells in nonlymphoid tissues, such as the brain. Understanding the contribution of CD4 T cells to the development of a robust CD8 T_{RM} compartment will allow us to generate durable and long-lasting protection from repeat viral infections in tissues that are not readily accessible to the peripheral immune response.
2) IFNs are a pleiotropic family of cytokines that potently inhibit viral replication, and IFNs have been implicated in alleviating PyV burden in vivo and in vitro. However, the contribution of IFNs to the defense against PyV-encephalitis remains largely unknown.
3) T cells are critical components of the defense against PyV infection in both mouse and humans. However, T cells can also contribute to brain diseases because of their cytotoxic capabilities. Evaluating the contribution of T cells to MuPyV pathogenesis will allow us to understand neuroprotective and neurodegenerative responses during brain infection.

The **overall aim** of this dissertation is to better understand the host-derived factors that prevent MuPyV replication in the brain and the periphery, with the goal of elucidating host defenses that can be modulated to promote viral control. Our **overall hypothesis** is that PyV defense arises from a combination of brain-derived molecules, such as IFNs, and that the interactions of the immune system generate multifunctional responses.

First, we investigate the functionality of CD8 T cells in the absence of CD4 T cells, an identified risk factor for the development of PML. Second, we elucidate the roles of type I, II, and III IFNs in the development of anti-PyV immune responses and antiviral defense in the brain. Finally, we investigate the contribution of MuPyV and T cells to demyelination in a novel mouse model of PyV-associated brain encephalitis.

1.5.1 To investigate the impact of CD4 T cell deficiency on the magnitude and function of CD8 bT_{RM} during persistent MuPyV infection. Previous work has shown that unhelped CD8 T cells fail to control antigen upon secondary exposure and have impaired memory differentiation. Deficiencies in CD4 T cells predispose patients to the development of PML, and mutations in the CD4 T cell epitope impair CD4 and CD8 T cell responses and antiviral control. However, the importance of CD4 T cells in the maintenance of CD8 T cells during persistent brain infection remains unknown. Using CD4 T cell-deficient mice and antibody-mediated depletion of CD4 T cells, we found that CD4 T cells are necessary for the development of CD8 bT_{RM}. Unhelped CD8 T cells had substantial changes to their transcriptome, remained dependent on the circulation, and were unable to control reinfection. These data provide new insights into the factors governing PML susceptibility in CD4 T cell-deficient individuals.

1.5.2 To elucidate the role of type I, II, and IIII IFNs on MuPyV infection in the brain. The members of the IFN family promote antiviral defense in brain resident cells, with different subsets having differing susceptibilities to each IFN family member. The efficacy of IFNs in inducing antiviral defense in brain resident cells has been demonstrated in vitro, but their role on PyV replication in the brain remains unknown. Using mice deficient in either type I, II, or III IFNs or their common signaling molecule, STAT1, we demonstrate that IFNs do not contribute

substantially to the control of persistent MuPyV infection. STAT1, however, dictates the infiltration of immune cells into the brain and their functionality and the extent of hydrocephalus following MuPyV inoculation. In addition to mediating the downstream signaling of IFNs, STAT1 is also involved in the signaling of many other molecules, suggesting that defense against MuPyV infection in the brain is multifaceted.

1.5.3 To determine the contribution of T cells and virus to the pathogenesis of MuPyV infection. Because most brain resident cells are terminally differentiated, the effector mechanisms used by T cells are detrimental to brain recovery. Post-mortem analysis of PML-IRIS brains reveals colocalization of T cells and infected cells, suggesting that T cells contribute to disease. In Chapter 3, we describe a novel mouse model of MuPyV brain infection that is relevant for understanding virus-associated demyelination and document that T cell infiltration is a critical component of MuPyV control in the brain, spleen, and kidney.

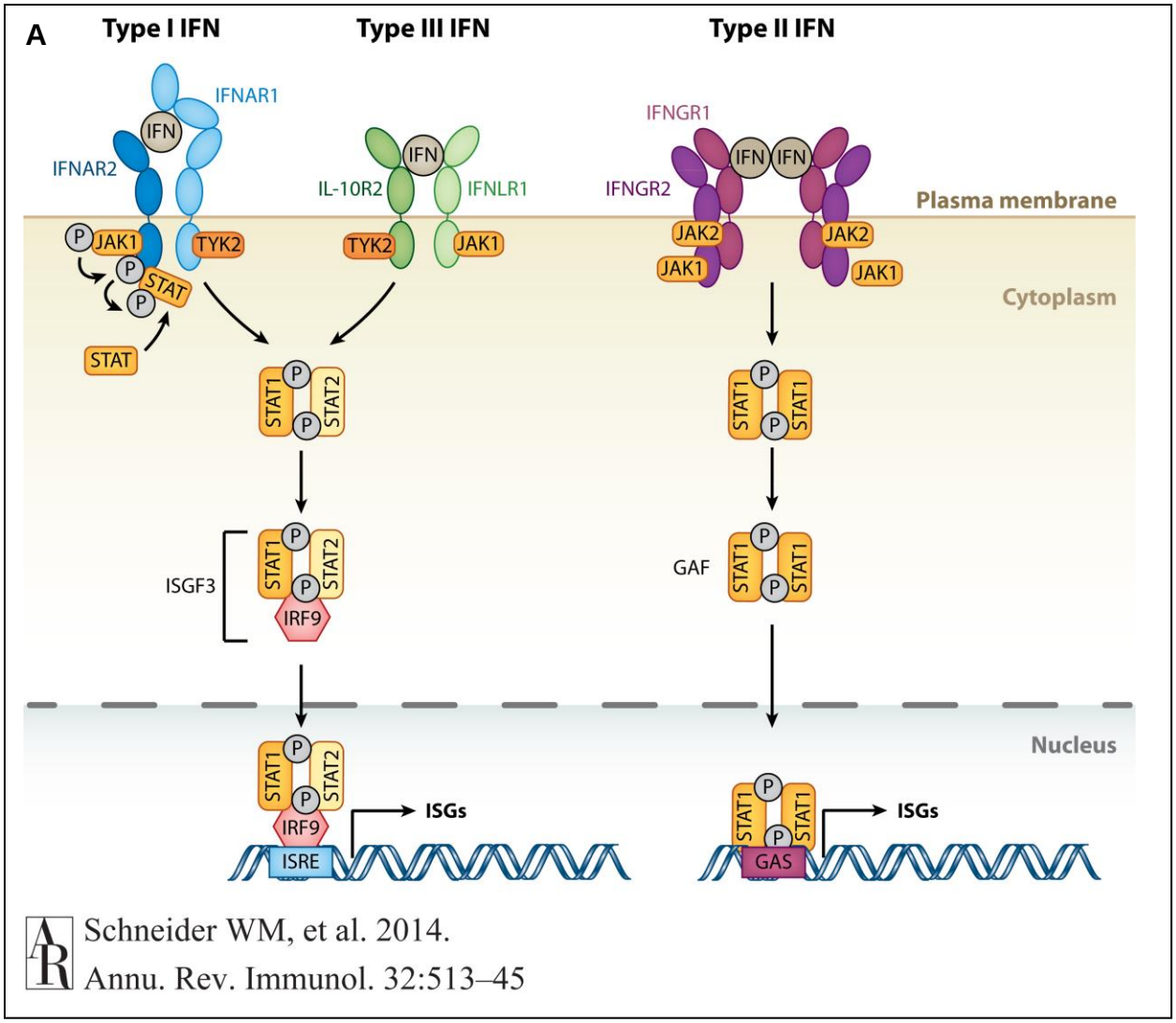

Fig 1-1: The IFN signaling cascade. (A) Schematic of the receptors and downstream signaling molecules of the three members of the IFN family [93].

Chapter 2

CD4 T cells control development and maintenance of brain-resident CD8 T cells during polyomavirus infection

Mockus TE, Shwetank, Lauver MD, Ren, HM, Netherby, CS, Salameh T, Kawasawa YI, Yue F, Broach JR, and Lukacher AE (2018) CD4 T cells control development and maintenance of brain-resident CD8 T cells during polyomavirus infection. PLoS Pathogens.

Abstract

Tissue-resident memory CD8 T cells (CD8 T_{RM}) defend against microbial reinfections at mucosal barriers; determinants driving durable CD8 T_{RM} responses in non-mucosal tissues, which often harbor opportunistic persistent pathogens, are unknown. JC polyomavirus (JCPyV) is a ubiquitous constituent of the human virome. With altered immunological status, JCPyV can cause the oft-fatal brain demyelinating disease progressive multifocal leukoencephalopathy (PML). JCPyV is a human-only pathogen. Using the mouse polyomavirus (MuPyV) encephalitis model, we demonstrate that CD4 T cells regulate development of functional antiviral brain-resident CD8 T cells (bT_{RM}) and renders their maintenance refractory to systemic CD8 T cell depletion. Acquired CD4 T cell deficiency, modeled by delaying systemic CD4 T cell depletion until MuPyV-specific CD8 T cells have infiltrated the brain, impacted the stability of CD8 bT_{RM}, impaired their effector response to reinfection, and rendered their maintenance dependent on circulating CD8 T cells. This dependence of CD8 bT_{RM} differentiation on CD4 T cells was found to extend to encephalitis caused by vesicular stomatitis virus. Together, these findings reveal an intimate association between CD4 T cells and homeostasis of functional bT_{RM} to CNS viral infection.

2.1 Introduction

T_{RM}, the largest memory T cell subset, are non-recirculating cells parked in both nonlymphoid and lymphoid tissues [71, 135, 136]. The importance of CD8 T_{RM} cells in limiting infections, their distinct transcriptional profile, the signals driving their differentiation, and their capacity to control re-infections at mucosal portals of pathogen entry are well documented [71, 137]. Far less is known about the requirements for establishing CD8 T_{RM} cells in non-mucosal tissues, particularly those populated by large populations of non-renewable cells, such as the brain, where rapid control of infection may prove lifesaving. Recent studies using acutely resolved viral meningo-encephalitidies have revealed the durability of CD8 bT_{RM} and their role in clearing CNS viral infections [84]. However, little is known of the requirements for establishing and maintaining CD8 T_{RM} cells to persistent viral CNS infections.

PyV are natural pathogens that persist as silent, lifelong infections in healthy hosts of many vertebrates. Fourteen polyomaviruses to date have been identified as constituents of the human virome, but several [BKPyV, JCPyV, and Merkel cell polyomavirus (MCPyV)] are opportunistic pathogens known to cause life-threatening diseases in immunocompromised individuals [19]. JCPyV is acquired in early adolescence probably via gastrointestinal routes of infection, reaches seropositivity rates over 60% by sixty years of age, and persists in the kidney, urinary tract, bone marrow, and possibly the brain [138, 139]. With altered immune status as a consequence of HIV/AIDS, immune-modulating therapeutics for autoimmune diseases (e.g., natalizumab for relapsing-remitting multiple sclerosis), and biologic anti-cancer agents, JCPyV can cause progressive multifocal leukoencephalopathy (PML) [19]. PyVs productively infect and persist only in their host reservoir species. An acknowledged impediment to understanding PML pathogenesis and the immunovirologic factors that put patients at risk for PML is the absence of tractable animal models [140]. Human astrocytes/oligodendrocytes engrafted in brains of $RAG2^{-/-}MBD^{sh/sh}$ mice support JCPyV replication and virus-induced loss of these glial cells results in

demyelination [26]. However, deciphering the immunological deficits that predispose patients to PML remains to be determined.

CD4 T cells are necessary for regulating the phenotype and function of CD8 memory T cells in lymphoid organs [60]. In acute viral infections, CD8 T cells primed in the absence of CD4 T cells ("unhelped" CD8 T cells) lose the ability to produce effector cytokines such as IFNγ, TNFα, IL-2, as well as the cytolytic protein Granzyme-B, and are unable to control primary infection or infections by reencountered pathogens [61-63]. Furthermore, memory differentiation is aberrant in unhelped CD8 T cells, as demonstrated by impaired upregulation of CD62L, IL-7Rα (CD127), and the CD27 costimulatory molecule [64, 65]. Recall responses of unhelped memory CD8 T cells to infection with vaccinia virus are restrained by PD-1 [141], and vaccine-elicited unhelped CD8 T cells express multiple inhibitory receptors [142]. Unhelped CD8 T cells infiltrate the brain in response to vesicular stomatitis virus (VSV) [76] and lymphocytic choriomengitis virus (LCMV) [84]. Other models of central nervous system (CNS) viral infection, however, suggest that CD4 T cell help is necessary for CD8 T cell function and CD8 bT_{RM} development. Unhelped CD8 T cells cannot control West Nile Virus (WNV) infection and gradually lose the ability to produce effector cytokines [143]. CD8 T cells in the CNS of CD4 T cell-deficient mice inoculated intracerebrally with a neurotropic mouse coronavirus had reduced IFNγ and Granzyme-B expression, impaired viral control, disrupted memory differentiation, and increased apoptosis [144-146]. CD4 T cell help to CD8 T cells and B cells is also pivotal in the control of measles virus encephalitis [147, 148]. For PML, it is interesting to note a case report documenting isolation of JCPyV DNA carrying a mutation that ablates a JCPyV-specific CD4 T cell epitope [31]. These studies highlight the discrepant data on the dependence of CD4 T cell help for sustaining CD8 bT_{RM} formation during CNS viral infections, and point toward the possibility that such CD4 T cell dependence may be context-dependent.

Mouse polyomavirus (MuPyV) is a ubiquitous natural mouse pathogen that establishes a lifelong infection [19, 149]. MuPyV infects a wide variety of cells such as epithelial cells, mesenchymal cells, macrophages, and dendritic cells [150, 151]. MuPyV persistently infects multiple organs including the spleen, brain, kidney, and bone marrow, with the site of inoculation affecting the organ distribution of persistent viral infection [152]. Mice lacking secondary lymphoid organs fail to generate an anti-MuPyV CD8 T cell response [153]. Previous work has shown that CD8 T cells contribute a large part of the host defense against MuPyV infection in the periphery [58, 59].

In this study, we asked whether CD4 T cell help was essential for generating CD8 bT_{RM} in mice infected with MuPyV. Upon i.c. MuPyV inoculation, virus-specific CD8 T cells are recruited to the brain and establish a CD8 bT_{RM} population [74, 154, 155]. MuPyV inoculated i.c. spreads systemically [154]. We found that unhelped virus-specific CD8 T cells infiltrate the brain and are functional during early stages of MuPyV infection, but fail to control virus during reinfection. We previously described the contrast in dependence of brain-infiltrating CD4 T cells, but not of CD8 T cells, on their circulating counterparts [154]. Here, we found that maintenance of unhelped CD8 T cells required resupply from CD8 T cells in the vasculature. The transcriptome of unhelped CD8 T cells showed pronounced upregulated expression of genes involved in pathways of CD8 T cell development and homeostasis. Moreover, CD4 T cell insufficiency impaired differentiation of functional virus-specific CD8 bT_{RM} not only at the stage of naïve CD8 T cell priming, but also after MuPyV-specific CD8 T cells had infiltrated the brain. The importance of CD4 T cells for homeostasis of virus-specific CD8 T cells during a persistent viral encephalitis has clear clinical ramifications for establishing durable immunosurveillance of persistent CNS infections.

2.2 Results

2.2.1 CD4 T cells are dispensable for the recruitment, maintenance, and function of brain-infiltrating MuPyV-specific CD8 T cells

A large body of evidence has shown that CD4 T cell deficiency during recruitment of naïve CD8 T cells has negative consequences on memory CD8 T cell differentiation [60]. To ask whether availability of CD4 T cell help during priming of virus-specific CD8 T cells affected recruitment and maintenance of CD8 T cells during MuPyV encephalitis, CD4 T cells were depleted by intraperitoneal (i.p.) administration of CD4 mAb before MuPyV infection and weekly thereafter until endpoint. CD4 T cell-sufficient and -deficient mice showed similar frequency and number of CD8 T cells specific for the dominant D^bLT359 epitope in both the brain and spleen in acutely (day 8 p.i.) and persistently (day 30 p.i.) infected mice (**Fig 2-1A & B)**. The helped and unhelped virus-specific CD8 T cell responses in the spleen decreased similarly between days 8 and 30 p.i. In contrast, the frequency and number of virus-specific CD8 T cells in the brain did not significantly change between days 8 and 30 p.i. in either CD4 T cell-sufficient or –deficient mice **(Fig 2-1A & B**). In addition, unhelped MuPyV-specific CD8 T cells in the brain proliferated similarly as compared to helped CD8 T cells and expressed Bcl-2 (**Fig 2-2A & B**). Independent confirmation of these results was made using MHC $II^{-/-}$ mice inoculated i.c. with MuPyV, where no differences were found in the frequency or number of virus-specific CD8 T cells in the brains of MHC $II^{-/-}$ and wild type (WT) mice (**Fig 2-1C & D**). This equivalence in helped vs unhelped virus-specific CD8 T cell responses in the brain mirrors that reported for WT and MHC $II^{-/-}$ mice given VSV intranasally (i.n.) [76]. CD4 T cell availability did not affect the pattern of effector/memory differentiation of MuPyV-specific CD8 T cells in either the brain or spleen based on surface co-expression of KLRG1 and CD127, and expression of the transcription factors T-bet, eomesodermin (eomes), TCF-1, and Blimp-1 (**Fig 2-2C-H**).

We next asked whether unhelped CD8 T cells exhibited functional deficits. Previous studies have shown that CD4 T cell help is necessary for the development of functionally competent CD8 T cells [60]. In contrast, similar numbers and frequencies of helped and unhelped D^bLT359-specific CD8 T cells produced IFN-γ, TNF-α, and IL-2, and retained cytotoxic effector potential (i.e., intracellular granzyme B and peptide-induced CD107 cell surface expression) during acute and persistent MuPyV infection (**Fig 2-3A & B)**. In the spleen, however, fewer unhelped D^bLT359-specific CD8 T cells produced IFNγ in persistently infected mice (**Fig 2-4A**). Helped and unhelped D^bLT359-specific CD8 T cells in the brain had similar sensitivity to antigen stimulation, as evidenced by the expression of IRF4 (**Fig 2-3C**), a transcription factor upregulated by TCR engagement [156]. Furthermore, IFNγ mRNA and CXCL9 mRNA, an IFNγ-induced chemokine, were upregulated compared to uninfected control mice similarly in brains of CD4 T cell-sufficient and -deficient mice (**Fig 2-3D)**. Although no difference in viral load was observed in brains of CD4 T cell-deficient and -sufficient mice during acute infection, viral loads trended higher during persistent infection in the absence of CD4 T cells (**Fig 2-3E**). Thus, CD4 T cells appear not to overtly impact the magnitude, differentiation, or function of virus-specific CD8 T cells infiltrating the brains of MuPyV-infected mice.

2.2.2 CD4 T cells are essential for the development of bT_{RM}

As we recently reported, approximately 40% of D^bLT359-tetramer$^+$ CD8 T cells in the brain express CD103 in persistently infected mice [74]. In CD4 T cell-deficient mice, few CD103$^+$ MuPyV-specific CD8 T cells were detected in the brain 30 days after MuPyV inoculation (**Fig 2-5A & B** and **2-6A**), although these cells expressed CD69 at levels similar to those in CD4 T cell-sufficient mice (**Fig 2-5C)**. During WNV infection of the brain, TGF-β produced from regulatory T cells is important for the upregulation of CD103 [157]. In our model, FoxP3$^+$CD25$^+$ CD4 T cells infiltrate the brain but constitute only 5% of CD44$^+$ CD4 T cells in WT mice (**Fig 2-6B**). After stimulation with PMA/ionomycin, brain CD4 T cells showed a transient 4-fold increase in TGFβ

mRNA compared to unstimulated CD4 T cells (**Fig 2-6C**). IL-21 has also been associated with establishing CD8 T_{RM} and their expression of CD103 [158]. CD4 T cells produced >100-fold more IL-21 mRNA after PMA/ionomycin stimulation (**Fig 2-6D**). Together, these data support the possibility that TGF-β and IL-21 contribute to upregulating CD103 on the virus-specific CD8 T cells during MuPyV infection. Furthermore, unhelped virus-specific CD8 T cells had higher PD-1 expression compared to helped virus-specific CD8 T cells (**Fig 2-5D** and **2-6E & F**). Diminished expression of CD103, a commonly used marker of T_{RM} cell differentiation, and elevated PD-1 expression raised the possibility that CD4 T cell help qualitatively modulated MuPyV-specific CD8 bT_{RM} residing in the brain.

We recently demonstrated that systemic depletion of CD8 T cells after their entry into the brain did not impact their maintenance, while i.p. administration of a depleting CD4 mAb led to a dramatic decline in numbers of CD4 T cells in the brain [154]. These data indicated that brain-resident CD8 and CD4 T cells during MuPyV encephalitis showed a dichotomy in their dependence on cells in the circulation. We asked whether maintenance of unhelped MuPyV-specific CD8 T cells in MuPyV-infected mouse brain retained independence from the vascular compartment. To do this, CD8 T cell-depleting mAb was given at day 10 p.i., which was after MuPyV-specific CD8 T cells had infiltrated the brain [154] (**Fig 2-5E**). In CD4 T cell-sufficient mice, depletion of circulating CD8 T cells had no effect on the number of total CD8 T cells or D^bLT359-specific CD8 T cells in the brain at day 30 p.i. **(Fig 2-5E**). In marked contrast, the number of total CD8 T cells and D^bLT359-specific cells declined approximately 100-fold in CD4 T cell-deficient mice depleted of circulating CD8 T cells at this timepoint (**Fig 2-5E)**. Together, these data suggest that CD4 T cell availability for development and maintenance of CD8 bT_{RM} is critical during persistent viral CNS infections.

A differential dependence of CD4 T cell help on development of virus-specific CD8 T_{RM} in different viral systems may depend on the type of viral infection. To explore this possibility, we used a recombinant VSV encoding the D^bLT359 epitope (rVSV-LT359) [159]. CD4 T cell-

sufficient and -deficient mice had similar frequencies of D^bLT359-specific CD8 T cells in the brain 30 days after rVSV-LT359 i.n. inoculation (**Fig 2-7A**). This result confirms that of Wakim et al. who found no differences in antigen-specific CD8 T cell responses between WT and CD4 T cell-deficient mice in brains of mice with VSV encephalitis [76]. We further observed that unhelped virus-specific CD8 T cells in brains after i.n. rVSV-LT359 inoculation failed to upregulate CD103 (**Fig 2-7B**). PD-1 expression on unhelped CD8 T cells, however, was not significantly higher (**Fig 2-7C**). Systemic CD8 T cell depletion resulted in loss of D^bLT359-specific CD8 T cells in CD4 T cell-depleted mice, but not in CD4 T cell-sufficient mice given αCD8 (**Fig 2-7D**). Using primers against VSV genomic RNA (gRNA), we were able to detect low levels of VSV gRNA during persistence in both CD4 T cell-sufficient and –deficient mice (**Fig 2-7E**). Similarly, a previous study reported persistent VSV gRNA after i.n. infection, but detected no VSV mRNA at the same time point [160]. Collectively, these data indicate that CD4 T cell help is essential for generating CD8 bT_{RM} in both VSV and MuPyV CNS infections.

To exclude the possibility that antibody-mediated CD4 T cell depletion increased the permeability of the BBB and allowed CNS access by anti-CD8α, we measured extravasation of sodium fluorescein into brains of CD4 T cell-sufficient and -deficient mice 10 days after MuPyV infection. CD4 T cell-deficient mice showed no change in the concentration of sodium fluorescein dye in the brain, indicating that the integrity of the BBB was unaltered by systemic CD4 T cell depletion (**Fig 2-8A**). Furthermore, systemically administered CD8 T cell-depleting mAb did not stain CD8 T cells in the brain parenchyma, irrespective of CD4 T cell status (**Fig 2-8B**). Unhelped virus-specific CD8 T cells expressed the adhesion molecules VLA-4, PSGL1, and LFA-1, suggesting that CD4 T cell availability did not alter the ability of these cells to home to and traffic into the infected brain (**Fig 2-8C**). To ask whether unhelped CD8 T cells remained in the vasculature and, thus, directly exposed to depleting anti-CD8α, we performed intravascular staining with FITC-conjugated CD45 mAb. No difference in the ratio of extravascular to intravascular total and virus-specific CD8 T cells was seen between helped and

unhelped mice (**Fig 2-8D**). Collectively, these data confirm that bT_{RM} become dependent on hematogenous replenishment in the absence of CD4 T cell help.

2.2.3 CD4 T cells promote MuPyV-specific CD8 bT_{RM} function

A central defect of unhelped memory CD8 T cells in lymphoid tissues is their failure to expand upon reencountering cognate antigen [161]. CD8 T_{RM} accelerate control of viral reinfection in nonlymphoid tissues [71]; however, a requirement for CD4 T cell help for CD8 bT_{RM} to retain their recall response capability is unknown. We previously showed that MuPyV-infected mice, which possess potent neutralizing virus antibodies, mount recall responses in the brain after i.c. challenge with homologous MuPyV [155]. We asked whether availability of CD4 T cell help affects recall responses of virus-specific CD8 T cells to MuPyV reinfection and ability to control the challenge infection. Mice were depleted of circulating CD4 T cells before i.c. inoculation with MuPyV and then reinfected i.c. with MuPyV at day 30 p.i. (**Fig 2-9A)**. At day 5 after reinfection, viral load was significantly higher in CD4 T cell-deficient mice reinfected with MuPyV compared to CD4 T cell-sufficient mice with reinfection (**Fig 2-9B**). However, the viral load was not significantly higher than CD4 T cell-deficient mice receiving mock rechallenge (**Fig 2-9B**). Although the viral load was trending lower in rechallenged CD4 T cell-sufficient mice, the difference did not reach statistical significance (**Fig 2-9B**). This loss of viral control was observed despite similar numbers and proliferation of brain virus-specific CD8 T cells **(Fig 2-9C & D**). Although MuPyV-specific CD8 T cells proliferated rapidly in the reinfected mice, no significant increase was seen in the number of D^bLT359^+ CD8 T cells in the brain upon rechallenge. This discrepancy between cell proliferation and numbers suggests engagement of a concurrent cell death process. Interestingly, no difference in IRF4 was seen between CD4 T cell helped and unhelped virus-specific CD8 T cells, implying comparable levels of TCR activation and IFNγ production (**Fig 2-9E**). Yet, the frequency of $IFN\gamma^+$ CD8 T cells upon ex vivo LT359 peptide stimulation was lower in rechallenged CD4 T cell-deficient than -sufficient mice

(**Fig 2-9F)**; although significant, there was <10% difference between the mock vehicle injected persistently infected rat IgG and CD4 T cell-deficient groups. Using IFNγ eYFP reporter mice to visualize effector function by MuPyV-specific CD8 T cells *in situ*, we found that a significantly higher fraction of $CD103^+$ than $CD103^-$ cells produced IFNγ upon reinfection, with $CD103^-$ D^bLT359 tetramer$^+$ CD8 T cells in both CD4 T cell-sufficient and -deficient mice producing little IFNγ (**Fig 2-9G**). This defect was not due to a decrease in $CD103^-$ cells in brain (**Fig 2-9G**). Without rechallenge, $CD103^-$ T cells from CD4 T cell -sufficient and -deficient mice have similar IFNγ-eYFP production to $CD103^+$ CD8 T cells (**Fig 2-9H**). These results indicate that CD4 T cells during recruitment and maintenance of CD8 bT_{RM} are necessary for effective control of MuPyV CNS reinfection and improved ability to produce IFNγ.

Absence of virus-neutralizing antibodies may be associated with increased viral burden, with the consequent high antigen levels driving virus-specific T cell dysfunction. However, the contribution of antiviral antibodies to offsetting T cell exhaustion depends on the experimental viral system. MuPyV infection elicits a virus-neutralizing CD4 T cell-independent IgG response directed to VP1, the major polyomavirus capsid protein [162, 163]. Similarly, influenza virus infection also generates a T cell-independent influenza-specific IgG that helps resolve primary influenza infection and prevents reinfection [164]. Despite a decrease in αVP1 IgG titers in CD4 T cell-depleted mice at day 30 p.i., sera from CD4 T cell-deficient and -sufficient mice exhibited strong virus-neutralization capability during acute and persistent infection (**Fig 2-10A & B**). To formally exclude an effect of MuPyV-neutralizing antibodies on peripheral viral load and T cell function during MuPyV rechallenge, WT and MHC $II^{-/-}$ mice were passively immunized with a neutralizing VP1 IgG mAb [165] from day 10 p.i. to MuPyV i.c. reinfection at day 30 p.i (**Fig 2-10C**). Despite passive immunization, unhelped virus-specific CD8 T cells still exhibited significant deficits in IFNγ production (**Fig 2-10D**), while PD-1 expression was increased compared to CD4 T cell-sufficient mice (**Fig 2-10E**). Viral loads were similar in $MHCII^{-/-}$ mice with and without mAb VP1 treatment (**Fig 2-10F**). Serum from $MHCII^{-/-}$ and WT mice that were

passively immunized with αVP1 possessed similar virus-neutralization capabilities (**Fig 2-10G**). These data demonstrate that virus-specific antibodies did not rescue the unhelped CD8 T cell response.

2.2.4 Helped and unhelped MuPyV-specific CD8 T cells in the brain have distinct transcriptomes

The common defect in IFNγ production by $CD103^-$ MuPyV-specific CD8 T cells in WT and CD4 T cell-deficient mice led us to survey the transcriptional landscape of $CD103^+$ and $CD103^-$ D^bLT359 tetramer$^+$ CD8 T cells sorted from brains of persistently infected WT and $MHCII^{-/-}$ mice (**Fig 2-11A**); for this analysis, we refer to D^bLT359 tetramer$^+$ CD8 T cells from MHC-$II^{-/-}$ mice as $MHCII^{-/-}$-$CD103^-$ CD8 T cells and D^bLT359 tetramer$^+$ $CD103^-$ and $CD103^+$ CD8 T cells from WT mice as $CD103^-$ and $CD103^+$. 377 transcripts were differentially expressed between $CD103^-$ and $MHCII^{-/-}$-$CD103^-$ CD8 T cells, whereas 267 transcripts were differentially expressed between $CD103^+$ and $MHCII^{-/-}$-$CD103^-$ CD8 T cells (**Fig 2-12A & B**). Only 73 transcripts, however, were differentially expressed between helped $CD103^-$ and $CD103^+$ CD8 T cells (**Fig 2-12A & B**). These data reveal that WT-$CD103^-$ and WT-$CD103^+$ cells had similar transcriptomes, both of which were substantially different from the transcriptomes of MHC $II^{-/-}$-$CD103^-$ cells. Our recent report showing similar phenotype and function by brain-resident, MuPyV-specific CD8 T cells irrespective of CD103 expression [74] are in line with the highly overlapping transcriptomes of WT-$CD103^+$ and WT-$CD103^-$ CD8 T cells. These findings support accumulating evidence that caution is warranted when considering CD103 as a stereotypical marker of T_{RM} differentiation [71, 155]. Ingenuity pathway analysis of $MHCII^{-/-}$-$CD103^-$ vs $CD103^-$ CD8 T cells revealed significant aberrations in the activation state and homeostasis of unhelped CD8 T cells. $MHCII^{-/-}$-$CD103^-$ exhibited significant downregulation of pathways including cdc42, actin cytoskeleton remodeling, and actin-based motility, which are essential for cell migration (**Fig 2-12C**). Additionally, $MHCII^{-/-}$-$CD103^-$ CD8 T cells had downregulated RhoA signaling, which has

recently been identified as a central regulator of CD4 T cell viability, proliferation, and migratory capacity in the CNS of EAE mice [166]. Notably, MHCII$^{-/-}$-CD103^{-} CD8 T cells had significant downregulation of Runx3 (**Table 2-1**), a recently identified component of the transcription factor signature of CD8 T_{RM} [167]. MHCII$^{-/-}$-CD103^{-} CD8 T cells also showed significant upregulation of phosphoinositide pathways **(Fig 2-12C**). Gain-of-function mutations in phosphoinositide pathways have been reported to promote exhaustion and senescence of CD8 T cells [168, 169]. MHCII$^{-/-}$-CD103^{-} CD8 T cells differentially expressed genes involved in mitochondrial function; mitochondrial dysfunction is highly prevalent in CD8 T cells isolated from HIV^{+} patients [170]. By comparison to MuPyV-specific CD8 T cells in brains of MHC-II$^{-/-}$ mice, the CD103^{+} and CD103^{-} cells in brains of WT mice shared most of the same significant gene expression pathways (**Fig 2-11B)**. Thus, unhelped CD8 T cells during persistent MuPyV infection have a profoundly altered transcriptome in a pattern indicating defective homeostasis and activation.

2.2.5 CD4 T cells are necessary for MuPyV-specific CD8 bT_{RM} homeostasis

Because CD4 T cell deficiency is often an acquired rather than an inherited condition, we asked whether delayed systemic deletion of CD4 T cells affected development of functionally competent CD8 bT_{RM} during MuPyV encephalitis. We therefore started i.p. administration of CD4 T cell-depleting mAb at day 10 p.i. (**Fig 2-13A**). The number of CD4 T cells significantly declined in the brain with systemic anti-CD4 depletion (**Fig 2-13B**). Although no difference was seen in the number of virus-specific CD8 T cells or viral load in the brain with delayed CD4 T cell depletion (**Fig 2-13C & D**), the frequency of virus-specific CD103^{+} CD8 T cells was significantly lower at 30 days p.i. compared to CD4 T cell-sufficient mice (**Fig 2-13E**). Because the frequency of CD103^{+} D^{b}LT359-specific CD8 T cells was significantly reduced in CD4 T cell-deficient mice, we asked whether a decline in CD4 T cells affected development of virus-specific CD8 T_{RM} cells after CNS infiltration. To this end, systemic CD4 T cell depletion began at day 10 p.i., coupled with circulating CD8 T cells at day 20 p.i. (**Fig 2-13F**). The number of total CD8 T

cells and MuPyV-specific CD8 T cell and the gMFI of CD8 on the MuPyV-specific CD8 T cells were significantly reduced in CD4 T cell-deficient mice (**Fig 2-13G**). We have previously published that increased CD8 gMFI marks bT_{RM} [154]. We next assessed the ability of these unhelped D^bLT359-specific CD8 T cells to control MuPyV challenge infection (**Fig 2-13H**). Five days after reinfection, the number of D^bLT359-specific CD8 T cells was not significantly different between CD4 T cell-sufficient and -deficient mice (**Fig 2-13I**), but the frequency of IFNγ-producing cells was significantly lower (**Fig 2-13J**). Virus levels, however, were the same between CD4 T cell-sufficient and –deficient mice (**Fig 2-13K**). These data support the concept that CD4 T cells are required to sustain functional CD8 bT_{RM} to persistent viral encephalitis.

2.3 Discussion

CD4 T cells modulate the differentiation program of pathogen-specific CD8 T cells that establish permanent residence as memory cells in mucosal barrier tissues, but their role in driving T_{RM} development in non-barrier tissues is less understood [60]. In this study, we determined that CD4 T cell help was essential for establishment and maintenance of CD8 bT_{RM} to MuPyV encephalitis. CD4 T cells guided the differentiation of MuPyV-specific CD8 bT_{RM} during naïve T cell priming and were required for maintenance of functional antiviral CD8 bT_{RM} in brains of persistently infected mice. Notably, CD4 T cell insufficiency resulted in diminished effector competence of antiviral CD8 T cells encountering MuPyV reinfection in the brain. An ongoing dependence on CD4 T cells for induction and maintenance of virus-specific CD8 bT_{RM} to a persistent CNS infection has clear clinical implications for individuals whose immune status is altered by infection or immunomodulatory therapeutic agents.

Accumulating evidence supports the likelihood that JCPyV adapts to selective pressure applied by virus-specific CD4 T cells. JCPyV recovered from PML patients carry mutations in the VP1 capsid protein that affect binding to sialylated glycans, which serve as receptors for JCPyV entry into host cells [171]. Thus, JCPyV-PML VP1 mutations are thought to alter viral tropism and endow JCPyV with neuropathic potential. Recent evidence, however, supports the alternative possibility that these VP1 mutations serve an immune evasion purpose by preventing recognition by neutralizing antibodies [172] and by ablating VP1-specific CD4 T cell epitopes [31]. These findings have motivated efforts to isolate monoclonal antibodies capable of broadly cross-neutralizing WT and VP1 mutant JCPyVs to protect patients at-risk of and as therapeutics for PML [173]. In the pre-combination antiretroviral therapy era, PML had an approximately 5% incidence in patients with HIV/AIDS, a disease initiated by profound CD4 T cell deficiency [174]. Individuals with idiopathic CD4 T cell lymphopenia, which manifest no overt changes in CD8 T cells, B cells, or NK cells, are also at elevated risk for PML [175]. JCPyV VP1/LT-specific CD8 T cell adoptive immunotherapy in a PML patient drove viral DNA below

PCR detectability in the CSF and improved neurological status [176]. Our data together with these studies suggest that preserving and augmenting anti-JCPyV CD4 T cells or providing "helper" cytokines in PML-susceptible individuals, and using such interventions to supplement CD8 T cell immunotherapy for PML, could promote differentiation of brain-infiltrating CD8 T cells into CD8 bT_{RM} and improve disease prognosis.

Upon peripheral LCMV infection, CD4 T cell deficiency is associated with sustained high viral load, which in turn, upregulates checkpoint inhibitory receptors (e.g., PD-1) on virus-specific CD8 T cells, with blockade of these receptors driving recovery of effector competence and control of persistent infection [177-179]. In the MuPyV system, however, CD4 T cell deficiency did not result in higher virus levels, and helped and unhelped CD8 T cells had equivalent functional competence (**Fig 2-3**). Yet, PD-1 expression was increased on unhelped virus-specific CD8 T cells (**Fig 2-6**). Similarly, unhelped CD8 T cells that infiltrate HSV-1-infected sensory ganglia upregulate PD-1, retain effector functionality, and maintain latency [180]. Together, these data raise the intriguing possibility that the major role of CD8 T cells in the persistently infected CNS may be to control resurgent viral infection.

RNA-seq analyses revealed profound differences in the transcriptomes of helped vs unhelped MuPyV-specific CD8 T cells from the brains of persistently infected mice. Pathway analyses point toward significant defects in cell migration by unhelped CD8 T cells, which may impair their ability to co-localize with virus-infected cells (**Fig 2-12**). Changes in mitochondrial function and loss of RhoA signaling pathways in unhelped CD8 T cells suggest that unhelped CD8 T cells may inadequately survey the infected tissue due to their defective T cell activation and metabolism [166, 181]. Also, depressed functional integrity of unhelped CD8 T cells may necessitate resupply of new effector T cells from the circulation for their brain maintenance.

The nature of CD4 T cell help changes over the course of persistent viral infections. A large body of literature documents that the magnitude of the CD8 T cell response during persistent viral infections is regulated, in part, by IL-21 and IL-2 produced by CD4 T cells [182-

184]. Other studies, however, have shown that IL-10, usually considered an immunosuppressive cytokine, can promote maturation of memory CD8 T cells [185]. CD4 T cells may also indirectly affect the quantity and quality of CD8 T cell responses via helping anti-viral antibody production and affinity maturation to control extent of persistent infection [60]. Maintenance of CD8 T cells during persistent MuPyV infection may also depend on de novo priming of naïve virus-specific CD8 T cells. Ongoing de novo recruitment over an infection that changes dynamically, including progressing from systemic to tissue-localized infection, could contribute to CD8 T cell heterogeneity [186]. De novo recruitment of MuPyV-specific CD8 T cells is CD4 T cell-dependent; thus, the level of availability of CD4 T cell help may conceivably regulate this avenue for CD8 T cell differentiation, including those that populate a T_{RM} cell compartment [187]. Similarly, in mice persistently infected with the neurotropic strain of mouse hepatitis virus, naïve CD4 and CD8 T cells were primed and recruited to the CNS [188]. In sum, these studies demonstrate that the nature of CD4 T cell help is dynamic.

Virus-specific CD8 T cells control infections in the CNS via cytopathic and non-cytopathic effector mechanisms [189]. We previously reported that MuPyV infection was controlled in mice lacking TNF receptors or perforin and/or Fas as efficiently as in WT mice, and that IFNγ and IFN-I inhibited MuPyV replication *in vivo* [58, 59, 190]. Likewise, IFNγ and IFN-I inhibited JCPyV replication in established human glial cell lines and primary human glial cells [55, 191]. Noteworthy is an incidental observation in a phase III clinical study to evaluate the effectiveness of IFNγ on reducing incidence of opportunistic infections in HIV/AIDS subjects where none of the subjects in the IFNγ cohort developed PML as opposed to a 10% incidence in the placebo group [52]. In this study, we found that reinfection with MuPyV was more efficiently controlled in CD4 T cell-sufficient than -deficient mice when CD4 T cells were systemically depleted at the time of naïve virus-specific CD8 T cell priming; however, in MuPyV-infected mice where CD4 T cell depletion was delayed, no difference in viral control was seen on i.c. reinfection (**Fig 2-13**). Because MuPyV-specific CD8 T cells suffered a deficit in IFNγ

functionality in early and delayed CD4 T cell-deficient situations, IFNγ may not be the sole anti-MuPyV effector mechanism. In this connection, PML has also been diagnosed in patients with autoimmune rheumatic diseases, albeit not as frequently as in HIV/AIDS patients [192], and anti-TNFα treatment was associated with a low incidence of PML in these patients [193].

Unlike the high frequency of $CD103^+$ memory CD8 T cells detected in tissues following resolution of acute viral infections [18, 76], fewer than half of MuPyV-specific CD8 T cells express CD103, an αE integrin that pairs with β7 to bind E-cadherin and retains T cells in tissues [74]. The role of CD103 in maintaining CD8 T_{RM} appears to vary between tissues; its expression is particularly important for retention in small intestine mucosal epithelium and skin epidermis [194, 195]. Interestingly, we found that virus-specific CD8 bT_{RM} expressing CD103 had superior IFN-γ activity upon CNS re-infection with MuPyV (**Fig 2-9**). *Yersinia pseudotuberculosis*-specific CD8 T_{RM} lacking CD103 localize with infectious foci in the intestinal lamina propria, where early inflammatory cues from infiltrating macrophages control the size of the $CD103^-$ population [83]. However, no geographic differences based on CD103 expression have been described for CD8 bT_{RM} responding to brain infections [75, 84]. Studies are ongoing to define anti-MuPyV effector mechanism(s) in the CNS and potential preferential expression of effector activities by antiviral CD8 T cells.

We previously reported and confirmed here that stable maintenance of brain-infiltrating CD4 T cells to MuPyV encephalitis depends on ongoing replenishment from the vascular compartment; in sharp contrast, numbers of virus-specific CD8 T cells in the brain are unaltered by systemic CD8 T cell depletion [154]. Using the VSV encephalitis mouse model, we determined that CD4 T cell help also rendered virus-specific CD8 T cells susceptible to systemic CD8 T cell depletion. Thus, we found that the link between CD4 T cell help and establishment of CD8 bT_{RM} applies to both persistent (i.e., MuPyV) and acute (i.e., VSV) encephalitis. Loss of CD4 T cells either during naïve CD8 T cell priming or even after CD8 T cell effectors have accessed the CNS renders brain-localized CD8 T cells dependent on those in the circulation.

Evidence presented here supports the concept that an intact systemic CD4 T cell compartment is essential for preserving a steady-state détente between CD8 bT_{RM} and persistent viral infection in the CNS.

2.4 Materials and Methods

Ethics statement

All experiments involving mice were conducted with the approval of Institutional Animal Care and Use Committee (Protocol 46194) of The Pennsylvania State University College of Medicine in accordance with the Guide for the Care and Use of Laboratory Animals of the National Institutes of Health. The Pennsylvania State University College of Medicine Animal Resource Program is accredited by the Association for Assessment and Accreditation of Laboratory Animal Care International (AAALAC). The Pennsylvania State University College of Medicine has an Animal Welfare Assurance on file with the National Institutes of Health's Office of Laboratory Animal Welfare; the Assurance Number is A3045-01.

Mice

Adult (6-12 wks of age) female and male C57BL/6 (B6) mice were purchased from the National Cancer Institute (Frederick, MD). Adult female and male B6.129-H2-*Ab1*^{tm1Gru} N12 mice (MHC class II-deficient) were purchased from Taconic Farms (Germantown, NY). Adult female and male C.129S4(B6)-*Ifng*$^{tm3.1Lky}$/J mice (IFN-γ eYFP reporter) were purchased from The Jackson Laboratory (Bar Harbor, ME). Mice were bred and housed in accordance with the guidelines of the NIH Guide for the Care and Use of Laboratory Animals and the Institutional Animal Care and Use Committee at the Penn State College of Medicine.

Viruses and Infections

MuPyV.A2 was prepared in baby mouse kidney cells as described [196]. Mice were infected intracerebrally (i.c.) with $3x10^5$ PFU MuPyV.A2 in 30 µL as described [154]. For rechallenge, mice were inoculated i.c. with $3x10^5$ PFU MuPyV.A2 in 30 µl at day 0, re-inoculated i.c. with $3x10^5$ PFU MuPyV.A2 in 30 µl or vehicle at day 30 p.i., then euthanized 4-5 days later. Recombinant VSV expressing the MuPyV D^bLT359 epitope (VSV.LT359) was grown and titered

on BHK-21 cells (ATCC: CCL-10) [159]. Mice were infected intranasally with $5x10^4$ PFU rVSV-LT359 diluted in PBS.

T Cell Depletion and αVP1 Administration

Mice were injected intraperitoneally (i.p.) with 250 µg rat anti-CD4 or 250 µg rat anti-CD8α (clone GK1.5 clone YTS169.4, respectively; Bio X Cell, West Lebanon, NH) or ChromoPure whole rat IgG (Jackson ImmunoResearch Laboratories, West Grove, PA) as indicated. Depletion was confirmed in peripheral blood by flow cytometry-based cell number assay using Absolute Count Standard (Bangs Laboratories, Fishers, IN). For passive immunization studies, the mice were injected i.p. with 250µg rat anti-VP1 (provided by Robert Garcea, CU Boulder, CO) or Chromopure whole rat IgG beginning at day 10 p.i. and continuing weekly.

T Cell Isolation and Flow Cytometry

Mononuclear cells from brains were isolated from transcardially perfused or intravascularly stained mice by collagenase-DNAse digestion and percoll gradient centrifugation as described [154]. Mononuclear cells were isolated from spleen as described [155]. For intravascular staining, animals were injected i.v. with FITC-conjugated anti-CD45 (clone 30-F11, BD Biosciences) through the tail vein three minutes before the brains were excised as described [197]. After isolation from perfused or intravascularly stained mice, cells were stained with Fixable Viability Dye (eBioscience, San Diego, CA), APC-D^bLT359 tetramers (NIH Tetramer Core Facility, Atlanta, GA), and the following surface antibodies: CD8α (clone 53-6.7, eBioscience), CD44 (clone IM7, eBioscience), PD-1 (clone RMPI-30, Biolegend), Tim-3 (clone RMT3-23, Biolegend), 2B4 (clone m2B4(B6)4581, Biolegend), CD103 (clone M290, BD Horizon), CD69 (clone HI.2F3, Biolegend), CD49d (clone MRF4.8, Biolegend), CD162 (clone 2PH1, BD Biosciences), CD11a (clone 2D7, BD Biosciences), CD127 (clone A7R34, Biolegend), KLRG1 (clone 2F1, BD Biosciences), CD25 (clone PC61.5.3, Invitrogen) and CD4

(clone RM4-5, BD Biosciences). For intracellular staining, cells were permeabilized and fixed in FoxP3 buffer fixation and permeabilization solutions (Thermo Fisher Scientific, Waltham, MA), and stained for T-bet (clone 4B10, Biolegend), eomes (clone Dan11mag, Invitrogen), Ki-67 (clone 2F1, BD Biosciences), and Bcl-2 (clone BCL/10C4). For intracellular cytokine stimulation assays, lymphocytes were isolated from brain and spleen, cultured in DMEM/10% FBS for 5 h at 37ºC with or without 1 µM LT359 peptide [198], stained with Fixable Viability Dye, anti-CD8α, and anti-CD44, then permeabilized and fixed in FoxP3 buffer fixation and permeabilization solutions. Intracellular staining included anti-IFNγ (clone XMG1.2; Biolegend), anti-TNFα (clone XMG1.2; Biolegend), anti-IL-2 (clone JES6-5H4, Biolegend), anti-CD107a (clone 1D4B, BD Biosciences), anti-CD107b (clone ABL-93, BD Biosciences), anti-Granzyme-B (clone GB11, BD Biosciences), and anti-IRF4 (clone IRF4.3E4, Biolegend). CD4 T cells were stained with anti-CD4 and anti-CD44, permeabilized as described, and then stained with FoxP3 (clone FJK-16s, Invitrogen). Lymphocytes isolated from IFN-γ eYFP reporter mice were surface stained with anti-CD8α and anti-CD44. The intracellular signal of YFP was amplified by staining with anti-GFP (clone FM264G, Biolegend). Samples were acquired on a BD LSRFortessa (BD Bioscience, San Jose, CA) or BD LSR II (BD Biosciences, San Jose, CA) and analyzed using FlowJo software (FlowJo, LLC, Ashland, OR).

Anti-VP1 ELISA and Antibody neutralization:

MuPyV major capsid protein VP1-specific ELISA were performed as described [198]. 10-fold serial dilutions of VP1 mAb (provided by Robert Garcea, CU Boulder, CO) was used to obtain a standard curve on each of the 96-well plates, and the VP1-specific IgG concentrations were calculated using this standard. Antibody neutralization assays were conducted in NµMG cells. 10 µg of VP1 mAb (positive control), rat IgG (negative control), or sera diluted 1:10 from MuPyV i.c. infected mice were incubated at 37C for 1 hr with 5 x 10^3 pfu/mL of MuPyV. The mixtures were then placed on 5 x 10^4 adherent NMuMG cells in 12-well plates and incubated at 37C for 1

hr. mRNA was harvested 24 hrs later and subjected to viral large T antigen quantification as previously described [199]. 0% neutralization was determined based on the mean number of LT transcripts observed with MuPyV when incubated with IgG. 100% neutralization is set at the limit of detection for the PCR assay.

Quantitative PCR

For quantifying viral genome DNA copies, Real-Time® PCR was performed on samples containing 10 ng DNA purified from brain and spleen using the Maxwell 16 nucleic acid isolation system (Promega, Madison, WI) as described [200]. For quantifying mRNA transcripts, total RNA was isolated from brain tissue per the manufacturer's instructions. cDNA was prepared using random primers and RevertAid H Minus Reverse Transcriptase Enzyme (ThermoFisher Scientific, Leesport, PA). SYBR green quantitative PCR with gene-specific primers from IDT Technologies (Coralville, IA) for IFN-γ, TGF-β, IL-21 (fwd 5'-CTATGTGTTCTAGGAGAGATGCTG-3', rev 5'-GGAGGAAAGAAACAGAAGCACA-3'), and CXCL9 mRNAs and 18s rRNA was performed on ABI StepOnePlus Real-Time PCR System (ThermoFisher Scientific) using previously published primer sequences [201-204]. Relative fold change over uninfected control mice was determined using the threshold cycle ($2^{-\Delta\Delta Ct}$) method [203]. For detection of VSV gRNA, cDNA was prepared as above and SYBR green qPCR was carried out with primers amplifying VSV gRNA (fwd 5'-ATGTCACTGCAAGGCCTAAGA-3', rev 5'-ATCTCTCCTACCGCCTGATCC). VSV genomes per copy of 18S RNA was determined by $2^{(18S\ CT\ -VSV\ CT)}$. For the stimulation of CD4 T cells, WT mice were inoculated i.c. with MuPyV. At sacrifice, the brains were digested as described [154]. CD4 T cells were purified from total brain homogenates using the EasyStep™ Mouse CD4 Positive Selection Kit II CD4 positive selection kit (Stemcell Technologies, Vancouver, Canada). Purified CD4 T cells were stimulated with PMA (50ng/ml) and Ionomycin (1ug/ml) for 3 hours at 37°C. After stimulation, the cells were lysed in 1 ml of Trizol and cDNA was prepared as described above.

BBB Permeability Assay

100 µl of 100 mg/ml sodium fluorescein dye (Sigma Aldrich, St. Louis, MO) was injected i.p. into mice at day 10 after i.c. inoculation with MuPyV.A2 or at 24 h after LPS administration (100 µg/µl). After 45 min, mice were cheekbled and transcardially perfused with PBS + 10% heparin. A 3 mm section was taken from the cerebrum, then processed as described [128] with fluorescein concentrations calculated using a standard curve.

Immunofluorescence Microscopy

Mice were treated i.p. with 250µg of anti-CD4 or Rat IgG 4 days and 1 day before i.c. inoculation with MuPyV. At day 10 p.i., the mice received 250 µg of anti-CD8α i.p. The mice were sacrificed 15 hours after receiving CD8 T cell depletion. At sacrifice, the mice were perfused with 10mL of 10% heparin in PBS followed by 10mL of 4% paraformaldehyde (PFA). Spleens and brains were postfixed in 4% PFA for 6 hours and then sucrose dehydrated in 30% sucrose. 12µm sections of brain and spleen were taken on a Leica biosystem cryostat (model CM1850, Buffalo Grove, IL). Sections were stained with rabbit anti-CD8A (Sino Biological Inc., Wayne, PA) primary antibody and secondary antibodies goat anti-rabbit (Jackson ImmunoResearch, West Grove, PA) and goat anti-rat (Jackson ImmunoResearch).

RNA-Sequencing and Gene Expression Pathway Analysis

Mononuclear cells were isolated from brains as previously described [154] and pooled from three mice into groups designated WT-CD103^{+}, WT-CD103^{-}, and MHCII$^{-/-}$-CD103^{-}. The cells were stained with DAPI (Sigma Aldrich, Germany), CD44, CD8, APC-D^{b}LT359 tetramer, and CD103 and then sorted on a BD FACS Aria SORP-high performance cell sorter. The collected cells were lysed with 1% IGEPAL CA-630 (Sigma-Aldrich) and immediately frozen on dry ice for storage at -80°C until further processing. The cDNA libraries were prepared using the SMARTer

Ultra Low Input RNA Kit for Sequencing – v4 (TAKARA Bio, CA) and Nextera XT DNA Library Prep Kit (Illumina, CA) as per the manufacturer's instructions. The unique barcode sequences were incorporated in the adaptors for multiplexed high-throughput sequencing. The final product was assessed for its size distribution and concentration using BioAnalyzer High Sensitivity DNA Kit (Agilent Technologies, CA). The libraries were pooled and diluted to 2 nM in EB buffer (Qiagen, MD) and then denatured using the Illumina protocol. The denatured libraries were diluted to 10 pM by pre-chilled hybridization buffer and loaded onto HiSeq SR Rapid v2 flow cells on an Illumina HiSeq 2500 (Illumina, San Diego, CA) and run for 64 cycles using a single-read recipe (HiSeq Rapid SBS Kit v2, Illumina) according to the manufacturer's instructions. Illumina CASAVA pipeline (released version 1.8, Illumina) was used to obtain de-multiplexed sequencing reads (fastq files) passed the default purify filter. Reads were mapped to the mm10 transcriptome with STAR [205] and gene-level quantification performed with RSEM [206]. Differential tests were performed in DESeq2 using the SARTools pipeline [207]. The list of differentially upregulated and downregulated genes with FDR < .05 was imported to Ingenuity Pathway Analysis software (Qiagen, Hilden, Germany) for pathway enrichment analysis using Ingenuity Knowledge Base (IKB) as the reference set. All analysis was done using the software contextual analysis settings for mouse CD8 T cells. The enrichment significance by *P*-value between the gene list and the canonical pathway analysis was measured by Fisher's exact test. The enrichment factor is the ratio of the number of genes in a given pathway divided by the total number of genes in the pathway.

Statistical Analysis

Experimental data were analyzed on Prism 6.07 (GraphPad, La Jolla, CA) using Mann-Whitney *t*-test, one-way ANOVA, and two-way ANOVA with Tukey or Sidak’s multiple comparisons test. Error bars indicate mean $\pm$ SD. All experiments were replicated independently.

2.5 Figures and table

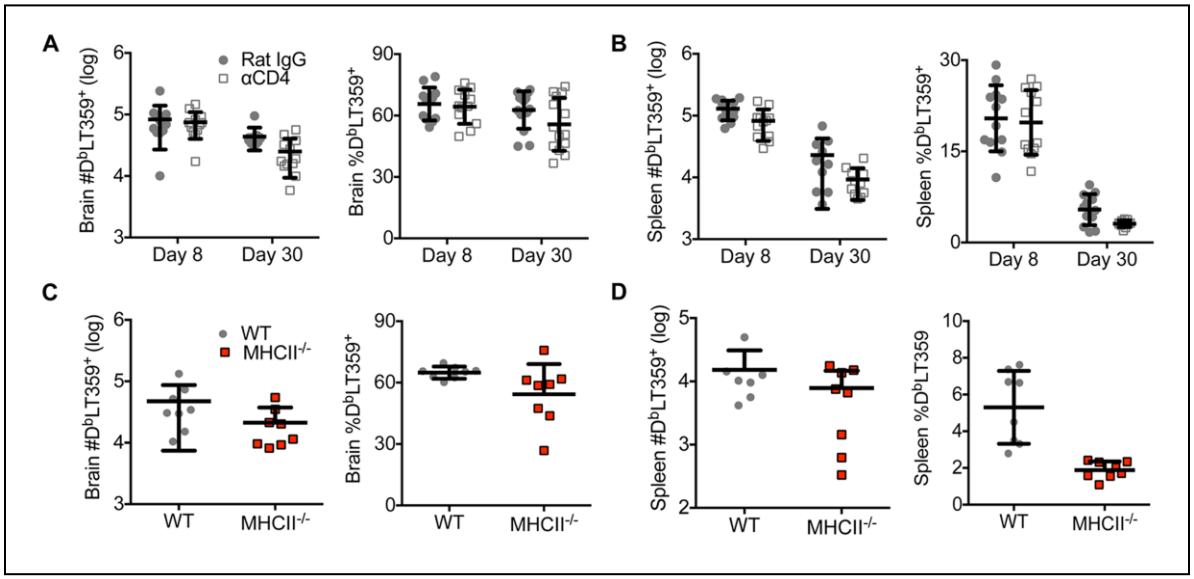

Fig 2-1: Brain and spleen MuPyV-specific CD8 T cell responses in CD4 T cell-sufficient and--deficient mice. (A, B) Number (left) and frequency (right) of $CD8^+$ $CD44^{hi}$ D^bLT359 $tetramer^+$ in brain (A) and spleen (B) during acute (day 8 p.i.) and persistent (day 30 p.i.). **(C, D)** Number (left) and frequency (right) of $CD8^+$ $CD44^{hi}$ D^bLT359 $tetramer^+$ in brain (A) and spleen (B) during persistent (day 30 p.i.) infection in WT and $MHCII^{-/-}$ mice. Mean ± SD of 7-10 mice per group from 2 independent experiments.

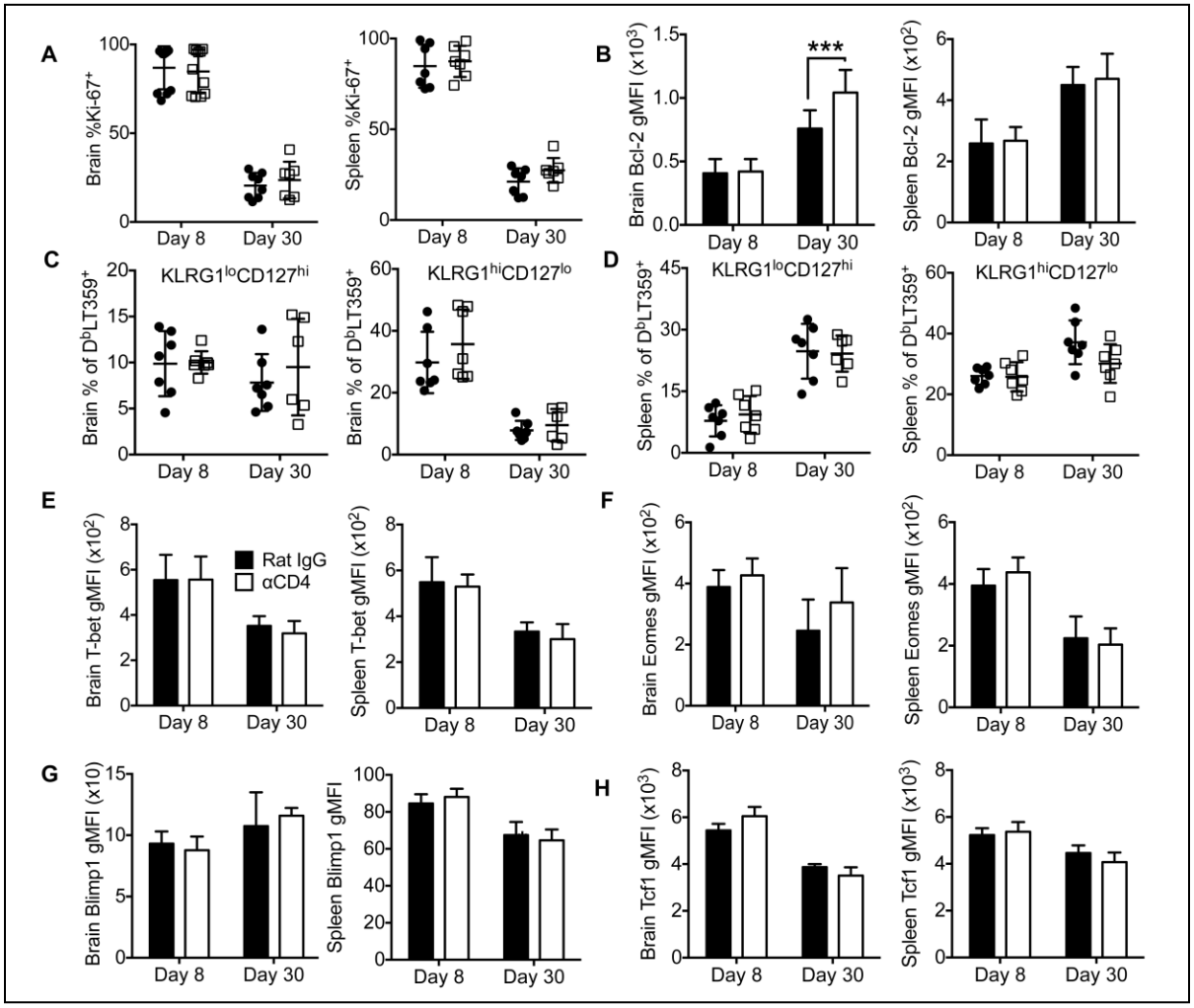

Fig 2-2: Characterization of helped and unhelped virus-specific CD8 T cells . (A) Frequency of Ki-67$^+$ D^{b}LT359 tetramer$^+$ CD8 T cells from brains (left) and spleens (right) at days 8 and 30 p.i. **(B)** gMFI of Bcl-2 on D^{b}LT359 tetramer$^+$ CD8 T cells from brains (left) and spleens (right). **(C, D)** Frequency of KLRG1^{lo}CD127^{hi} (left) or KLRG1^{hi}CD127^{lo} (right) D^{b}LT359 tetramer$^+$ CD8 T cells from brains (C) and spleens (D). **(E-H)** gMFI of T-bet (E), eomes (F), blimp-1 (G), and Tcf1 (H) in brain (left) and spleen (right) D^{b}LT359 tetramer$^+$ CD8 T cells at days 8 and 30 p.i. Mean $\pm$ SD of 7-12 mice per group from two-three independent experiments (A-F) and of 3-4 mice from one independent experiment (G,H). ****P*<0.001, two-way ANOVA with Sidak's multiple comparisons test (A-H)

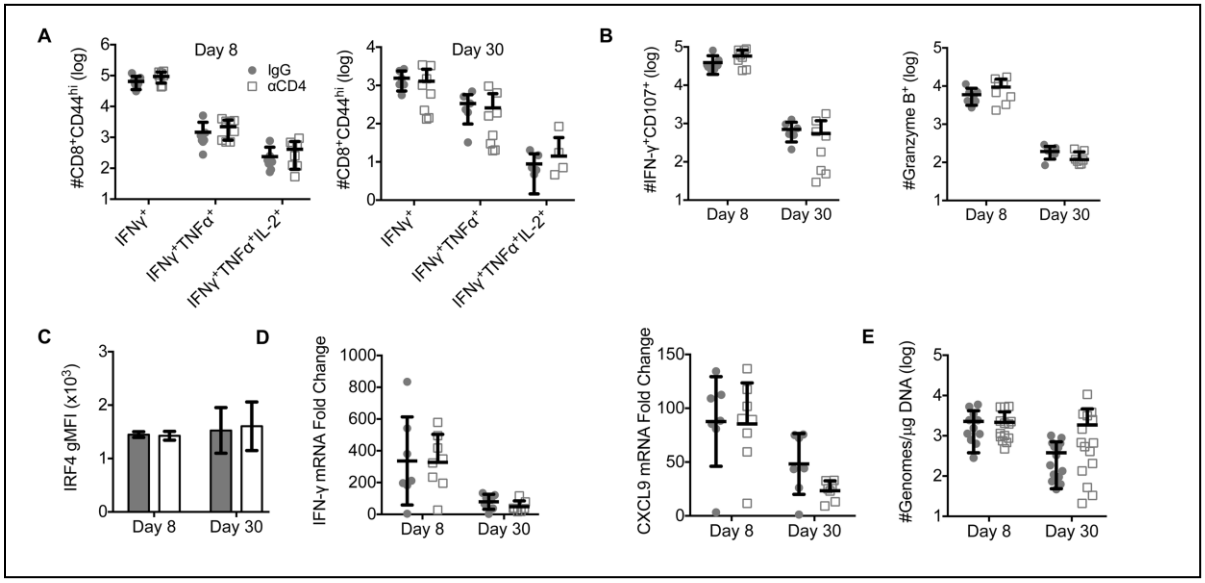

Fig 2-3: Unhelped virus-specific CD8 T cells in the brain remain functional. (A) Number of IFNγ$^+$, IFNγ$^+$ TNFα$^+$, and IFNγ$^+$TNFα$^+$ IL-2$^+$ CD44^{hi} CD8 T cells from brains at days 8 (left) and 30 (right) p.i. following *ex vivo* stimulation with LT359 peptide. **(B)** Number of IFNγ$^+$ CD107$^+$ (left) and Granzyme-B$^+$ CD44^{hi} CD8 T cells from brain at days 8 and 30 p.i. There was a significant decrease in the number of IFNγ$^+$ CD107$^+$ (P<0.0001) and Granzyme-B$^+$ (P<0.0001) between days 8 and 30 p.i. **(C)** Ex vivo staining for IRF4 in helped and unhelped D^{b}LT359 tetramer$^+$ CD8 T cells isolated from brain. **(D)** Quantitative PCR analysis for fold change of IFNγ (left) and CXCL9 (right) mRNA compared to housekeeping gene 18s rRNA at days 8 and 30 p.i. There was a significant decrease in IFNγ (P=0.0002) and CXCL9 (P=0.0003) mRNA between days 8 and 30 p.i. **(E)** Real-Time® PCR analysis of viral genome copies from brains at days 8 and 30 p.i. Mean ± SD of 7-10 mice per group from 2 independent experiments (A-D) or 13-15 mice per group from 3 independent experiments (E), two-way ANOVA with Tukey's multiple comparisons test (A-E)

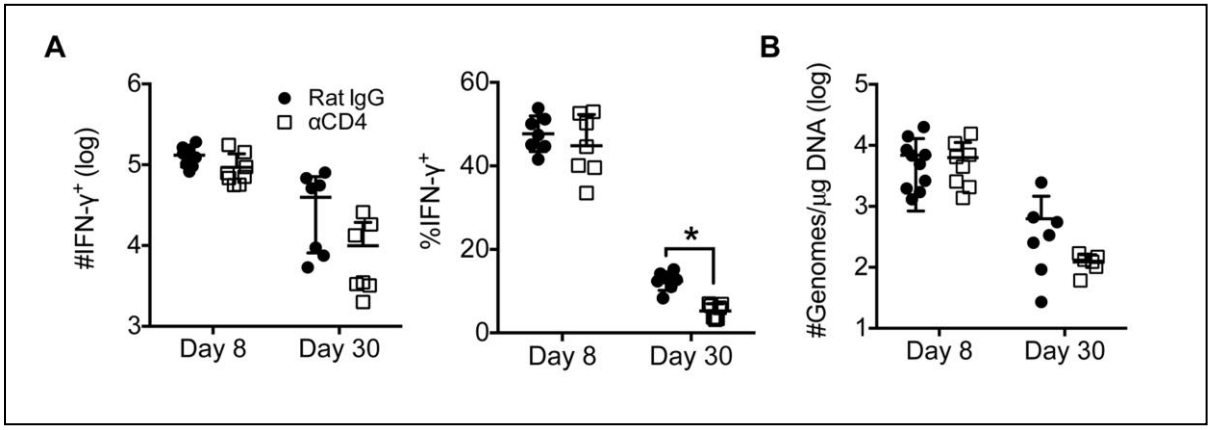

Fig 2-4: Unhelped splenic MuPyV-specific CD8 T cells have reduced function. (A) Number (left) and frequency (right) of IFNγ^{+} CD44^{hi} CD8 T cells from spleens at days 8 and 30 p.i. following *ex vivo* stimulation with LT359 peptide. **(B)** Quantitative PCR analysis of viral genome copies from spleen at days 8 and 30 p.i. (A & B) Mean ± SD of 6-10 mice per group from two independent experiments. *P<0.05, two-way ANOVA with Sidak's multiple comparisons test.

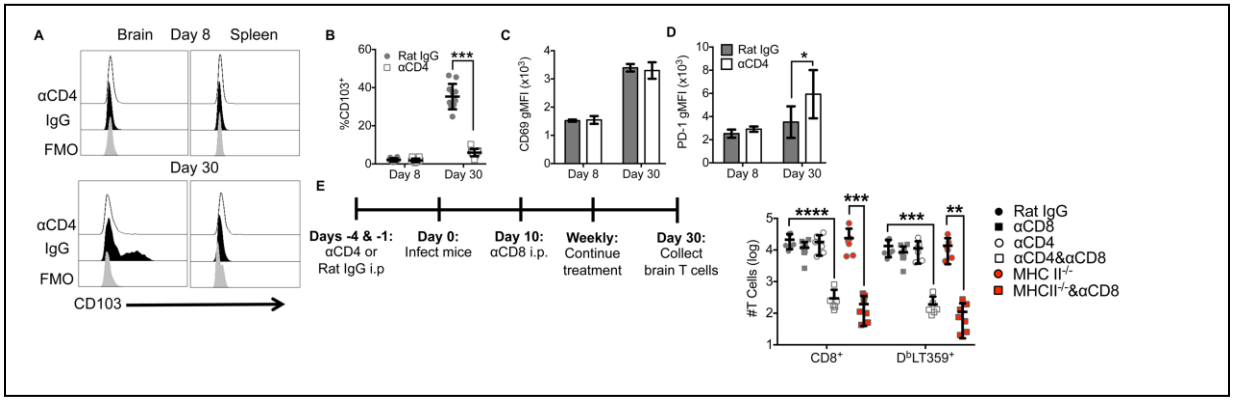

Fig 2-5: Unhelped MuPyV-specific CD8 T cells in the brain are not maintained upon systemic CD8 T cell depletion. (A) Representative histogram of $CD103^+$ and $CD103^-$ D^bLT359 tetramer$^+$ CD8 T cells from brain and spleen at days 8 and 30 p.i. **(B)** Frequency of $CD103^+$ D^bLT359 tetramer$^+$ CD8 T cells from brain at days 8 and 30 p.i. **(C, D)** CD69 (C) and PD-1 (D) gMFI on D^bLT359 tetramer$^+$ CD8 T cells from brain at days 8 and 30 p.i. **(E)** Experimental design, and number of total CD8 T cells and D^bLT359 tetramer$^+$ CD8 T cells from brains at day 30 p.i. Mean ± SD of 8-12 mice per group from 3 independent experiments (A-D) or 6-10 mice per group from 3 independent experiments (E & F). *$P \leq 0.05$, **$P \leq 0.01$, ***$P \leq 0.001$, ****$P \leq 0.0001$, two-way ANOVA with Tukey multiple comparisons test

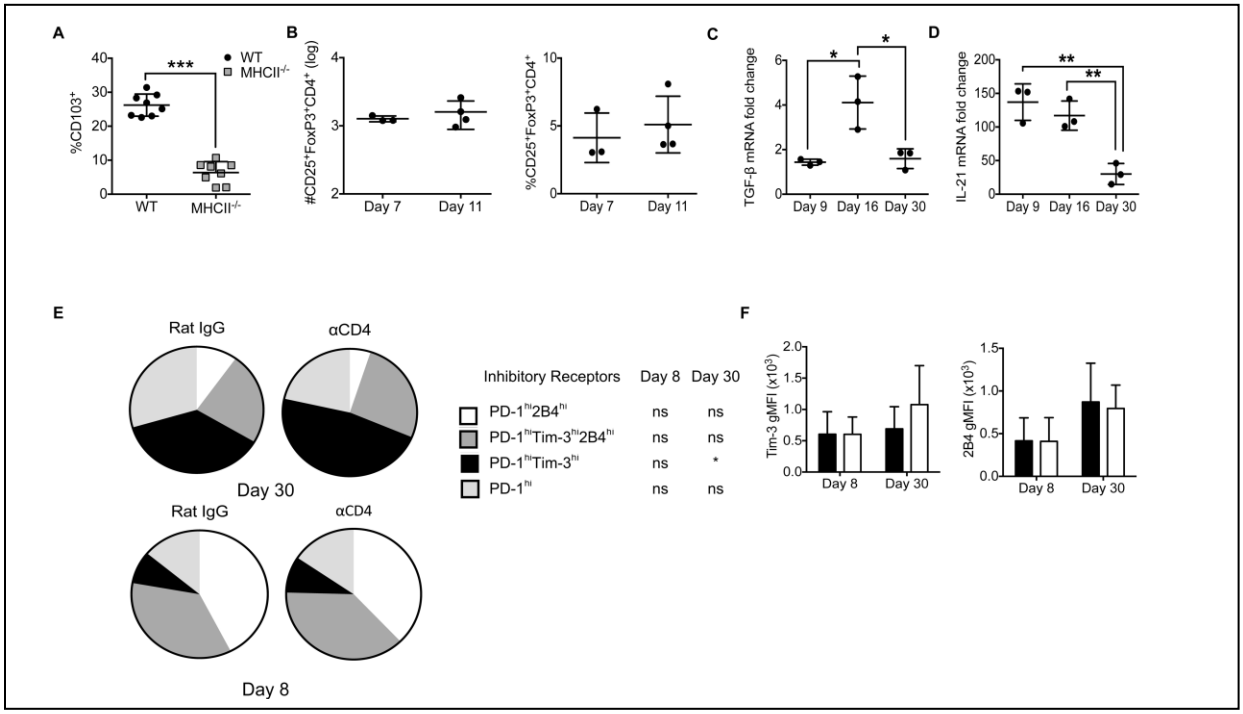

Fig 2-6: bT_{RM} development is impaired in MHCII$^{-/-}$ mice and unhelped CD8 T cells have increased expression of inhibitory receptors. (A) Frequency of CD103^{+} D^{b}LT359 tetramer^{+} CD8 T cells from brain. **(B)** Number (left) and frequency (right) of FoxP3^{+}CD25^{+} CD4 T cells at days 7 and 11 p.i. **(C,D)** TGFβ (C) and IL-21 (D) mRNA from CD4 T cells isolated from brain and stimulated with PMA/ionomycin. **(E)** Coexpression of Tim-3 and 2B4 on PD-1^{hi} D^{b}LT359 tetramer^{+} CD8 T cells at days 30 (top) and 8 (bottom) p.i. **(F)** gMFI of PD-1, Tim-3, and 2B4 on brain D^{b}LT359 tetramer^{+} CD8 T cells at days 8 and 30 p.i. Mean ± SD of 6-8 mice per group from two independent experiments (A, E, F) or 3-4 mice from one experiment (B-D). *P<0.05, ***P<0.001, one-way ANOVA (A-D), unpaired Student's t-test with Welch's correction (E-F)

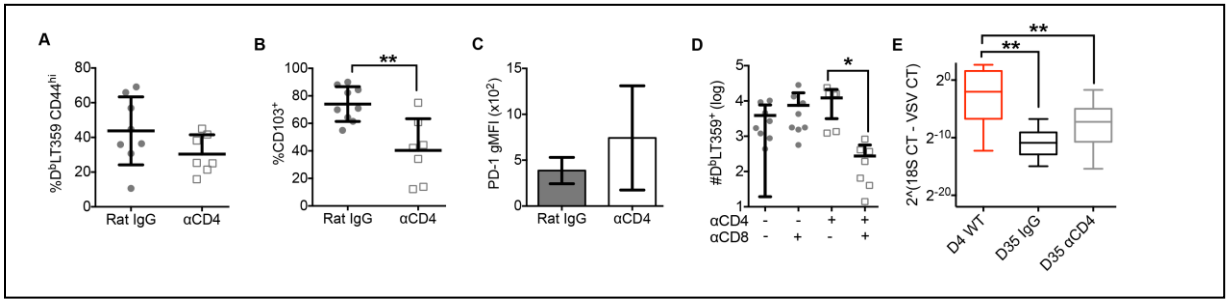

Fig 2-7: CD4 T cell help is essential for the development of CD8 bT$_{RM}$ in response to VSV infection. (A) Frequency of D^{b}LT359 tetramer$^+$ CD8 T cells from brains 30 days post-VSV infection. **(B)** Frequency of CD103$^+$ D^{b}LT359 tetramer$^+$ CD8 T cells from brains 30 days post-VSV infection. **(C)** gMFI of PD-1 expression on D^{b}LT359 tetramer$^+$ CD8 T cells. **(D)** Number of D^{b}LT359 tetramer$^+$ CD8 T cells from brains 30 days post-VSV infection. (**E**) Quantitative PCR analysis of VSV gRNA from brain at day 4 (control) or day 35 p.i. Mean ± SD of 3-4 mice per group from 2 independent experiments. *$P \leq 0.05$, **$P \leq 0.01$, Mann-Whitney *t*-test (A-C) and one-way ANOVA (D)

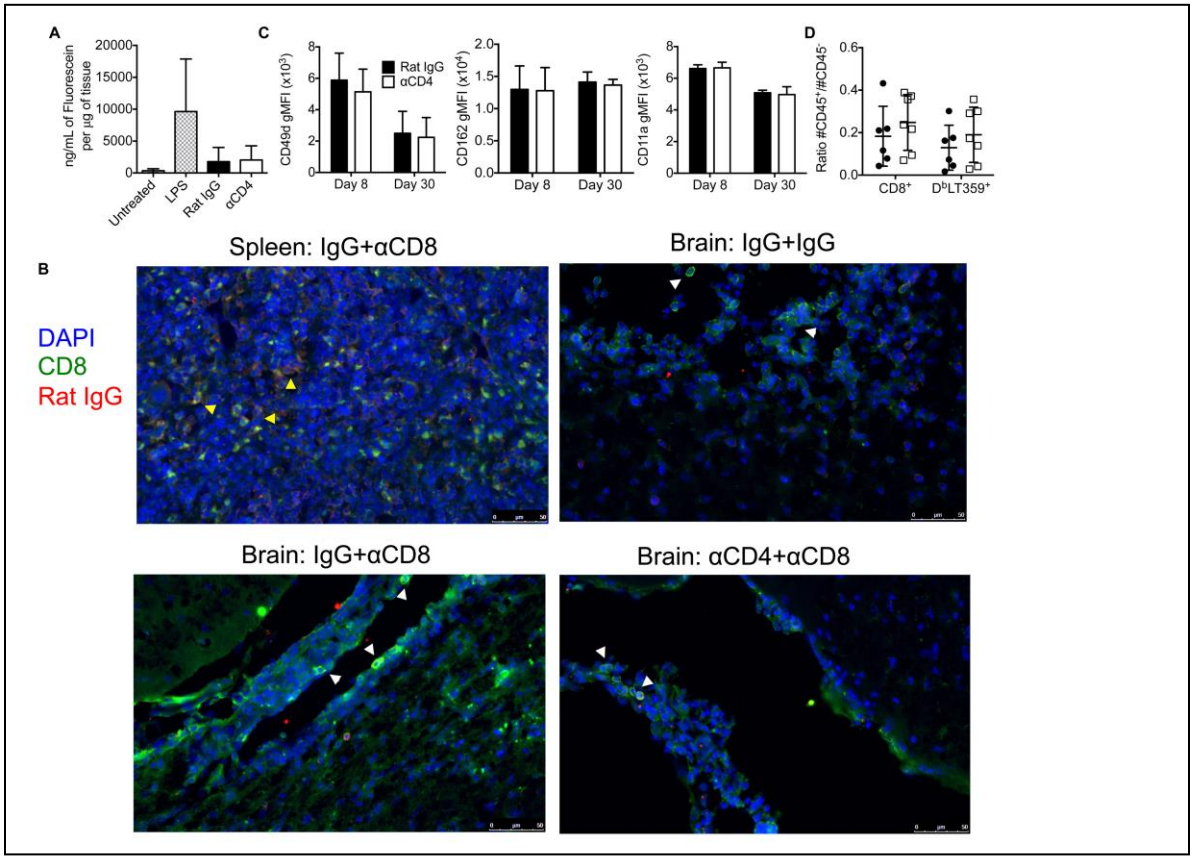

Fig 2-8: CD4 T cell depletion does not change BBB permeability, adhesion molecule expression on CD8 T cells, or extravascular location of brain CD8 T cells. (A) BBB permeability was measured 10 days p.i. by the accumulation of sodium fluorescein dye in the brain. **(B)** The ability of CD8 T cell depleting rat mAb given at day 10 p.i. to access spleen and brain CD8 T cells in CD4 T cell-depleted and rat IgG control-treated mice was analyzed the next day by examining colocalization of rat IgG and anti-CD8 in these organs. White arrows indicate CD8 T cells and yellow arrows CD8 T cells that were stained with both CD8 and rat IgG. **(C)** gMFI of CD49d (left), CD162 (middle), and CD11a (right) on helped and unhelped D^bLT359 tetramer$^+$ cells from blood. **(D)** Ratio of CD45$^+$ (intravascular)/CD45$^-$ (extravascular) total CD8 T cells and D^bLT359 tetramer$^+$ CD8 T cells from brain. Mean $\pm$ SD of 3-8 mice per group from two independent experiments.

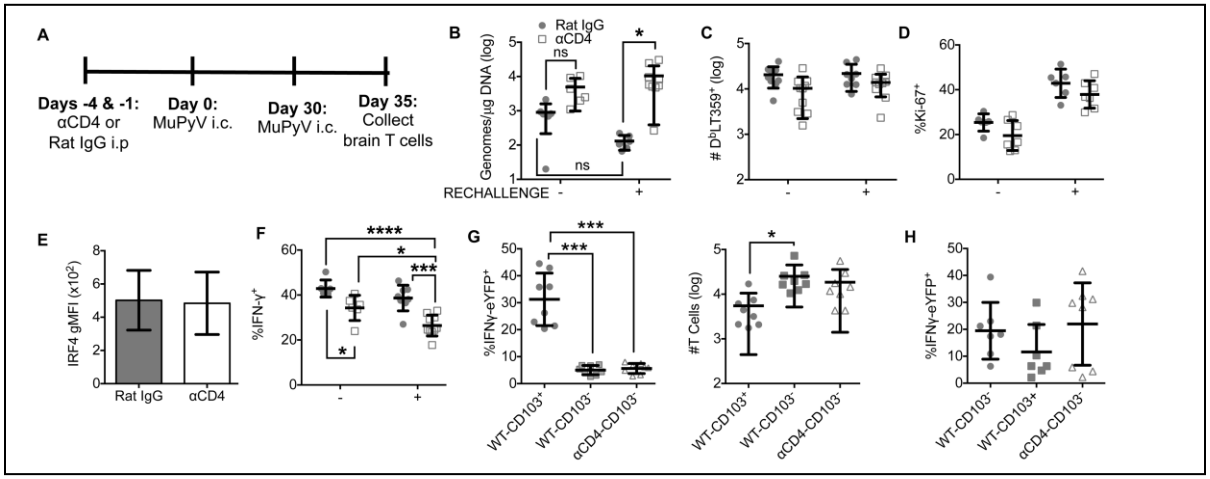

Fig 2-9: Reduced effector activity of unhelped CD8 T cells in the brain upon reinfection.

(A) Experimental design. **(B)** Real-Time® PCR analysis of viral genome copies from brain. **(C)** Number of D^bLT359 tetramer$^+$ CD8 T cells from brain. **(D)** Frequency of Ki-67$^+$$D^bLT359$ tetramer$^+$ cells from the brain. **(E)** *Ex vivo* staining for IRF4 in D^bLT359 tetramer$^+$ CD8 T cells. **(F)** Frequency of IFNγ$^+$CD44^{hi} CD8 T cells from brain following *ex vivo* stimulation with LT359 peptide. **(G)** Frequency (left) of IFNγ-eYFP$^+$ cells and number (right) of D^bLT359 tetramer$^+$ WT-CD103$^+$, WT-CD103$^-$ cells, and αCD4-CD103$^-$ cells from the brains of IFNγ-eYFP mice at day 5 post reinfection. **(H)** Frequency of IFNγ-eYFP$^+$ cells 30 days p.i. Mean ± SD of 9-10 mice per group from 3 independent experiments (A-F) or 8 mice per group from two independent experiments (G, H). ns = not significant, *$P \leq 0.05$, ***$P \leq 0.001$, Two-Way ANOVA with Tukey multiple comparisons test (B-F) and one-way ANOVA (G,H).

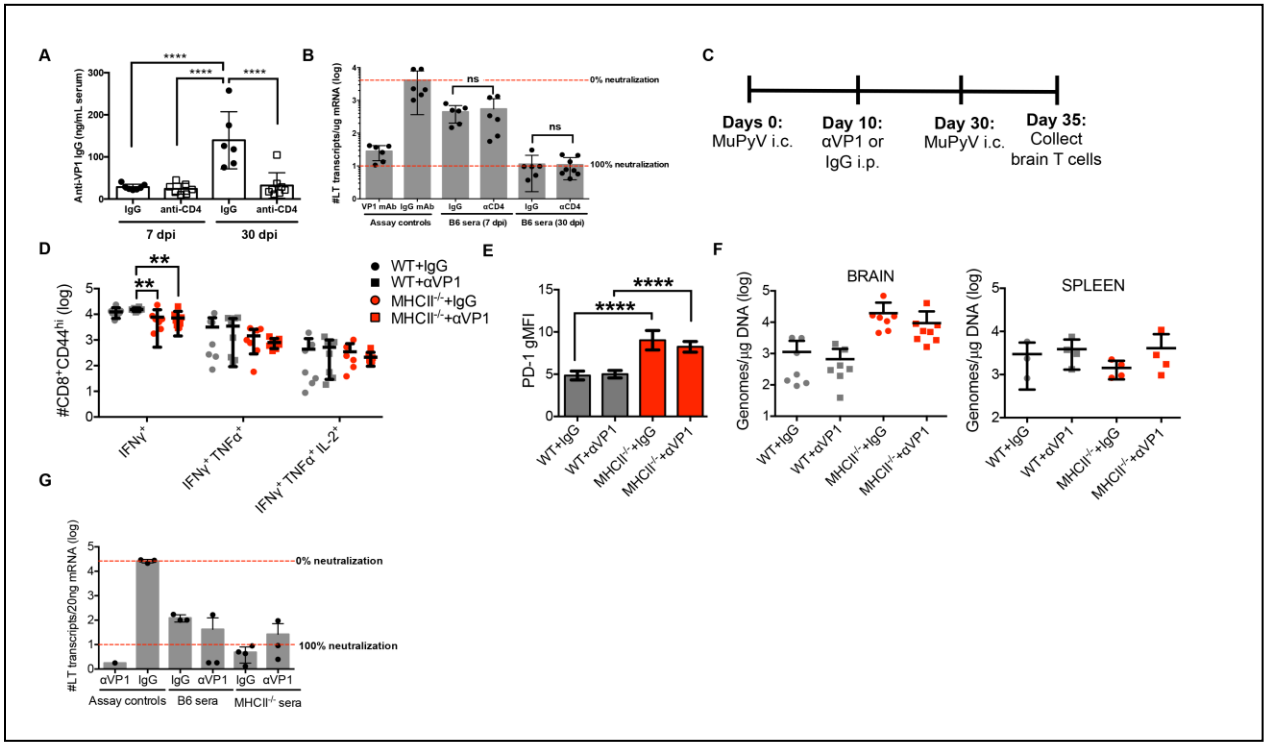

Fig 2-10: Unhelped CD8 T cell functionality upon reinfection is independent of neutralizing antibodies. (A) Anti-VP1 IgG levels in serum at days 7 and 30 p.i. **(B)** Neutralization assay of antibodies from serum at days 7 and 30 p.i. Assay controls indicate cells treated with only IgG or VP1 mAb. **(C)** Experimental design. **(D)** Frequency of IFNγ^{+}, IFNγ^{+} TNFα^{+}, and IFNγ^{+} TNFα^{+} IL-2^{+} CD44^{hi} CD8 T cells from brains 5 days post rechallenge stimulated ex vivo with LT359 peptide. **(E)** PD-1 gMFI on D^{b}LT359^{+} CD8 T cells. **(F)** Real-Time® PCR analysis of viral genome copies from brain five days post rechallenge. Mean + SD of 7-8 mice per group from two independent experiments (A-B) or 4 mice per group from one experiment (C-E). **(G)** LT mRNA assay showing neutralization capacity of serum from WT and MHCII$^{-/-}$ mice at 5 days after i.c. rechallenge with MuPyV. Assay controls indicate cells treated with only IgG or VP1 mAb.ns = not significant, *$P \leq 0.05$, ****$P \leq 0.001$, two-way ANOVA with Tukey multiple comparisons test (D) and one-way ANOVA (E)

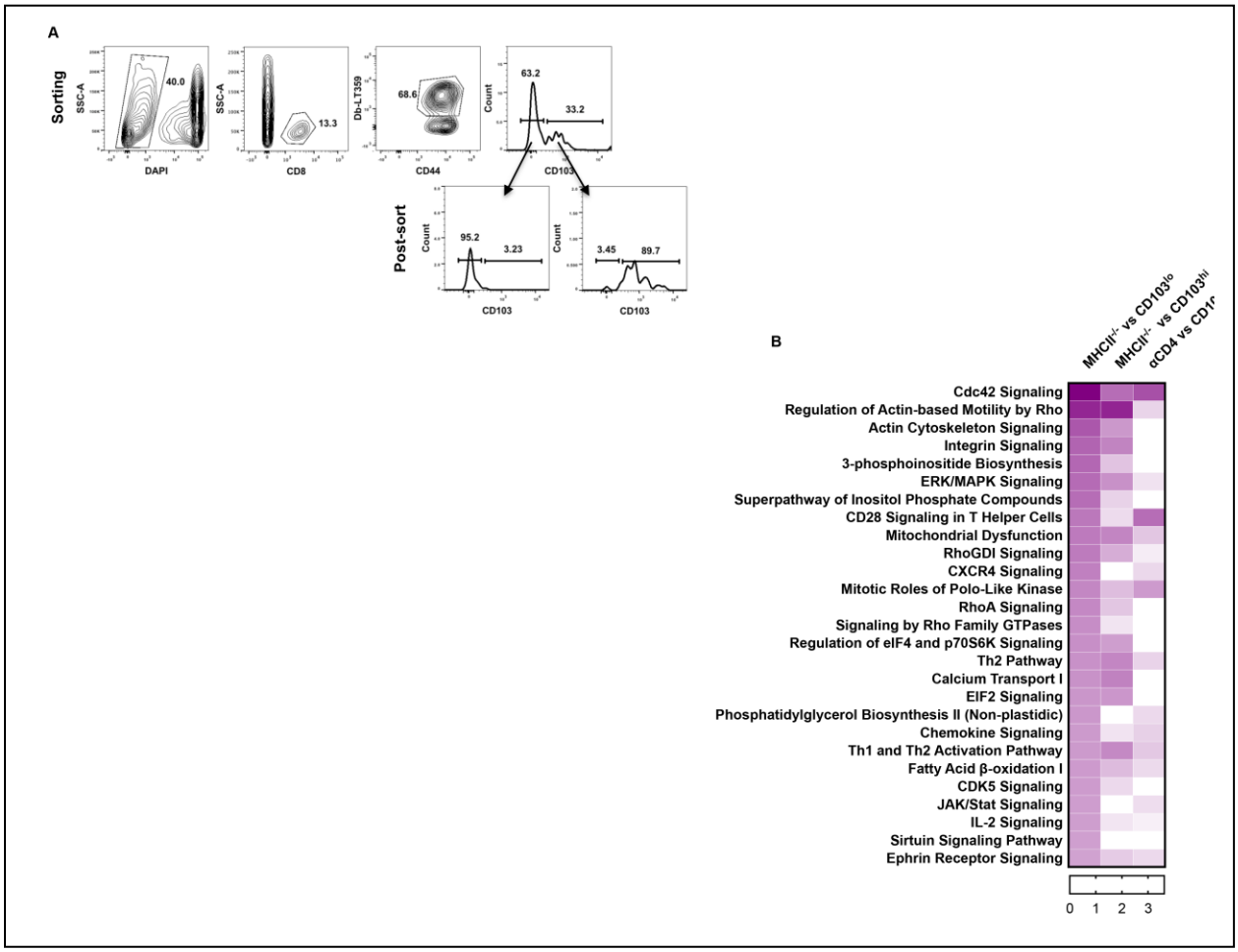

Fig 2-11: FACS-sorting strategy for CD103$^-$, CD103$^+$ and MHCII$^{-/-}$-CD103$^-$. (A) Mononuclear cells harvested from brains of B6 and MHCII$^{-/-}$ mice at day 30 after i.c. inoculation with MuPyV were stained with D^{b}LT359 tetramers, CD8, CD44, and CD103. **(B)** Heat map representing the differentially expressed pathways from the Ingenuity pathway analysis between MHCII$^{-/-}$-CD103$^-$ and CD103$^-$ and MHCII$^{-/-}$-CD103$^-$ and CD103$^+$.

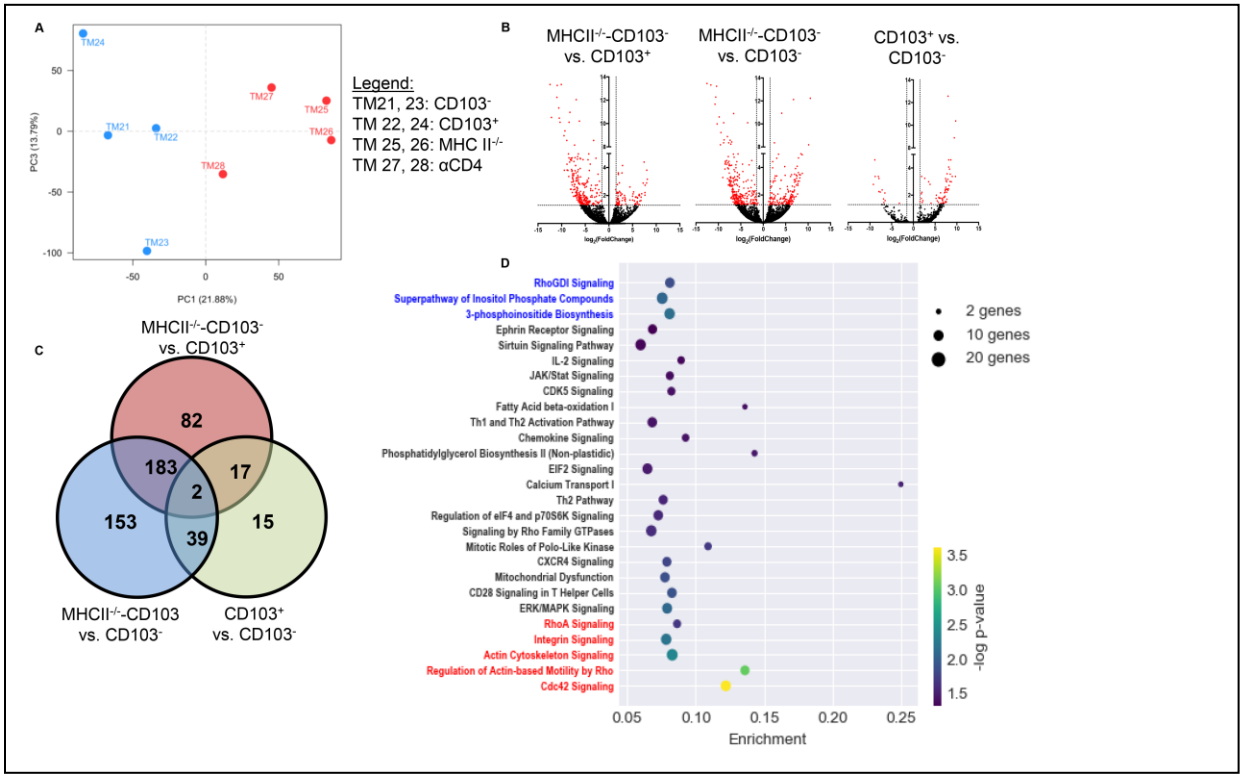

Fig 2-12: Helped and unhelped MuPyV-specific CD8 T cells in the brain have distinct transcriptional profiles. (A) Principal component analysis plot. **(B)** Volcano plot representation of differential expression analysis of transcripts of MHCII$^{-/-}$ vs WT-CD103^{+} (left) MHCII$^{-/-}$ vs CD103^{-} (middle), and CD103^{+} vs CD103^{-} (right). Red represents differentially expressed transcripts over the cut-off of a q-value $\leq$ 0.05 and the X-axis represents the fold change. **(C)** Venn diagram showing the number of differentially expressed genes in MHCII$^{-/-}$-CD103^{-} vs CD103^{+} (top), MHCII$^{-/-}$-CD103^{-} vs CD103^{-} (left bottom), and CD103^{+} vs CD103^{-} (right bottom). **(D)** Ingenuity pathway analysis of differentially expressed transcripts between MHCII$^{-/-}$-CD103^{-} and CD103^{-}. Y-axis represents pathway and X-axis represents enrichment factor. Bubble size represents the number of differentially expressed transcripts and color represents the *P*-value calculated by Fisher's Exact test. Blue labels indicate upregulated pathways and red labels indicate downregulated pathways with a cut-off z score $\leq$ 2.0.

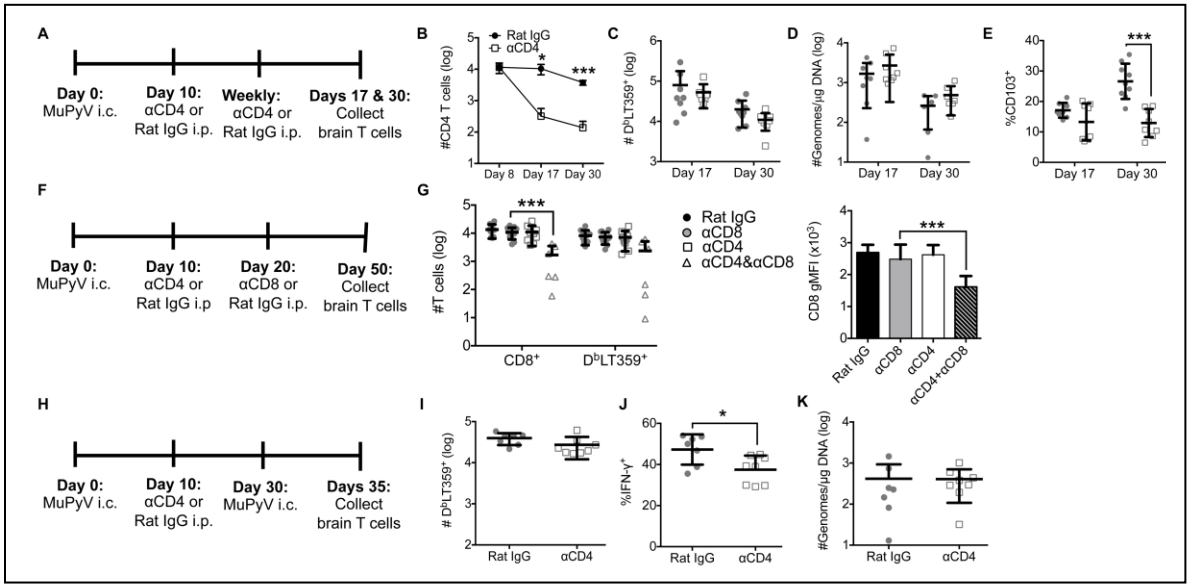

Fig 2-13: Delayed systemic CD4 T cell depletion affects bT_{RM} differentiation/maintenance. **(A)** Experimental design. **(B)** Number of CD4 T cells in brain. **(C)** Number of virus-specific CD8 T cells from brain at 17 and 30 days p.i. **(D)** Real-Time® PCR analysis of viral genome copies from brain. **(E)** Frequency of $CD103^+$ D^bLT359-specific CD8 T cells in brain at days 17 and 30 p.i. There was a significant increase in $CD103^+$ CD8 T cells (p=0.0132) in Rat IgG-treated mice between days 8 and 30 p.i. **(F)** Experimental design. **(G)** Number of total and virus-specific CD8 T cells (left) and gMFI of CD8 on D^bLT359 $tetramer^+$ CD8 T cells (right) in brain upon systemic depletion of CD4 and/or CD8 T cells. **(H)** Experimental design. **(I)** Number of D^bLT359 $tetramer^+$ CD8 T cells from brain. **(J)** Frequency of $IFN\gamma^+CD44^{hi}$ CD8 T cells from brain upon *ex vivo* stimulation with LT359 peptide. **(K)** Real-Time® PCR analysis of viral genome copies from brain. Mean ± SD of 8 mice per group from two independent experiments. *$P \leq 0.05$, ***$P \leq 0.001$, two-way ANOVA with Sidak's multiple comparisons test (B-E,G), one-way ANOVA (G), and Mann-Whitney test (I-K).

Pathway name	-log(p-value)	%↑	%↓	Gene List
Cdc42 signaling	3.62	6	7	CD3G, FOS, JUN, PPP1R12A, ARPC2, PAK2, EXOC2, HLA-DOB, ARPC3, MYL12B, MYL12A
Regulation of Actin motility by Rho	3.07	2	12	RAC2, PFN1, PPP1R12A, ARPC2, PAK2, ARPC3, MYL12B, MYL12A
Actin Cytoskeleton Signaling	2.38	3	6	RAC2, PFN1, PPP1R12A, GNA12, ARPC2, PAK2, TRIO, ARPC3, TLN1, MAP2K1, MYL12B, MYL12A
Integrin Signaling	2.20	2	6	RAC2, CAPNS1, PFN1, PPP1R12A, ARPC2, PAK2, ITGA6, ARPC3, TLN1, MAP2K1, MYL12B, MYL12A
3-phosphoinositide Biosynthesis	2.15	6	2	PTPN6, PPP1R12C, SYNJ1, PTPN2, PPP1R12A, DUSP1, PPP1R13B, ICOS, MTMR2, PPP2R5E, DUSP2
ERK/MAPK signaling	2.09	4	4	RAC2, FOS, PPP1R12A, PPP2CA, DUSP1, PAK2, TLN1, PPP2R5E, MAP2K1, DUSP2, EIF4EBP1
Superpathway of inositol phosphate compounds	2.07	6	2	PTPN6, PPP1R12C, SYNJ1, PTPN2, PPP1R12A, DUSP1, PPP1R13B, ICOS, MTMR2, PPP2R5E, DUSP2, PPIP5K2
CD28 signaling in T helper cells	1.91	6	3	CD3G, FOS, PTPN6, JUN, ARPC2, HLA-DOB, ARPC3, MALT1, MAP2K1
Mitochondrial Dysfunction	1.88	1	7	HSD17B10, SDHB, NDUFS8, NDUFB7, ATPAF1, NDUFB8, GPX4, AIFM1, APP, PINK1
RhoGDI Signaling	1.86	3	5	PPP1R12C, PPP1R12A, GNA12, ARPC2, PAK2, ARPC3, ARHGDIB, MYL12B, MYL12A
CXCR4 Signaling	1.79	5	3	FOS, JUN, EGR1, GNA12, PAK2, LYN, MAP2K1, MYL12B, MYL12A
Mitotic Roles of Polo-like Kinase	1.70	4	7	HSP90AB1, PPP2CA, PLK3, PPP2R5E, RAD21
RhoA Signaling	1.68	2	6	PFN1, PPP1R12A, GNA12, ARPC2, ARPC3, MYL12B, MYL12A
Signaling by Rho Family GTPases	1.61	4	3	FOS, PPP1R12C, JUN, PPP1R12A, GNA12, ARPC2, PAK2, ARPC3, MAP2K1, MYL12B, MYL12A
Regulation of eIF4 and p70S6K Signaling	1.58	4	3	PPP2CA, RPS23, RPS21, EIF4A2, RPS15A, EIF2S3, PPP2R5E, MAP2K1, EIF4EBP1
Th2 Pathway	1.56	3	5	RUNX3, CD3G, IL2RG, JUN, MAF, ICOS, CXCR6, HLA-DOB
Calcium Transport I	1.54	0	25	ANXA5, ATP2B4

EIF2 Signaling	1.49	5	2	RPL22, RPL18A, RPS23, RPL39, RPL26, RPS21, EIF4A2, RPS15A, EIF2S3, MAP2K1, RPLP0
Phosphatidylglycerol Biosynthesis II (Non-plastidic)	1.47	10	5	AGPAT5, GPAT4, MBOAT7
Chemokine Signaling	1.43	7	2	FOS, JUN, PPP1R12A, CCL5, MAP2K1
Th1 and Th2 Activation Pathway	1.43	3	4	RUNX3, CD3G, IL2RG, JUN, MAF, IL6R, ICOS, CXCR6, HLA-DOB
Fatty Acid β^2-oxidation	1.42	0	14	HSD17B10, ECHS1, SCP2
CDK5 Signaling	1.41	5	3	PPP1R12A, PPP2CA, EGR1, ITGA6, PPP2R5E, MAP2K1
JAK/STAT Signaling	1.39	7	1	FOS, PTPN6, JUN, PIAS1, SOCS4, MAP2K1
IL-2 Signaling	1.37	5	4	FOS, IL2RG, JUN, CSNK2B, MAP2K1
Sirtuin Signaling Pathway	1.36	1	4	TIMM8A, POLR2F, SDHB, GADD45B, JUN, NDUFS8, NDUFB7, NDUFB8, H1F0, LDHA, ABCA1, APP
Ephrin Receptor Signaling	1.32	2	5	RAC2, RGS3, GNA12, ARPC2, PAK2, SH2D3C, ARPC3, MAP2K1

Table 2-1: Differentially expressed genes from pathways indicated by Ingenuity pathway analysis. Table indicating the –log (p-value), frequency of upregulated (indicated %↑) transcripts, frequency of downregulated (labeled as %↓) transcripts, and list of transcripts differentially expressed in each pathway.

Chapter 3: STAT1 mediates neuroinflammation during persistent MuPyV-encephalitis

Abstract

JCPyV causes the devastating brain-demyelinating disease PML in individuals with immunosuppression from HIV/AIDS, immunomodulatory therapies for the treatment of autoimmune disease, or hematological malignancies. No effective anti-JCPyV therapies are available, and the understanding of risk factors predisposing patients to PML development is limited. Type I, II, and III IFNs mediate antiviral defense at the level of the immune system and the infected cell in many organs, including the brain. We have previously published that type I and II IFNs contribute to viral control in the periphery, but their efficacy in the brain remains unknown. In this study, we provide evidence that type I IFNs mediate viral control during acute brain infection, but no single IFN contributed substantially to viral control during persistent MuPyV infection. However, mice deficient in STAT1, the common downstream effector of the IFN receptor family, developed severe hydrocephalus and had an increased infiltration of immune cells into the brain. We further found that STAT1-mediated protection occurs at the level of the immune system and the infected cell as deficiencies in STAT1 in infected cells slightly worsened MuPyV-induced hydrocephalus. Together, these findings demonstrate that STAT1 is a critical component of the antiviral defense against MuPyV infection.

3.1 Introduction

IFNs exhibit a range of antiviral activity both directly, through the induction of an antiviral state in the infected cell, and indirectly, through modulation of immune cells by activating innate immune cells and upregulating MHC complexes on APCs [110, 208-210]. IFNs can be classified into three types: type I, II, and III IFNs. Type I IFNs, consisting of IFN -α, -β, -ω, -ε, and -κ, signal through the heterodimeric IFN-α/β receptor (IFNAR) complex [211]. Nearly all cell types are capable of producing and responding to type I IFNs, including neurons, astrocytes, microglia, and oligodendrocytes [92]. In contrast, IFNγ, the sole member of the type II family of IFNs, signals through the IFNγR [212]. IFNγ production is restricted to immune cells such as T cells, NK cells, and NKT cells [93]. The recently defined type III IFNs, consisting of IFN -λ1, -λ2, -λ3, and -λ4, signal through the heterodimeric IFNLR [213, 214]. Type III production is restricted to cells of epithelial and endothelial lineage [105]. Although the members of the IFN family signal through disparate receptors, nearly all downstream activities are mediated by activation of the JAK/STAT signaling pathway [93]. The unique receptor expression of and responsiveness to the IFN family defines cell-intrinsic immune programs, allows tissue-specific responses to pathogens, and overall fine tunes the immune response.

The activation of JAK/STAT pathways requires binding of IFN to its receptor. Once the receptor is bound, the JAK kinases and STAT family members are phosphorylated and activated [93]. STAT1 is considered to be the canonical IFN signaling molecule because all members of the IFN family signal through STAT1, but IFN signaling does involve other members of the STAT family, such as STAT2. It is worth noting that other cytokine signaling pathways also involve STAT1, such as the members of the common γ and β chain cytokine families [131]. There is some evidence of STAT1-independent IFN signaling, for instance the activation of extracellular signal regulated kinase (Erk1/2) in neurons as the primary IFNγ induced pathway during measles virus encephalitis [215]. Activated STAT1/STAT2

heterodimers and STAT1 homodimers translocate into the nucleus where they bind ISRE and GAS, respectively, in the regulatory regions of IFN-related genes [93, 216]. The transcription of IFN-related genes induces potent antiviral defenses against many viral infections, including PyVs.

PyVs infect a wide range of host species, including 14 that infect humans, but all PyVs exhibit strict host specificity [20, 21]. In immunocompetent individuals, PyV infection is a silent, asymptomatic infection that persists lifelong in the host [139]. However, upon immunosuppression from HIV/AIDS infection, immunomodulatory therapies for the treatment of autoimmune diseases, or hematological malignancies, one of the human PyV, JCPyV, causes the often-fatal, demyelinating disease PML [217]. PML is marked by subcortical demyelination, likely resulting from the infection and dysfunction of astrocytes and oligodendrocytes [25]. JCPyV has recently been found to be associated in the development of other diseases such as JCPyV encephalopathy, JCPyV-GCN, and JCPyV-meningitis, demonstrating that JCPyV can induce a variety of brain diseases [30]. The incidence of JCPyV-associated diseases in at-risk populations is still relatively rare, suggesting that there may be other unidentified determinants that predict PML development. In many CNS-tropic animal infection models, such as WNV, *Streptococcus pneumoniae*, Sindbis virus, and HSV, type I, II, and III IFNs limited viral infection by modulating the permeability of the BBB and inducing an antiviral state within infected oligodendrocytes and astrocytes [92, 105, 111, 119, 128]. In the context of PyV infection, treatment of human fetal glial cells or renal epithelial cells with recombinant IFNγ or type I IFNs inhibited JCPyV replication [53, 55, 218]. Although no direct role of type III IFNs on PyV replication has been demonstrated, IFNλ signaling at the BBB was found to be protective during WNV infection [128]. Currently, no effective anti-PyV agents are available. Understanding host susceptibility, defining host immunological interactions, and developing therapies against PyVs are critical for alleviating PyV-associated morbidities.

Intracerebral (i.c.) inoculation of mice with MuPyV, a natural mouse pathogen , provides the opportunity to understand PyV pathogenesis and immunity in an immunocompetent host. MuPyV and JCPyV are genetically and structurally similar, and they both establish persistent, asymptomatic infections in their respective hosts [19, 149]. Previous work from our group found that IFNγ and Type I IFNs mediate viral control in the kidney and spleen, respectively [58, 190]. In this study, we asked if type I, II, or III IFNs or STAT1, which is necessary for IFN signaling, confer protection against MuPyV pathogenesis in the brain. Using i.c. MuPyV infection, we found that while type I IFNs contribute to viral control during early, acute MuPyV brain infection, the absence of a single IFN did not lead to poorer control of persistent MuPyV infection. Furthermore, the absence of type I, II, or III IFNs did not affect the development of anti-MuPyV immune responses or protection against MuPyV-induced demyelination and hydrocephalus during persistent infection. However, we demonstrate that loss of STAT1 signaling leads to unchecked immune infiltration and extensive hydrocephalus in the brain. Our work described is bolstered by a recent study correlating increased PML risk with STAT1 mutations, and suggests that STAT1 signaling plays a critical role in the control of PyV replication in the brain [56].

3.2 Results

3.2.1 Type I IFNs regulate viral control during acute MuPyV infection in the brain and spleen

A large body of evidence has shown that type I, II, and III IFNs control many neuro- and gliotropic viral infections, such as coronavirus, WNV, and measles virus, in mice [16, 104, 128, 219-221]. Additionally, patients with mutations in type I, II, or III IFNs are susceptible to HSV encephalitis and other mycobacterial infections [222]. To ask whether the IFN family affects MuPyV replication in the brain, WT mice, mice deficient in receptors for type I IFNs ($IFNAR^{-/-}$), type I and III IFNs ($IFNLR1^{-/-}IFNAR^{-/-}$), type II IFNs ($IFN\gamma R^{-/-}$), and mice deficient in STAT1 ($STAT1^{-/-}$) were infected i.c. with MuPyV. During acute (day 8 p.i.) MuPyV infection, $IFNLR1^{-/-}$ $IFNAR^{-/-}$ and $STAT1^{-/-}$ mice had significantly higher viral load in the brain compared to WT mice (**Fig 3-1A**). However, although no significant difference in viral loads was found between WT and $IFNAR^{-/-}$ mice, the viral load in $IFNAR^{-/-}$ mice was trending higher during acute infection (**Fig 3-1A**). Additionally, $IFNAR^{-/-}$ and $IFNLR1^{-/-}IFNAR^{-/-}$ had similar viral loads, suggesting that viral control in the brains of $IFNLR1^{-/-}IFNAR^{-/-}$ mice may be mediated by type I and not type III IFNs (**Fig 3-1A**). Similarly, type I IFN was important for viral control in the spleen during acute infection, as demonstrated by significantly higher viral load in the spleens of $IFNAR^{-/-}$ and $IFNLR1^{-/-}IFNALR^{-/-}$ mice compared to WT mice (**Fig 3-1B**).

Statistical analyses revealed a significant decrease ($P<0.0001$) in viral loads between acute and persistent (30 days p.i.) infection in the brains of WT mice and of mice lacking type I, II, or III IFN receptors (**Fig 3-1A**). The similar viral control In mice lacking type II IFNs contrasts our previous work showing increased MuPyV load in the kidney during persistent infection in $IFN\gamma R^{-/-}$ mice (**Fig 3-1A**, [58]). These results suggest that IFNγ is not the dominant mechanism of viral control in all tissues, mirroring the heterogeneity in the level of IFNγR expression throughout the body [223]. Taken together, these results indicate that the contribution of type I IFNs to viral control is most critical during acute MuPyV infection in the brain and spleen.

3.2.2 STAT1 protects against brain pathology during MuPyV encephalitis

Aberrations in the homeostatic balance of type I, II, and III IFNs exacerbate progression of many brain diseases in humans, including Alzheimer's Disease, progressive MS, and relapse remitting MS, due to insufficient or excessive immune surveillance of the brain [118, 129]. To ask whether loss of IFNs accentuated MuPyV-pathology, we measured the integrity of the BBB and development of hydrocephalus in MuPyV-infected mouse brains. BBB permeability, indicated by the extent of extravasation of intravascularly (i.v.) administered sodium fluorescein dye into the brain at day 9 p.i., was increased in infected $IFNAR^{-/-}$, $IFNLR1^{-/-}IFNAR^{-/-}$, and $STAT1^{-/-}$ mice compared to infected WT mice and sham-infected mice, demonstrating that type I IFNs and, potentially, type III IFNs tighten the BBB during viral infection (**Fig 3-2A**). This result reflects previous studies documenting increased BBB permeability following infection with WNV in the absence of type I and III IFNs [128, 224]. However, IFNγ responsiveness was dispensable for maintenance of BBB integrity as $IFN\gamma R^{-/-}$ had similar fluorescein accumulation compared to infected WT and sham-infected mice (**Fig 3-2A**). Because differences in brain permeability can reflect deficits in the BBB, composed of endothelial cells lining the vasculature of the brain, or in the blood-CSF barrier, composed of ependymal cells lining the ventricles, we next measured the size of the lateral ventricles and the dorsal third ventricle [225, 226]. Infected $STAT1^{-/-}$ mice had increased lateral ventricle and dorsal third ventricle size compared to sham-infected mice and infected WT mice, demonstrating that STAT1 is protective against MuPyV-induced hydrocephalus (**Fig 3-2B-I**). In contrast, loss of IFNγ, type I IFNs, or IFNλ had no effect on hydrocephalus development (**Fig 3-2B-I**).

To ask if STAT1 promotes antiviral defense in the infected cell itself, we infected mice with a modified MuPyV containing an 84-nucleotide miRNA sequence corresponding to STAT1 (STAT1 miRNA virus) or a scrambled sequence (miR124 virus). Mice infected with the STAT1 miRNA virus had trending higher ventricle volume compared to mice infected with miR124, but more mice are needed to verify this claim. (**Fig 3-3A-E**). However, the ventricles in mice

infected with the STAT1 miRNA virus were not as large as in the mice with global STAT1 deficiency (**Fig 3-2B & 3D**), suggesting that loss of STAT1 in the infected cell is only partially responsible for the observed pathology.

Subcortical demyelination is a hallmark of PML [227]. Because extensive hydrocephalus was observed in STAT1$^{-/-}$ mice, we next asked whether IFNs were protective against MuPyV-induced demyelination. Quantitative histopathologic analyses revealed that the percent of myelination in the cingulum, external capsule, and dorsal hippocampal commissure was similar between infected and sham-infected WT mice and mice deficient in type I IFN, IFNγ, and IFNλ receptors or deficient in STAT1, suggesting that IFNs do not confer protection against demyelination (**Fig 3-4A**). Analysis of the entire brain section revealed no difference in the density of Luxol Fast Blue (LFB) color in infected and sham-infected WT and STAT1$^{-/-}$ mice (**Fig 3-4B**). However, infected STAT1$^{-/-}$ mice had trending higher incidences of neurodegeneration compared to infected WT and sham infected mice (**Fig 3-4C**). The neurodegeneration in STAT1$^{-/-}$ mice was primarily found in the grey matter surrounding the ventricles and the hippocampus, suggesting that compression by hydrocephalus could be influencing neuronal survival. Taken together, these results indicate that STAT1 confers protection against MuPyV-induced damage in the brain.

3.2.3 Mice deficient in STAT1 have increased myeloid infiltrates

Because STAT1$^{-/-}$ mice had extensive hydrocephalus without higher viral loads, we next asked if brain pathology reflected excessive immune activation. Previous work has shown that a loss of STAT1 causes aberrant activation of the inflammatory response [134]. In our PyV infection model, we found that mice deficient in STAT1 had increased neuroinflammation. At day 8 p.i., WT, IFNAR$^{-/-}$, IRNLR$^{-/-}$IFNAR$^{-/-}$, and IFNγR$^{-/-}$ mice had similar number and frequency of CD45^{hi}Ly6G^{+}Ly6C^{hi} (neutrophil-like) and CD45^{hi}Ly6G^{-}Ly6C^{lo} (monocyte-like) cells in the brain (**Fig 3-5A-C**). STAT1$^{-/-}$ mice had increased numbers of neutrophil-like cells in the brain

compared to WT mice (**Fig 3-5A-C**). This trend of increased inflammatory immune cells in STAT1$^{-/-}$ mice continued during persistent infection. Analysis of hematoxylin and eosin (H&E) stained sections revealed that WT mice had low levels of infiltrating monocytes and lymphocytes into the brain parenchyma. However, STAT1$^{-/-}$ mouse brains had increased numbers of macrophages and neutrophils surrounding the lateral ventricles, dorsal third ventricle, hippocampus, and dentate gyrus at 30 days p.i. (**Fig 3-6A**). STAT1$^{-/-}$ mice also had an attenuated ependymal lining infiltrated by inflammatory myeloid cells filled with eosinophilic content, suggesting that the cells are phagocytosing cellular debris such as neuropil (**Fig 3-6B-D).** Additionally, STAT1$^{-/-}$ mice had foci of inflammatory neutrophils and macrophages, which were not seen in WT mice. STAT1$^{-/-}$ mice also had increased numbers of neutrophils, mononuclear cells, and macrophages in the meninges compared to the relatively low numbers of macrophages in the meninges in WT mice at day 30 p.i. (**Fig 3-6E**). Myeloid cells, such as neutrophils, have been implicated in the pathogenesis of various neurodegenerative diseases, such as MS, suggesting that the increased infiltration of myeloid cells may exacerbate pathology in STAT1$^{-/-}$ mice [228]. In conclusion, the absence of STAT1 allows a persistent inflammatory environment.

Brain resident immune cells, such as microglia, can also contribute to an inflammatory state during viral infection. STAT1 phosphorylation by IFN signaling promotes the activation of pro-inflammatory microglia during insult, suggesting that a deficiency of STAT1 may induce an anti-inflammatory phenotype in microglia [229]. Flow cytometric analyses, however, revealed significantly more microglia in the brains of IFNAR$^{-/-}$ and STAT1$^{-/-}$ mice compared to WT mice during acute MuPyV infection (**Fig 3-7A**). Macrophages express IFNLR and IFNλ treatment of macrophages induced the production of IL-10, TNFα, and other cytokines, suggesting that a loss of IFNLR may negatively impact the activation of macrophage-derived cells, such as microglia [230]. The microglia from IFNAR$^{-/-}$ and IFNLR$^{-/-}$IFNAR$^{-/-}$ mice also had increased expression of MHC II (**Fig 3-7B**). We found that IFNγ from infiltrating virus-specific CD8 T cells

is necessary for the upregulation of MHC II on microglia (**Fig 3-8A & B**), and previous research has shown that IFNβ inhibits the expression of MHC II on microglia, which may, in part, explain the discrepancy between increased numbers without concurrent increased MHC II expression on microglia from STAT1$^{-/-}$ mice [231]. However, IFNAR$^{-/-}$ mice did not have a sustained inflammatory microglia or macrophage phenotype. During persistent MuPyV infection, STAT1$^{-/-}$ mice showed trending higher numbers of Iba1^{+} cells during persistent MuPyV infection compared to IFNAR$^{-/-}$ mice (**Fig 3-7C**). Iba1 stains both microglia and macrophages. Iba1^{+} cells accumulated near the ventricles in STAT1$^{-/-}$ mice, but elevated cell numbers were not seen in sham-infected STAT1$^{-/-}$ or infected IFNAR$^{-/-}$ mice (**Fig 3-7D-G**). The Iba1 staining on the cells in STAT1$^{-/-}$ was dark and found predominately on the cellular membrane, demonstrating that these cells are activated (**Fig 3-7D-G**). In conclusion, STAT1 deficiency promotes persistent activation of microglia and macrophages, further demonstrating increased damaging neuroinflammation following MuPyV infection in the absence of STAT1.

3.2.4 STAT1 deficiency results in increased CD8 T cell infiltration into the brain and aberrant resident memory development during MuPyV infection.

Previous studies have shown that STAT1 has anti-inflammatory, through the activation of suppressor of cytokine signaling, as well as pro-inflammatory effects on the innate and adaptive immune response [131, 232]. Our previous work has shown that the adaptive immune response, particularly the CD8 T cell response, is an important component of MuPyV control in many organs [154, 200]. IFN signaling is important for the development and maintenance of CD8 T cells responses [106, 130, 233]. During MuPyV infection, WT, IFNAR$^{-/-}$, IFNLR1$^{-/-}$IFNAR$^{-/-}$, and STAT1$^{-/-}$ mice had similar numbers of CD8 T cells specific for D^{b}LT359, the immunodominant CD8 T cell epitope, in the brain, and the numbers declined similarly between acute and persistent MuPyV infection (**Fig 3-9A**). IFNγR$^{-/-}$ mice had transiently higher numbers of D^{b}LT359-specific CD8 T cells in the brain during acute MuPyV infection compared to WT

mice, but this difference was lost during persistent infection, suggesting that IFNγ does not have a long-lasting impact on the recruitment of CD8 T cells to the brain (**Fig 3-9A**). Despite similar numbers of D^bLT359-specific CD8 T cells, $IFNAR^{-/-}$ and $IFNLR1^{-/-}IFNAR^{-/-}$ mice had a reduced frequency of D^bLT359-specific CD8 T cells during acute and persistent infection, which suggests that other non-D^bLT359-specific CD8 T cells may have been recruited or expanded (**Fig 3-9B**). In contrast, the spleens of WT, $IFNAR^{-/-}$, and $IFNLR1^{-/-}IFNALR^{-/-}$ mice had similar frequencies of D^bLT359-specific CD8 T cells during acute and persistent MuPyV infection, demonstrating that this deficit is brain-specific (**Fig 3-10A**). $STAT1^{-/-}$ mice also had a reduced frequency of D^bLT359-specific CD8 T cells during acute MuPyV infection in the brain, but this difference was lost during persistent infection (**Fig 3-9B**). $IFNAR^{-/-}$ and $STAT1^{-/-}$ mice had significantly increased numbers of total CD8 T cells in the brain during acute MuPyV infection, suggesting that $IFNAR^{-/-}$ and $STAT1^{-/-}$ mice have increased infiltration of D^bLT359-nonspecific CD8 T cells into the brain (**Fig 3-9C**).

We next asked whether the formation of T_{RM}, T_{CM}, and T_{EM} subsets in CD8 T cells was intact. CD8 T_{RM}, including CD8 bT_{RM}, act as the frontline defense against reinfection in non-lymphoid tissue, which is reinforced by the work presented in Chapter 2 demonstrating that poor CD8 bT_{RM} maintenance has negative consequences on viral control during reinfection. CD103 and CD69 are regarded as the canonical surface markers of CD8 T_{RM}, and we have previously shown that 80-95% and 40% of D^bLT359-specific CD8 T cells express CD69 and CD103, respectively, during persistent MuPyV infection in the brain [18, 74, 140, 199]. In this study, we found that mice deficient in type I IFN and III IFN receptors and STAT1 signaling had reduced expression of CD69 on D^bLT359-specific CD8 T cells in the brains of acutely and persistently infected mice (**Fig 3-9D**). Previous work has shown that CD69 is upregulated in response to TCR engagement and IFNα stimulation [234, 235]. The upregulation of CD69 antagonizes S1P1 expression – increased S1P1 expression allows chemotactic egress of lymphocytes from tissue - and S1P1 downregulation is required for the development of CD8 T_{RM}, suggesting that IFNAR-

$^{-/-}$, IFNLR1$^{-/-}$ IFNAR$^{-/-}$, and STAT1$^{-/-}$ mice have aberrant CD8 bT$_{RM}$ development [236, 237]. WT mice and mice deficient in type I, II, or III IFNs had similar frequencies of CD103^{+} D^{b}LT359-specific CD8 T cells in the brain at day 30 p.i., but STAT1$^{-/-}$ mice had a significantly reduced frequency of CD103^{+} D^{b}LT359-specific CD8 T cells (**Fig 3-9E**). Additionally, D^{b}LT359-specific CD8 T cells from STAT1$^{-/-}$ mice had elevated expression of PD-1 during acute and persistent infection (**Fig 3-9F**). Work from our lab has shown that high expression of PD-1 negatively impacts differentiation of D^{b}LT359-specific CD103^{+} CD8 T cells during persistent MuPyV infection, which may explain the loss of CD103^{+} D^{b}LT359-specific CD8 T cells seen in this study [74]. We next examined the ability of D^{b}LT359-specific CD8 T cells in the spleen to differentiate into CD8 T$_{EM}$ and T$_{CM}$ subsets. Previous work has shown that CD8 T cells with high CD127 expression are more likely to transition into memory cells whereas high KLRG1 expression distinguishes short-lived effector cells [238, 239]. In STAT1$^{-/-}$ mice, few CD127^{lo}KLRG1^{hi} (effector-like) MuPyV-specific CD8 T cells were detected during acute MuPyV infection in the spleen, and STAT1$^{-/-}$ mice had an increased frequency of CD127^{hi}KLRG1^{lo} (memory precursor) CD8 T cells compared to WT mice (**Fig 3-9G**). IFNAR$^{-/-}$ and IFNLR1$^{-/-}$IFNALR$^{-/-}$ mice also had a reduced frequency of effector-like MuPyV-specific CD8 T cells, but did not have a concurrent increased in memory precursor CD8 T cells (**Fig 3-9G**). WT and IFNγR$^{-/-}$ mice had similar frequencies of both populations of cells (**Fig 3-9G**). Taken together, these results suggest that T$_{EM}$ and T$_{CM}$ differentiation is intact in the absence of IFN and STAT1 signaling in the spleen, but STAT1 loss negatively impacts the differentiation of CD8 bT$_{RM}$.

3.2.5 CD8 T cells have increased effector function in the absence of STAT1

The aberrant memory differentiation in STAT1$^{-/-}$ mice suggested that these cells may have other deficits, such as in effector function. Previous work has shown that type I IFNs are necessary for the differentiation of naïve CD8 T cells into functionally competent effector CD8 T cells, and type III IFNs negatively modulate CD8 T cell responses during chronic viral infection

[106, 130]. Likewise, IFNγ affects CD8 T cell responses by the stimulation of MHC I receptors on infected cells [240]. Therefore, we next asked whether a lack of IFN sensitivity contributed to functional deficits. Following ex vivo stimulation with LT359 peptide, similar numbers of CD8 T cells isolated from the brains of WT, IFNAR$^{-/-}$, IFNLR1$^{-/-}$ IFNAR$^{-/-}$, and IFNγR$^{-/-}$ mice during acute and persistent MuPyV infection produced IFNγ and TNFα and retained the capacity for secretory degranulation (i.e. peptide-induced CD107 expression) (**Fig 3-11A**). In contrast, CD8 T cells isolated from STAT1$^{-/-}$ mice during acute and persistent MuPyV infection produced more IFNγ and CD107 following ex vivo stimulation (**Fig 3-11A**). MuPyV-specific CD8 T cells from the spleens of persistently infected STAT1$^{-/-}$ mice also produced more IFNγ following ex vivo stimulation, demonstrating that CD8 T cells from STAT1$^{-/-}$ mice have aberrant functionality (**Fig 3-10B**). For full biological activity, STAT1 must also be phosphorylated at the transactivation domain serine 727 (S727) once STAT1 has bound to DNA [241]. Knockin mice with point mutations in S727 (STAT1.S727A) have reduced antimicrobial defense and higher immune cell cytotoxicity [242]. We found that disruption in the ability of STAT1 to bind to DNA (mice labeled as B6.S727A) did not affect effector function or viral control in the spleen and brain, which mimics previous work showing that phosphorylation of S708, instead of S727, is more important for antiviral IFN signaling (**Fig 3-12A-C**) [243]. Excessive immune activity, especially increased IFNγ production, is highly toxic to terminally differentiated brain resident cells, such as neurons [244]. However, caution is warranted in translating ex vivo stimulation to in situ production as the methods utilized investigated the potential for IFNγ production. Despite similar functional competence, MuPyV-specific CD8 T cells from IFNAR$^{-/-}$, IFNLR1$^{-/-}$IFNALR$^{-/-}$, and STAT1$^{-/-}$ mice had reduced expression of IRF4, a transcription factor upregulated by TCR engagement [156], which may reflect decreased functional competence in the brain (**Fig 3-11B**). Virus-specific CD8 T cells from IFNAR$^{-/-}$, IFNLR1$^{-/-}$IFNALR$^{-/-}$, and STAT1$^{-/-}$ mice also had reduced expression of Nur77 following ex vivo stimulation, a transcription factor indicative of TCR stimulation strength [245], but similar production of effector cytokines, suggesting that the expression of IRF4 and

Nur77 may not indicate functionality (**Fig 3-11B & C**). More studies investigating the production of CD8 T cell effector cytokines in situ are needed to address this discrepancy.

3.2.6 CD8 T cells are necessary for survival of MuPyV-infected STAT1$^{-/-}$ mice

Although efficacious in alleviating brain viral burden, IFNγ is injurious to brain resident cells as shown by improved memory performance and hippocampal volume in IFNγKO mice in the absence of any apparent inflammation [246]. Furthermore, CD8 bT_{RM} represent an autonomous barrier against reinfection and excessive immune activation in the brain [84]. Based on these studies, we depleted CD8 T cells from STAT1$^{-/-}$ mice as a way to analyze the contribution of CD8 bT_{RM} and their effector function to the development of damage and viral control following i.c. MuPyV infection (**Fig 3-13A**). We found that depletion of CD8 T cells caused weight loss in STAT1$^{-/-}$ mice following MuPyV infection (**Fig 3-13B**). This weight loss was not due to the depletion of CD8 T cells in STAT1$^{-/-}$ mice as sham-infected mice did not lose weight following depletion (**Fig 3-13C**). Furthermore, these mice were unable to survive MuPyV infection and all depleted STAT1$^{-/-}$ mice were dead by two weeks after infection (**Fig 3-13D**). STAT1$^{-/-}$ mice had significantly increased viral load in the brain in the absence of CD8 T cells at terminal endpoint, underscoring their role in the control of MuPyV infection in the brain (**Fig 3-13E**). These results demonstrate that CD8 T cells, despite increased effector function, provide essential antiviral defense in the absence of STAT1.

3.3 Discussion

Using the mouse PyV-infection model, we provide evidence that STAT1 dampens the inflammatory response and alleviates brain damage following infection, which was not seen in mice deficient in type I IFN, type II IFN, or type I and III IFN receptors. Cell-intrinsic STAT1 signaling partially protected against MuPyV-induced encephalitis, but a global deficiency in STAT1 caused widespread and diffuse hydrocephalus, suggesting that STAT1 has effects on infected cells and other cells, including immune cells, simultaneously. Mice deficient in STAT1 have a sustained inflammatory signature consisting of inflammatory myeloid cells, T cells, and microglia. We show that the deviant T cell response is still necessary for survival in $STAT1^{-/-}$ mice, further supporting the notion that the adaptive immune response is a key component of protection from MuPyV infection.

IFNs program a state of antiviral resistance in infected cells and alarm innate and adaptive immune cells. In our study, we show that type I IFNs mediate viral control during acute MuPyV infection in the brain and spleen (**Fig 3-1**). The ability of type I IFNs to restrict viral replication is attributed to the induction of ISGs, and the resultant antiviral state in infected and bystander cells, and the activation of myeloid cells, B cells, T cells, and NK cells [247]. However, despite previous research from our group documenting the role of IFNγ in reducing viral burden in the kidney, this study found that IFNs were most important for viral control during acute MuPyV infection (**Fig 3-1,** [58]). This discrepancy between viral control in the brain and kidney may reflect the heterogeneity of immune populations responsible for viral control. Previous work has shown that T cells use tissue- and virus-specific methods of viral control, as shown by the targeted killing of infected cells during brain VSV infection versus the systemic release of IFNγ from CD8 T cells during influenza infection of the airway [18, 248]. Furthermore, the site of inoculation can affect the functionality of CD8 T cells and their dependence on CD4 T cells, suggesting that other immune cells may also reflect heterogeneity based on the site of inoculation [249]. Thus, these studies and ours document that IFNs are critical components of

the antiviral defense during acute infection, but another unknown mechanism promotes PyV-defense during persistent viral infection in the brain.

Over 50 cytokines and growth factors utilize the STAT family members to regulate cell growth, survival, and differentiation and the immune response, suggesting that viral control may be mediated by an IFN-independent mechanism during persistent MuPyV infection in the brain [250]. STAT1 is activated in response to the binding of growth factors, hormones, catecholamines, and cytokines in the beta chain receptor, gamma chain receptor, and IL-10 families to their respective receptors, although at a lower level than in response to IFNs [251-258]. Two of the growth factors that involve STAT1 signaling, epidermal growth factor (EGF) and vascular endothelial growth factor (VEGF), have potent effects on brain resident cells following trauma [259, 260]. EGF enhances oligodendrocyte development, and overexpression of EGFR accelerates myelin repair following lysolecithin-induced focal demyelination of the corpus callosum [261, 262]. Additionally, VEGF has been implicated in neuroprotection, neurogenesis, and brain vessel repair following ischemic and hemorrhagic stroke [263]. Furthermore, agnoprotein derived from JCPyV downregulated GM-CSF production from glial cells [264]. GM-CSF signals through the common beta chain receptor and phosphorylates STAT1 upon binding [255]., Thus, non-IFN cytokines may signal through STAT1 to provide anti-PyV defense. In conclusion, the phenotype observed in STAT1 deficient mice may reflect decreased sensitivity to other trophic factors or cytokines, especially given the absence of neuropathology in mice deficient in type I, II, or III IFN receptors.

In our study, we found that microglia have a prolonged activation state in $STAT1^{-/-}$ mice (**Fig 3-7**). The expression of numerous TLRs and PRRs in microglia, the brain's tissue-resident macrophage, allows them to respond rapidly and efficiently to viral infection in the brain [265]. Following stimulation by pathogens, microglia secrete proinflammatory factors such as glutamate, reactive oxygen species, cytokines, and chemokines that activate other glial cell subsets, such as astrocytes, and mobilize the peripheral immune response [266]. The varied

activities of microglia make them a critical component of antiviral defense in the brain. Although glial cell activation has beneficial effects such as pathogen clearance, uncontrolled and persistent activation can exacerbate brain damage via the continual production of inflammatory, neurotoxic mediators and protracted immune activity [265]. Thus, the activation of microglia in STAT1$^{-/-}$ mice may create a positive feedback loop that perpetuates brain resident and immune cell activation and increases brain pathology.

Our result demonstrating increased hydrocephalus in STAT1$^{-/-}$ mice (**Fig 3-2**) suggests that STAT1 mediates antiviral defense in ependymal cells during MuPyV encephalitis. Ependymal cells are a unique, ciliated, and terminally differentiated population of glial cells that line the ventricles of the brain and central canal of the spinal cord. The beating of ependymal cilia is important for the movement of the CSF through the brain and the adherens and tight junctions of ependymal cells constitute the brain parenchyma-CSF barrier [267, 268]. Disruption of ependymal cilia or adhesion by brain insult such as trauma or viral infection can cause hydrocephalus [267]. For example, the presentation of JCPyV meningitis in human patients is marked by hydrocephalus [30]. Hydrocephalus has also been associated with abnormal neurogenesis, most likely resulting from the loss of trophic support from ependymal cells to progenitor cells in the subventricular zone (SVZ) [267]. These pluripotent progenitor cells of the SVZ are able to differentiate into neurons and oligodendrocyte precursor cells (OPCs), and their loss has been shown to decrease remyelination in inflammatory conditions [269]. However, despite the predominant role of ependymal cells in brain damage during viral infection, the intrinsic antiviral defenses employed by ependymal cells remain largely unknown. Previous work has shown that ependymal cells are able to respond to type I and II IFNs, but these studies were limited and did not investigate type III IFNs [268]. Our data suggests that STAT1 promotes antiviral defense in ependymal cells following MuPyV infection, but further studies are needed to demonstrate what signaling molecule induces STAT1 activation.

STAT1 is a dynamic transcription factor that modulates the immunopathologic response. In our PyV-infection model, we found that STAT1$^{-/-}$ mice had an increased number of neutrophil-like cells, increased effector cytokine production from CD8 T cells following ex vivo peptide stimulation, and impaired CD8 bT_{RM} development in the brain (**Fig 3-5, 9, & 11**). In many viral infections, STAT1 deficiency results in an unrestrained immune response, especially in regard to neutrophils and CD8 T cells [134, 270-274]. Additionally, various cytokines that regulate CD8 T_{RM} development, such as IL-15 and IL-21, use STAT1 as a downstream effector, suggesting that STAT1 deficiency impairs memory differentiation of CD8 T cells [70, 275-277]. The accumulation of neutrophils and CD8 T cells in the brain are hallmarks of neuroinflammation [4]. The infiltration of neutrophils contributes to demyelination and cell loss in the CNS, as demonstrated by decreased cuprizone-induced demyelination and picornavirus-induced hippocampal pathology in the absence of neutrophils [228, 278-280]. Similarly, CD8 T cells were found to promote demyelination in the brain following infection with JHM strain of mouse hepatitis virus (JHMV) [281]. However, despite extensive brain damage from the activity of immune cells, the infiltration of immune cells is important for the control of brain infection. Neutrophils are among the first responders to microbial infection and are important for the recruitment of virus-specific lymphocytes into the infected CNS via permeabilization of the BBB [282]. Similarly, CD8 T cells, especially CD8 bT_{RM}, provide lasting immune surveillance of the CNS [84, 137]. Collectively, these studies demonstrate that STAT1 signaling functions as a homeostatic immune checkpoint by promoting the differentiation of memory CD8 T cells and reducing the infiltration and effector capability of the immune response in the brain.

The ubiquitous expression of STAT1 and IFN receptors in the CNS underscores their crucial role in controlling viral insult in the brain. In our study, we found IFNs, specifically type I IFNs, were important for viral control during acute infection, but IFN signaling did not play a role in the control of persistent viral infection. Similarly, IFNs had no effect on immune cell infiltration into the brain or the development of pathology resulting from MuPyV infection. However,

STAT1, the common downstream transcription factor of the IFN family, constituted a major part of PyV-defense. Mice deficient in STAT1 had increased viral loads and infiltration of immune cells, suggesting an aberrant neuroinflammatory landscape. Furthermore, brain pathology in STAT1-deficient mice was marked by hydrocephalus, which may reflect the absence of antiviral defense in ependymal cells. Depletion of CD8 T cells from $STAT1^{-/-}$ mice suggest that CD8 T cells may compensate for the loss of immune activity resulting from STAT1 deficiency, but this work is incomplete and requires investigation of the contribution of other immune cell subsets, such as neutrophils. Our findings raise the possibility that amplifying brain resident cell-intrinsic responses and promoting memory responses of CD8 T cells may offer a therapeutic avenue for alleviating PyV infection of the brain.

3.4 Materials and methods

Mice

Adult (6-12 wks of age) female and male C57BL/6 (B6) mice were purchased from the National Cancer Institute (NCI, Frederick, MD). Female C57BL/645.1 (SJL) were purchased from the NCI. IFNLR1$^{-/-}$IFNAR$^{-/-}$ mice were obtained from Dr. Sergei Kotenko at the University of Rutgers (Newark, NJ). IFNAR$^{-/-}$ and IFNγR$^{-/-}$ mice were obtained from Dr. Ziaur Rahman. STAT1$^{-/-}$ mice were obtained from Dr. Christopher Norbury with an approved MTA from Dr. Sergei Kotenko. All knockout mice are on a B6 background. Mice were bred and housed in accordance with the guidelines of the NIH Guide for the Care and Use of Laboratory Animals and the Institutional Animal Care and Use Committee at the Penn State College of Medicine. For survival studies, mice were sacrificed when considered moribund by the veterinary staff. For adoptive transfer studies, CD8 T cells were isolated from IFNγ$^{-/-}$ TCR-1 mice as described and injected i.v. into SJL mice [74].

Viruses and Infections

MuPyV.A2 was prepared in baby mouse kidney cells as described [196]. Mice were infected i.c. with 3x10^5 PFU MuPyV.A2 in 30 µL as described [154]. MuPyV.LT206 was prepared as described and mice were infected i.c. with 1.75x10^5 PFU [200]. The STAT1 miRNA and miR124 (scrambled virus) were generated by InFusion cloning technology. The early proteins of MuPyV are interpreted by introns of varying lengths, with a shared intron region (STIN) 53bps in length. Using InFusion cloning technology, 84 nucleotides miRNA hairpins were inserted into this STIN, corresponding to STAT1 miRNA or a scrambled sequence. The STAT1 and miR124 plasmids used were generously provided by Dr. Ben TenOever, Mount Sinai School of Medicine (New York, NY). Mice were infected i.c. with 3x10^9 genomic equivalents in 30µL.

CD8 T Cell Depletion

Mice were injected i.p. with 250 µg rat anti-CD8β or ChromoPure whole rat IgG (Jackson ImmunoResearch Laboratories, West Grove, PA) beginning 4 days before infection and continuing weekly. Depletion was confirmed in peripheral blood by flow cytometry-based cell number assay using Absolute Count Standard (Bangs Laboratories, Fishers, IN).

T Cell Isolation and Flow Cytometry

Mononuclear cells were isolated from brains by collagenase-DNAse digestion and percoll gradient centrifugation as described [154]. Mononuclear cells were isolated from spleen as described [155]. After isolation, cells were stained with Fixable Viability Dye (eBioscience, San Diego, CA), APC-D^bLT359 tetramers (NIH Tetramer Core Facility, Atlanta, GA), and the following surface antibodies: CD8α (clone 53-6.7, eBioscience), CD44 (clone IM7, eBioscience), PD-1 (clone RMPI-30, Biolegend), CD103 (clone M290, BD Horizon), CD69 (clone HI.2F3, Biolegend), CD127 (clone A7R34, Biolegend), KLRG1 (clone 2F1, BD Biosciences), Ly6C (clone HK1.4, Biolegend), Ly6G (clone 1A8, Biolegend), MHC II (clone M5/114 15.2, eBioscience), CD11b (clone M1/70, BD Biosciences), streptavidin (Biolegend), and CD45 (clone 30-F11, BD Biosciences). Additionally, cells were stained with the following biotinylated surface antibodies: Thy1.2 (clone 53-21, eBioscience), CD19 (clone 6D5, Biolegend), and NK1.1 (clone PK136, Biolegend). For intracellular cytokine stimulation assays, lymphocytes were isolated from brain and spleen, cultured in DMEM/10% FBS for 5 h at 37°C with or without 1µM LT359 peptide [198], stained with Fixable Viability Dye, anti-CD8α, and anti-CD44, then permeabilized and fixed in FoxP3 buffer fixation and permeabilization solutions. Intracellular staining included IFN-γ (clone XMG1.2; Biolegend), TNF-α (clone XMG1.2; Biolegend), IL-2 (clone JES6-5H4, Biolegend), CD107a (clone 1D4B, BD Biosciences), CD107b (clone ABL-93, BD Biosciences), Nur77 (clone 12.14, BD Biosciences), and IRF4 (clone IRF4.3E4, Biolegend). Samples were acquired on a BD LSRFortessa (BD Bioscience, San Jose, CA) or BD LSR II (BD Biosciences, San Jose, CA) and analyzed using FlowJo software (FlowJo, LLC, Ashland, OR).

Quantitative PCR

For quantifying viral genome DNA copies, Real-Time® PCR was performed on samples containing 10 ng DNA purified from brain and spleen using the Wizard® Genomic DNA Purification Kit (Promega, Madison, WI) as described [200]. Samples were run on an ABI StepOnePlus Real-Time PCR System (ThermoFisher Scientific) and concentrations were calculated based on a standard curve [201-204].

Histological processing and analysis

Mice were perfused with 10mL of 10% heparin in PBS followed by 10mL of 10% neutral buffered formalin (NBF). Skulls were post-fixed in 10% NBF overnight and brains excised the next day. 7µm sections of brain were taken on a microtome by the Comparative Medicine core. Formalin fixed paraffin embedded sections (FFPE) were stained with Luxol Fast Blue-Periodic Acid Schiff (LFB-PAS) for visualization of myelin fibers and Hematoxylin and Eosin (H&E) for cell infiltration as described [283]. LFB-PAS stained sections were digitally imaged on a Keyence BZ-X710 all-in-one fluorescence microscope and stitched together using ImageJ software (National Institutes of Health, Bethesda, MD). Analysis of myelin was performed and analyzed as described [284] or using the LFB-PAS deconvolution function in Image J. In brief, total brain sections were deconvoluted and the density of blue staining was quantified for the entire brain section. For ventricle size, the pixel area of the left and right lateral ventricles and dorsal third ventricle was divided by the total pixel area of the brain section or the cortex using Adobe Photoshop (San Jose, CA). Ventricle size was then expressed as a percent of the total brain area or cortex area. For immunohistochemistry (IHC), 10 µm FFPE brain sections were deparaffinized and rehydrated prior to antigen retrieval in 10 mM sodium citrate buffer (pH 6.0). Sections were permeabilized with 1% TritonX-100, stained with primary antibodies anti-GFAP (Dako, Carpinteria, CA) or anti-Iba (Dako) for 1 hr at RT, then stained with secondary biotinylated goat anti-rabbit (Vector, Burlingame, CA) for 1 hr at RT, followed by avidin-

conjugated horse radish peroxidase (VECTASTAIN Elite ABC Kit, Vector, Burlingame, CA). Staining was developed using the VECTOR NovaRED Peroxidase substrate kit (Vector, Burlingame, CA).

Inflammation, neurodegeneration, and meningitis scoring was done by Dr. Hannah Atkins, the Comparative Medicine veterinary pathologist. Each group represents brain sections within 1mm of each other. Scoring was completed on a four-point scale:

Neurodegeneration, Inflammation, and Meningitis Scoring			**IHC Intensity Scoring**	
Numerical Score	*Description*	*Definition*	*Numerical Score*	*Description*
0	Within normal limits	Tissue considered to be normal under the considering the age, sex, and strain of the animal concerned.	0	No Staining
1	Minimal	The amount of change barely exceeds that which is within normal limits.	1	Minimal
2	Slight	In general, the lesions are easily identified but of limited severity	2	Mild
3	Moderate	The lesion is prominent, but there is significant potential for increased severity	3	Moderate
4	Severe	The change occupies the majority of the organ	4	Strong

Microglia numbers represent the average of the number of Iba^+ cells within three defined areas 20µm from the lateral ventricles.

BBB Permeability Assay

100 µl of 100 mg/ml sodium fluorescein dye (Sigma Aldrich, St. Louis, MO) was injected i.p. into mice at day 10 after i.c. inoculation with MuPyV.A2 or at 24 h after LPS administration (100 µg/µl). After 45 min, mice were cheekbled and transcardially perfused with PBS + 10% heparin. A 3 mm section was taken from the cerebrum, then processed as described [128] with fluorescein concentrations calculated using a standard curve.

Statistical Analysis

Experimental data were analyzed on Prism 6.07 (GraphPad, La Jolla, CA) using Mann-Whitney tests, one-way ANOVA, and two-way ANOVA with Tukey or Sidak's multiple comparisons test. Error bars indicate mean ± SD. All experiments were replicated independently.

3.5 Figures

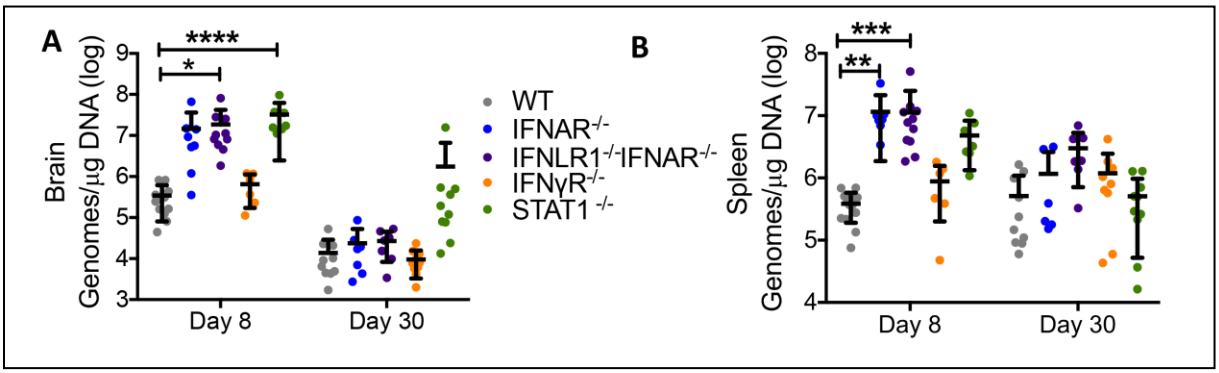

Fig 3-1: MuPyV load in the brains and spleens of WT mice and deficient in type I IFNs, IFNγ, IFNλ, or STAT1 during acute and persistent infection. (A,B) Real-time PCR® analysis of viral genome copies in brain (A) and spleen (B) at acute (day 8 p.i.) and persistent (day 30 p.i.) infection. Mean ± SD of 7-15 mice per group from 2-3 independent experiments. **P*<0.05, ***P*<0.01, ****P*<0.005, *****P*<0.001, Two-Way ANOVA

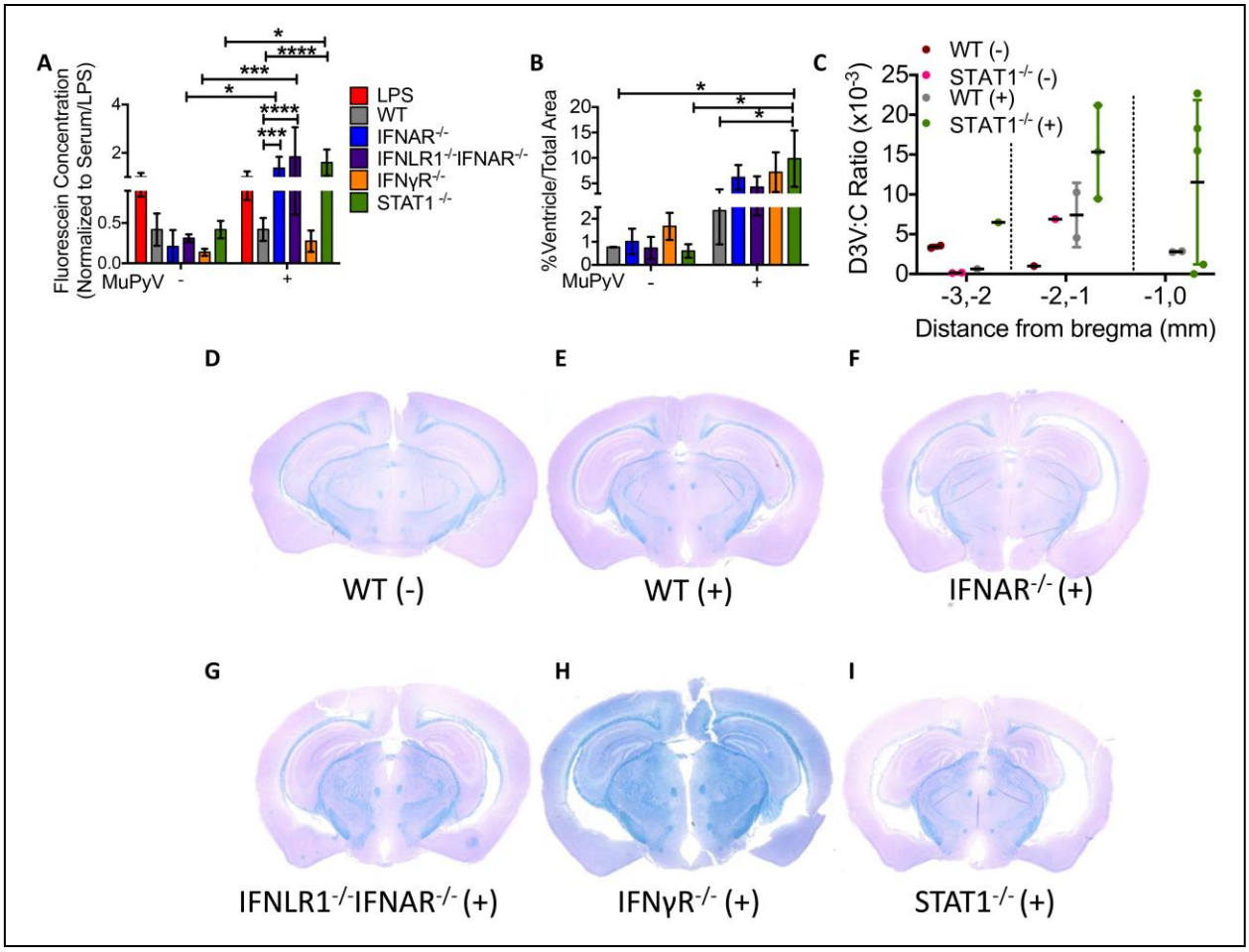

Fig 3-2: STAT1 signaling protects against MuPyV-induced brain pathology. (A) BBB permeability was measured 9 days p.i. by the accumulation of sodium fluorescein dye in the brain. LPS injected mice are positive controls for BBB permeability. **(B)** Percent of lateral ventricle volume from brain sections -2.70mm caudal to bregma. Brains removed 30 days p.i. **(C)** Ratio of dorsal third ventricle to cortex from brains at 30 days p.i. (-) indicates sham infected mice and (+) indicates MuPyV infected mice. **(D-I)** Representative LFB images of WT (D, E), IFNαR$^{-/-}$ (F), IFNaλR$^{-/-}$ (G), IFNγR$^{-/-}$ (H), and STAT1$^{-/-}$ (I) mouse brains -2.70mm caudal to bregma. Sections taken 30 days p.i. Mean ± SD of 7-15 mice per group from 2-3 independent experiments (A) or 2-5 mice per group from 1 independent experiment (B-I). *P<0.05, ***P<0.005, ****P<0.001, Two-Way ANOVA

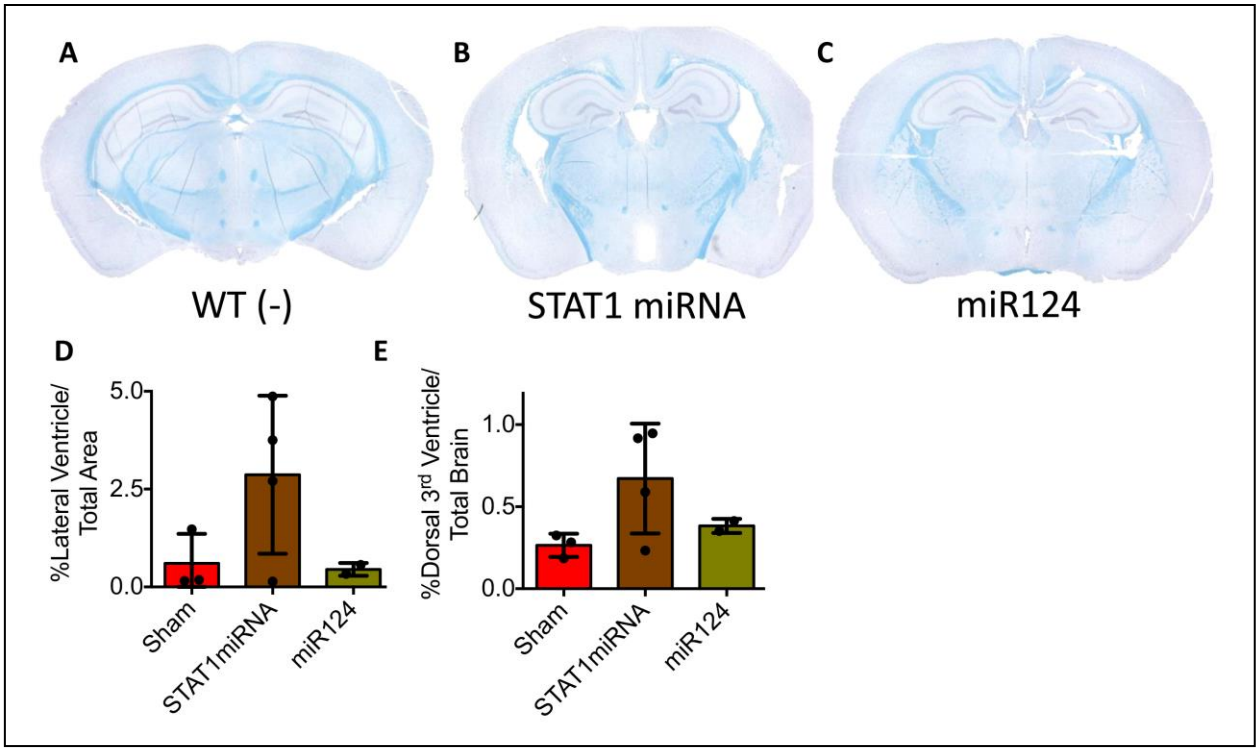

Fig 3-3: STAT1 deficiency in infected cells causes hydrocephalus. (A-C) Representative images of sham (A), STAT1 miRNA virus (B), and miR124 (C) infected mice at -2.70mm from bregma. Mice were sacrificed at day 30 p.i. **(D,E)** Percent of lateral ventricle (D) and dorsal third ventricle (E) in total brain from brain sections -2.70mm caudal to bregma. Mean ± SD of 2-5 mice per group from 1 independent experiment

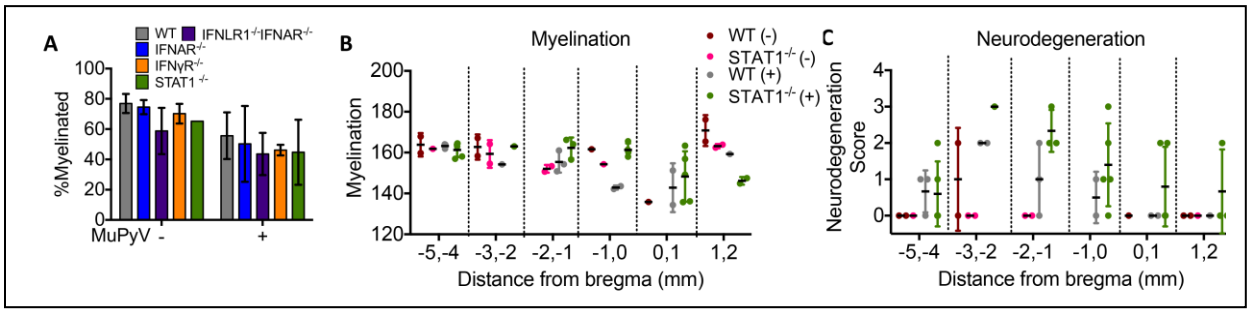

Fig 3-4: STAT1 deficiency does not affect demyelination. (A) Percent area myelinated in the cingulum, dorsal hippocampal commissure, and external capsule -2.70mm caudal to bregma. Brains removed 30 days p.i. **(B)** Demyelination in total brain section from STAT1$^{-/-}$ and WT mice 30 days p.i. (-) indicates sham infected mice and (+) indicates MuPyV infected mice. **(C)** Mouse brains were rated for the degree of neurodegeneration by a veterinary pathologist blinded to the identity of the experimental groups. Brains were removed 30 days p.i. Mean ± SD of 2-5 mice per group from 1-2 independent experiments (A-C)

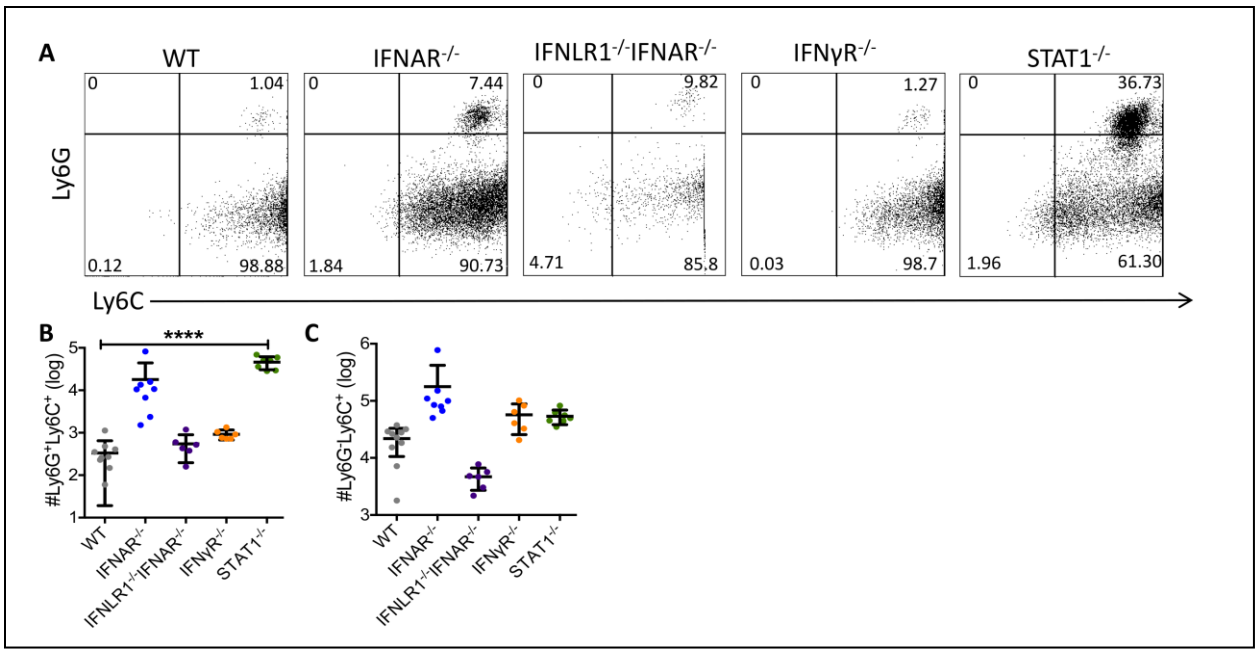

Fig 3-5: STAT1$^{-/-}$ mice have increased accumulation of inflammatory cells in the brain during acute MuPyV infection. (A) Representative flow histograms from brain at day 8 p.i. Frequencies shown are averages. **(B,C)** Number of Ly6G^{+}Ly6C^{+} (B) and Ly6G^{-}Ly6C^{+} (C) cells at day 8 p.i. Mean ± SD of 1-5 mice per group from 1 independent experiment. *P<0.05, **P<0.01, ****P<0.001, One-Way ANOVA

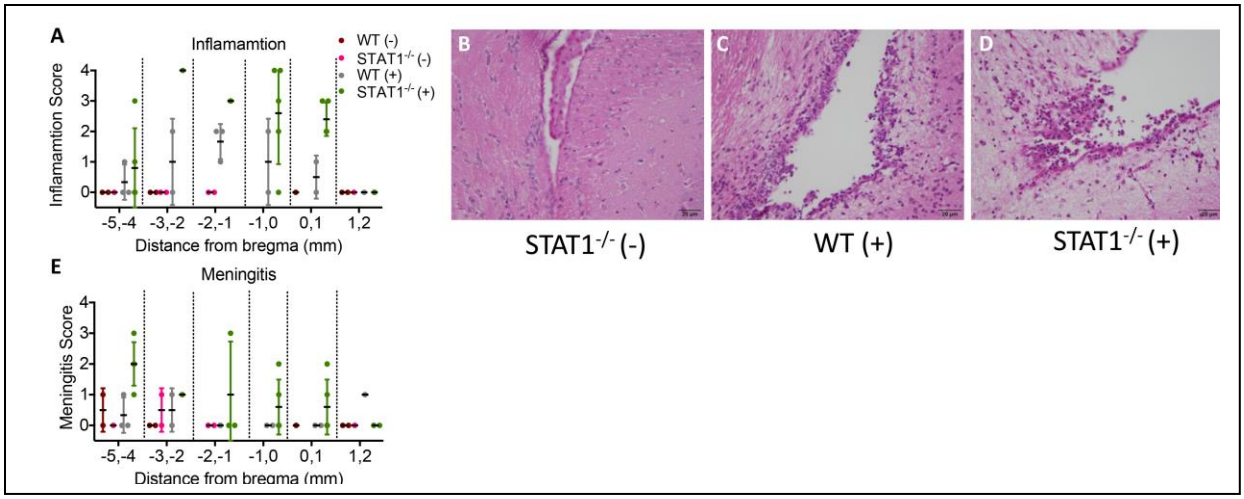

Fig 3-6: STAT1$^{-/-}$ mice have increased inflammation in the brain during persistent MuPyV infection. (A) Mouse brains were rated for the degree of inflammation by an examiner blinded to the identity of the experimental groups. (-) indicates sham infected mice and (+) indicates MuPyV infected mice 30 days p.i. **(B-D)** Representative H&E images of sham infected STAT1$^{-/-}$ mice (B) and MuPyV-infected WT (C) and STAT1$^{-/-}$ (D) mice 30 days p.i. **(E)** Mouse brains were rated for the degree of meningitis by an examiner blinded to the identity of the experimental groups. Mean ± SD of 1-5 mice per group from 1 independent experiment.

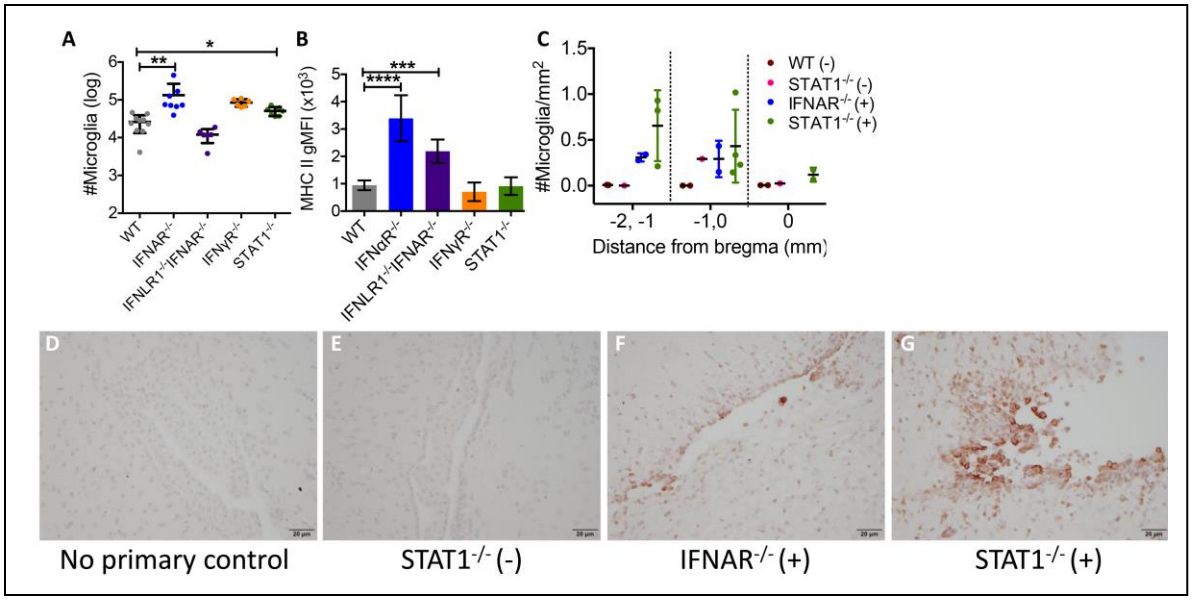

Fig 3-7: STAT1$^{-/-}$ mice have increased numbers of microglia in the brain during acute and persistent MuPyV infection. (A) Quantification of microglia at day 8 p.i. by flow cytometry. **(B)** gMFI of MHC II on microglia at 8 days p.i. **(C)** Number of microglia/mm^2 was quantified in FFPE brain sections by an examiner blinded to the identity of the experimental groups. (-) indicates sham infected mice and (+) indicates MuPyV infected mice 30 days p.i. **(D-G)** Representative images of Iba1 staining in FFPE sections from sham infected STAT1$^{-/-}$ mice (E) and MuPyV-infected IFNAR$^{-/-}$ (F) and STAT1$^{-/-}$ (G) mice 30 days p.i. Mean ± SD of 1-11 mice per group from 1-2 independent experiments *P<0.05, **P<0.01, ****P<0.001, One-Way ANOVA (A,B)

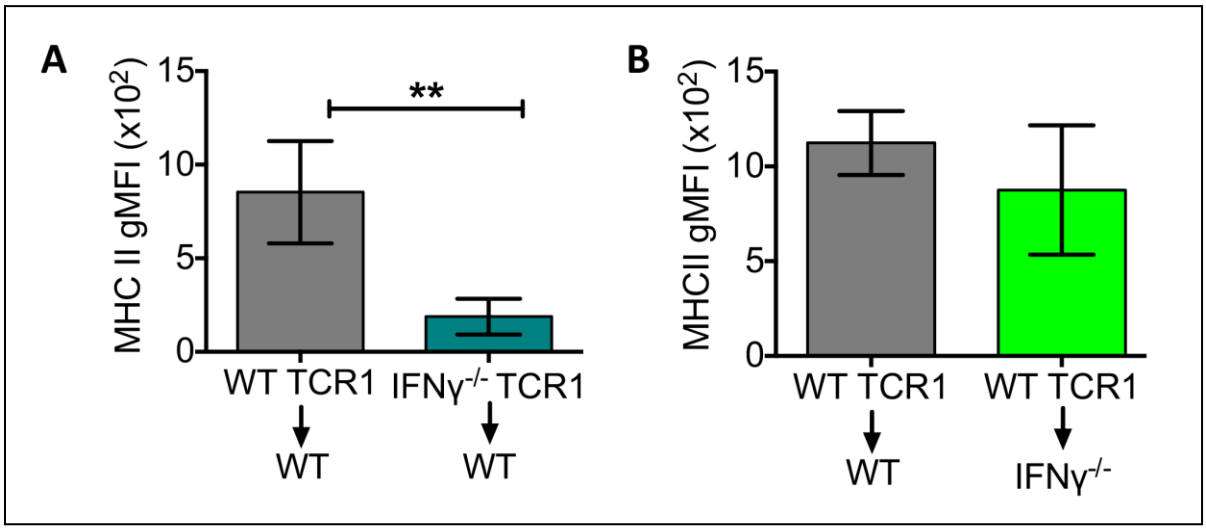

Fig 3-8: IFNγ from virus-specific CD8 T cells upregulates MHC II on microglia. (A) gMFI of MHC II on microglia following i.v. injection of WT TCR1 or IFNγ$^{-/-}$ TCR1 CD8 T cells at 8 days p.i. **(B)** Adoptive transfer of WT TCR1 into IFNγ$^{-/-}$ mice rescues MHC II expression. Mean ± SD of 3-7 mice per group from 1-2 independent experiments (A-D). ***P*<0.01, One-Way ANOVA, Mann Whitney test

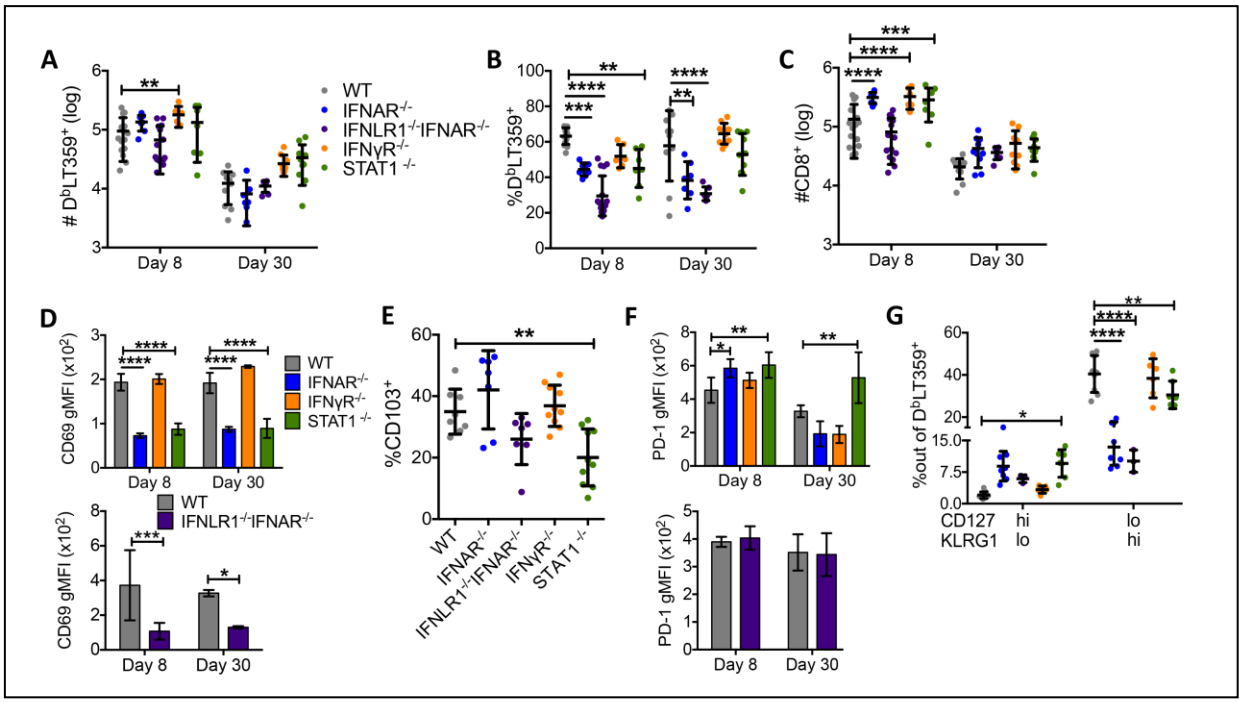

Fig 3-9: Loss of STAT1 signaling disrupts T_{RM}, but not T_{CM}, differentiation. (A,B) Number of total (A) and D^bLT359-specific (B) CD8 T cells from brain at days 8 and 30 p.i. **(C)** Frequency of D^bLT359-specific CD8 T cells from brain at days 8 and 30 p.i. **(D)** CD69 gMFI on D^bLT359-specific CD8 T cells from brain at days 8 and 30 p.i. **(E)** Frequency of $CD103^+$ D^bLT359-specific CD8 T cells in brain at day 30 p.i. **(F)** PD-1 gMFI on D^bLT359-specific CD8 T cells from brain at days 8 and 30 p.i. **(G)** Frequency of $CD127^{hi}KLRG1^{lo}$ and $CD127^{lo}KLRG1^{hi}$ D^bLT359-specific CD8 T cells from spleen at day 8 p.i. Mean ± SD of 4-11 mice per group from 1-2 independent experiments. **P*<0.05, ***P*<0.01, ****P*<0.005, *****P*<0.001, Two-Way ANOVA

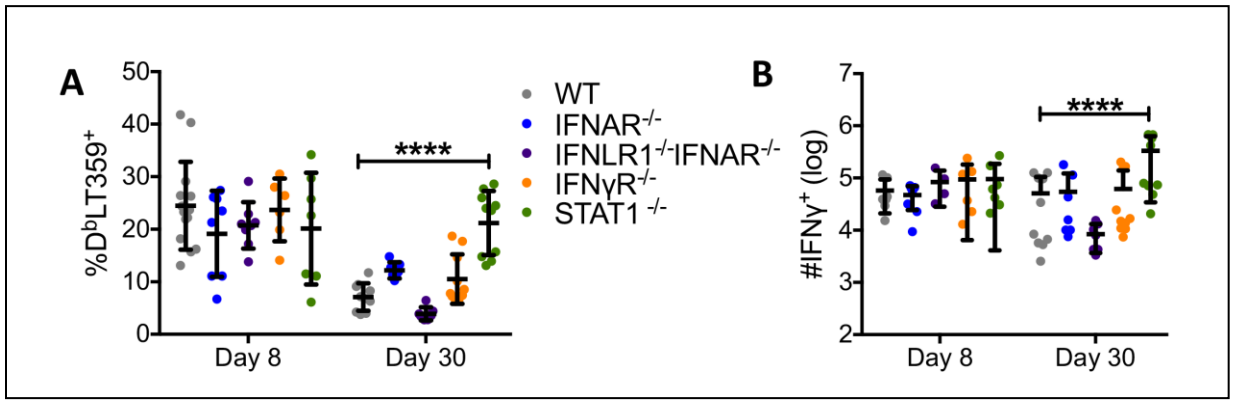

Fig 3-10: D^{b}LT359-specific CD8 T cells have increased function during persistent MuPyV infection in the spleen. (A) Frequency of D^{b}LT359-specific CD8 T cells from spleen at days 8 and 30 p.i. **(B)** Number of IFNγ$^+$ CD8 T cells from spleen at days 8 and 30 p.i. following ex vivo stimulation with LT359 peptide. Mean ± SD of 2-10 mice per group from 1-2 independent experiments. ****P<0.001, Two-Way ANOVA

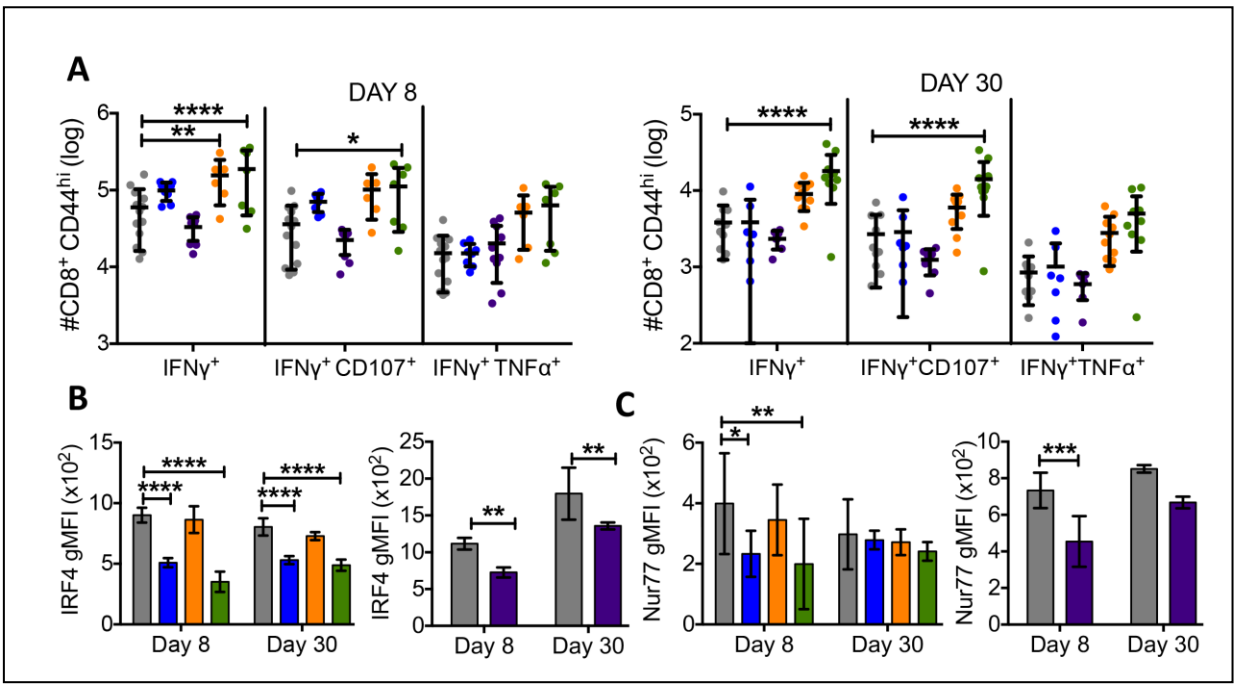

Fig 3-11: STAT1 signaling regulates function of D^bLT359-specific CD8 T cells. (A) Number of IFNγ⁺, IFNγ⁺CD107⁺, and IFNγ⁺TNFα⁺ CD8 T cells from brain at days 8 (left) and 30 (right) p.i. following ex vivo stimulation with LT359 peptide. **(B)** IRF4 gMFI on D^bLT359-specific CD8 T cells. **(C)** Nur77 gMFI on CD8 T cells following ex vivo stimulation with LT359 peptide. Mean ± SD of 2-10 mice per group from 2 independent experiments. **P*<0.05, ***P*<0.01, ****P*<0.005, *****P*<0.001, Two-Way ANOVA

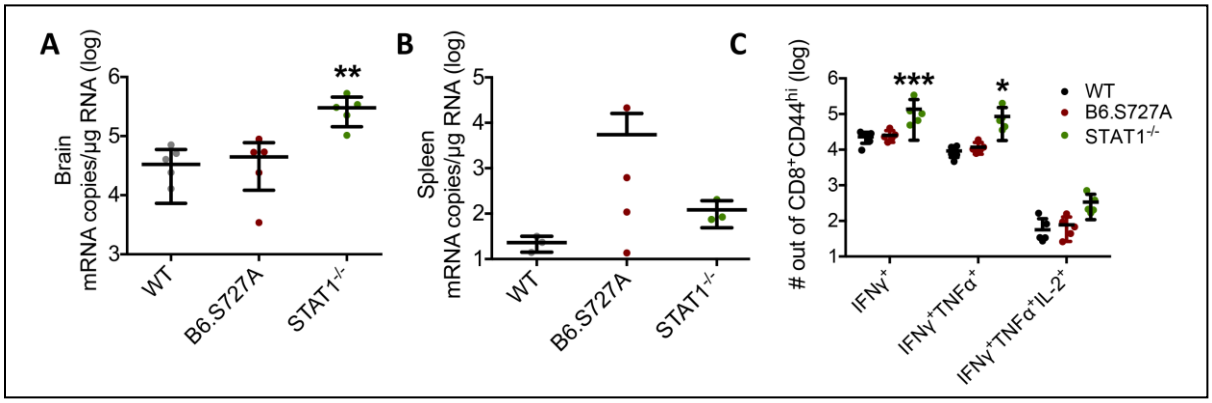

Fig 3-12: Mutated STAT1 binding has no effect on D^bLT359-specific CD8 T cell function.

(A,B) Real-time PCR analysis of viral genome copies in brain (A) and spleen (B) at day 14 p.i. **(C)** Number of $IFN\gamma^+$, $IFN\gamma^+TNF\alpha^+$, and $IFN\gamma^+TNF\alpha^+IL\text{-}2^+$ CD8 T cells from spleen at day 14 p.i. following ex vivo stimulation with LT359 peptide. Mean ± SD of 2-5 mice per group from 1 independent experiment. **P*<0.05, ***P*<0.01, ****P*<0.005, One-Way ANOVA

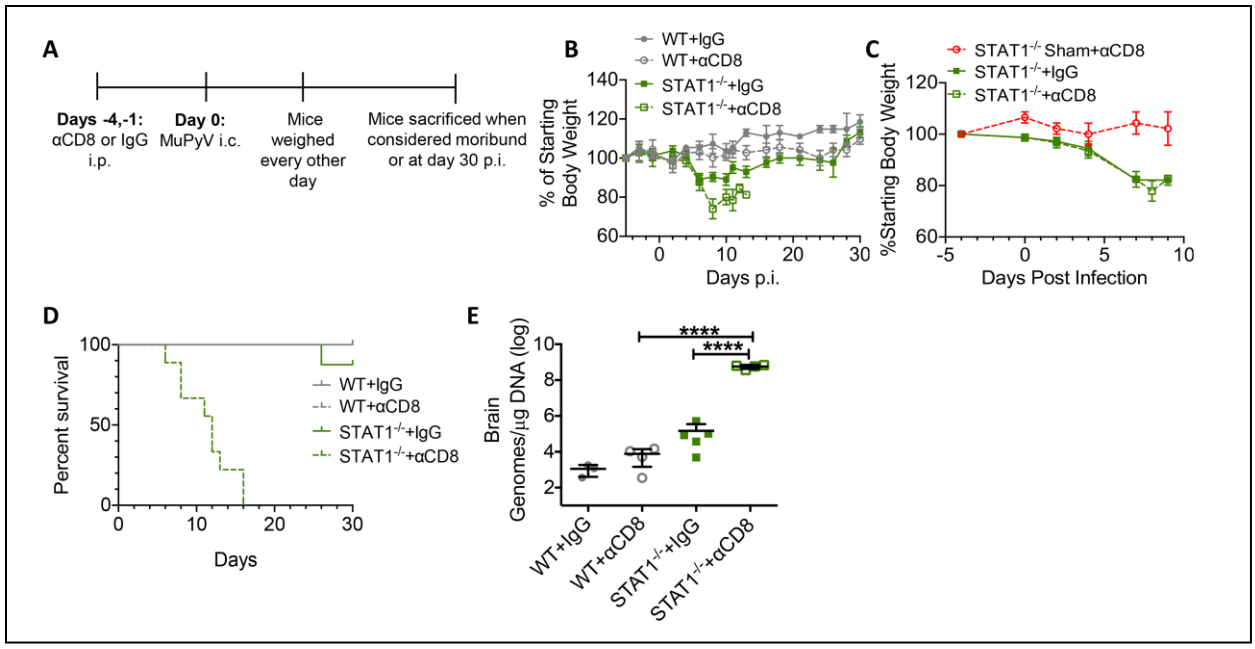

Fig 3-13: T cells are protective in STAT1$^{-/-}$ mice against lethal MuPyV infection. (A) Experimental design. **(B,C)** Percent body weight of female (B) and male (C) STAT1$^{-/-}$ and WT mice following rat IgG or αCD8 treatment. **(D)** Survival curve of STAT1$^{-/-}$ and WT mice following MuPyV infection. **(E)** Real-time PCR analysis of viral genome copies from the brains of STAT1$^{-/-}$ and WT mice sacrificed at terminal endpoint. Mean ± SD of 3-5 mice per group from 1 independent experiment.

Chapter 4

Brain infiltrating T cells protect against MuPyV-induced demyelination

Abstract

PML is marked by significant and diffuse white matter loss that leads to death or severe cognitive dysfunction. The widely held consensus is that JCPyV induces demyelination as a result of the lytic infection of oligodendrocytes, but this assumption is based on JCPyV infection of transformed fetal glial lines and post mortem analyses of PML brains. The sizeable gaps in our knowledge of PML pathogenesis necessitate the development of a tractable animal model. In this study, we document a novel mouse model of i.c. infection with MuPyV that mimics the histopathological hallmarks of PML, such as demyelination and infection of glial cells. Diffusion tensor magnetic resonance imaging (DTI) revealed extensive demyelination and hydrocephalus following MuPyV i.c. infection. Using this MuPyV encephalitis model, we found that demyelination was increased in the absence of infiltrating T cells. Together, these results validate the use of this model for understanding virus-associated demyelination.

4.1 Introduction

In immunocompetent hosts, JCPyV persists as a silent, asymptomatic pathogen in the kidneys, urinary tract, and, potentially, the brain [174, 285]. Upon immunosuppression from HIV/AIDS, immunomodulatory therapies for the treatment of autoimmune diseases, or hematological malignancies, JCPyV can cause the lethal disease PML [217, 286, 287]. Magnetic resonance imaging (MRI) of patients with PML shows single or multiple asymmetric, diffuse areas of demyelination in the subcortical white matter tracts of the brain [227]. This demyelination is thought to arise solely from the infection and death of oligodendrocytes [288]. However, this assumption is largely based on post mortem analyses, which only allow identification of the end stages of disease. The recognition of JCPyV as the causative agent in other neurological diseases, such as JCPyV-GCN, JCPyV-encephalopathy and JCPyV-meningitis, suggests that JCPyV has the capacity to infect multiple cell types of the brain [28, 29]. Elegant work utilizing i.c. infection with JCPyV in human fetal glial chimeric mice, in which human glia differentiated into viable oligodendrocytes and astrocytes in the mouse brain, showed productive infection of glial precursor cells and astrocytes, with oligodendrocytes rarely infected [26, 57]. The human chimeric white matter was demyelinated despite the overwhelming astrocyte-dependent infection [26]. Furthermore, JCPyV productively infects choroid plexus epithelial cells and meningeal cells in culture, suggesting that JCPyV infection of these cells may be an entry point for JCPyV into the brain [289]. In conclusion, these studies demonstrate the diversity of cell types capable of supporting JCPyV infection, and reveal the significant gaps in our understanding of the pathogenesis of PML.

Although once considered rare, interest in PML has grown because the risk of PML increases with the duration of immunomodulatory treatments for autoimmune disease – Natalizumab, an α4 blocking antibody for the treatment of MS, has a risk of 1% with treatment duration of over two years – and nearly all immunomodulatory therapies now come with a risk of PML development [217, 290]. Some of these immunomodulatory treatments target the migration

or function of T cells, and T cell deficiency is a known risk factor for the development of PML. The brain is largely bereft of T cells during homeostatic conditions, but T cells rapidly accumulate in the brain following viral infection. Commonly, antiviral T cells are primed in secondary lymphoid organs and recruited to the infected CNS by chemokine and integrin gradients [137]. Once in the brain, these T cells produce effector cytokines and differentiate into T_{RM}, which remain in the tissue and possess the ability to respond rapidly and specifically to repeat infection [18, 71]. Both peripheral and brain antigen-specific T cells protect the brain following JCPyV infection [43]. The efficacy of T cells in ameliorating PML is shown by improved survival when patients have peripheral JCPyV-specific T cells and worsened survival when mutations arise in the JCPyV epitope that CD4 T cells commonly recognize [31, 43]. However, T cells can also accentuate brain damage during PML. The only available therapy for PML is to reconstitute the immune system, but this can cause PML-IRIS. PML-IRIS is marked by a rapid clinical deterioration despite JCPyV control and a full or partial recovery of the immune system [291]. An increased number of CD8 T cells infiltrate the brain during PML-IRIS, and CD8 T cells are the dominant mononuclear cell infiltrate [49, 292]. Additionally, Granzyme-B^+ CD8 T cells are found juxtaposed to JCPyV-infected oligodendrocytes in the PML-IRIS brain [49]. Thus, T cells represent a double-edged sword in immune-mediated defense of the brain by both improving viral control and exacerbating damage following JCPyV infection.

The rarity of PML and the strict host specificity of PyVs has hampered the study of PML and the development of a tractable animal model. Use of an animal model with an intact immune system and a natural pathogen will help determine the impacts of the immune system and viral infection on the pathogenesis of PyV-associated diseases [140]. Thus, we propose using i.c. injection of MuPyV into mouse brains to study PyV-induced CNS encephalitis. MuPyV is structurally and genetically similar to JCPyV, and establishes a persistent, asymptomatic infection in many organs including the spleen, brain, kidney, and bone marrow [152]. In this study, we evaluated the viability of a novel mouse model of PyV-associated disease and used it

to interrogate the role of T cells in MuPyV-induced disease. We found that MuPyV productively infected glial cells in culture and colocalized with astrocytes and endothelial cells in situ. MuPyV infection demyelinated white matter tracts in the mouse brain, but the damage was predominantly in the caudal sections of the brain. Finally, we found that T cell infiltration is neuroprotective as T cell-deficient mice had worsened pathology and higher viral load. Our work described here validates a mouse model of PyV-associated and underscores the role of T cells in alleviating PyV-associated disease.

4.2 Results and Discussion

4.2.1 MuPyV productively infects brain resident cells.

Because JCPyV shows tropism for oligodendrocytes during PML, we asked if MuPyV is also able to infect cells of oligodendrocyte lineage. Using the conditionally immortalized N19 cell line, we found that MuPyV infected N19 cells *in vitro* **(Fig 4-1)**. It should be noted that the N19 cell line consists of oligodendrocytes at many stages of development, making the identification of the exact cell type infected complex. We next asked if MuPyV was able to infect cells in the brain using immunofluorescent staining for colocalization of VP1 with CNS cell-specific markers: glial fibrillary acidic protein (GFAP) for astrocytes and zonula occludens 1 (ZO-1) for ependymal cells (**Fig 4-2A-C**). Previous work has shown that oligodendrocytes and neurons are not infected by MuPyV (Shwetank et al., submitted). We found that astrocytes and ependymal cells were $VP1^{+}$, demonstrating that these cells are productively infected by MuPyV (**Fig 4-2A-C**).

4.2.2 Damage following MuPyV infection is more apparent in caudal brain sections.

PML is marked by demyelination in the subcortical white matter tracts of the brain [19]. However, the level of demyelination is variable, with some white matter tracts being demyelinated whereas others are largely intact. To investigate the extent of demyelination throughout the mouse brain, representative sections were taken from rostral and caudal areas of the brain. In rostral sections (**Fig 4-3A**), there is limited enlargement of the lateral ventricles and demyelination of the cingulum at 30 days p.i. (**Fig 4-3B & C**). Similar to the cingulum, other white matter tracts, such as those of the basal ganglia, are unaffected by MuPyV infection (**Fig 4-3B & C**). However, demyelination and hydrocephalus are more apparent in the caudal sections of the brain at 30 days p.i. (**Fig 4-3D-H**). In conclusion, these results indicate that MuPyV causes demyelination inconsistently throughout the mouse brain, which reflects current work demonstrating differences in viral control based on brain location [104].

Investigating individual sections of the mouse brain leaves the analysis prone to sampling error. Therefore, we decided to utilize DTI to better demonstrate the heterogeneity of damage resulting from MuPyV infection. Demyelinating lesions identified by MRI are the gold standard of diagnosis of PML, so this approach more closely approximates the human condition [293]. An acknowledged limitation of conventional MRI techniques is the spatial resolution (**Fig 4-4A & B,** [294]). DTI measures the random thermal motion, also called Brownian motion, of water to infer neuroanatomy(**Fig 4-4A & B [294]**). In our study, we have utilized three different parameters to interrogate structural loss following MuPyV infection: fractional anisotropy (FA), relaxation rate (R_2), and mean diffusivity (MD). FA measures the directional average of the diffusion of water. A higher FA indicates a more structured environment. R_2 indicates the rate of how quickly a proton relaxes to the static magnetic field. Thus, a higher R_2 indicates a denser environment. MD is a measurement of how much a proton can diffuse in a given area. A higher MD shows a loss of compartmentalization of the surrounding area. FA, R_2, and MD analyses demonstrate that damage was most evident in the caudal sections of the brain (**Fig 4-5A-C**). The red areas in the FA analysis indicate a loss of orderness of fibers surrounding the dorsal third ventricle (**Fig 4-5A**). R_2 measurements showed edema in the ventricles and white matter tracts such as the corpus callosum, anterior commissure, and fornix (**Fig 4-5B**). Similarly, MD measurements revealed reduced compartmentalization in the caudate and putamen, corpus callosum, fornix, and lateral ventricles (**Fig 4-5C**).

The brain is composed of several evolutionarily defined regions: the forebrain (telencephalon and diencephalon), midbrain (mesencephalon), and hindbrain (metencephalon and myencephalon), with the cerebral cortex being the most evolutionarily recent. The cell types and structures of these regions differ, and the advent of single-cell RNA Seq technologies has allowed the identification of many differentiated, distinct subtypes of neurons, astrocytes, oligodendrocytes, neural stem cells, and ependyma cells in areas once considered cellularly homogenous such as the striatum, mouse cortex, and hippocampus [295-297]. Furthermore, a

large body of research has documented varying degrees of susceptibility to viral infection in different cell types, which is supported by recent work showing the existence of separate immune programs in brain resident cells from evolutionarily distinct CNS regions [104, 298-300]. For example, granule cell neurons from the cerebellum have different innate immune signatures than cortical neurons from the cerebral cortex following infection with positive strand RNA viruses, which affects their susceptibility to infection [298]. Similarly, cerebellar astrocytes from mice and humans showed enhanced IFN responsiveness following WNV infection compared to cortical astrocytes, leading to improved host defense and suppressed neuroinflammation in the hindbrain [104]. Thus, the heterogenous pattern of demyelination we see following MuPyV infection may reflect preferential infection of cells types in the caudal parts of the mouse brain versus those in the rostral sections.

4.2.3 T cells are critical for MuPyV control and promote neuroprotection.

Deficiency in T cell-mediated surveillance of the brain is one of the dominant risk factors for the development of PML [19]. Therefore, we next asked whether T cell deficiency affected the replication of MuPyV and the development of pathology in the CNS using TCR$\alpha^{-/-}$ mice. We found that T cells mediated viral control in the brain, spleen, and kidney (**Fig 4-6A-C**). In the brain, T cell deficiency had no effect on viral load at day 10 p.i., but T cell-deficient mice had increased viral load at days 30 and 60 p.i. (**Fig 4-6A**). In the spleen, however, viral load was significantly or trending higher in T cell-deficient mice across all time points analyzed (**Fig 4-6B**). Similarly, viral load was higher in the kidney during acute and persistent MuPyV in the absence of T cells (**Fig 4-6C**). This discrepancy of viral control in the brain versus the spleen and kidney indicates different methods of viral control. T cell infiltration into the CNS following i.c. inoculation with MuPyV peaks by day 8 p.i., whereas the peak of T cell proliferation in the spleen is earlier [154, 190]. These data show that early MuPyV control in the brain is T cell independent. However, the increased viral load at days 30 and 60 p.i. demonstrate that T cells

are a critical component of antiviral defense during persistent infection. T cell independent control of acute MuPyV infection is supported by data presented in Chapter 3 showing that early MuPyV control is mediated by type I IFNs. Unfortunately, the cell or cells responsible for early MuPyV control in the brain remain unknown. In conclusion, the results discussed in this Chapter and in Chapter 3 show that the brain utilizes different methods of viral control during acute and persistent MuPyV infection.

Due to the higher viral load in TCRα$^{-/-}$ mice at days 30 and 60 p.i., we next asked if TCRα$^{-/-}$ had worsened pathology in the brain. Similar to the results discussed earlier, LFB-PAS staining of brain sections from WT and TCRα$^{-/-}$ mice revealed extensive demyelination in the caudal sections of the brain (**Fig A-7A-H**). Furthermore, T cell-deficient mice had enlarged lateral ventricles and decreased myelination of the cingulum, corpus callosum, and dorsal hippocampal commissure compared to MuPyV-infected WT and sham infected mice at 60 days p.i. (**Fig A-7E-H**). These results suggest that T cell are neuroprotective following MuPyV infection.

4.3 Conclusions

In conclusion, this work describes a novel mouse model of PyV-induced demyelination and encephalitis. Histological and MRI analyses reveal a heterogenous pattern of demyelination and hydrocephalus following MuPyV infection. Similar to risk factors for the development of PML in humans, T cell deficiency worsened disease pathogenesis. The development of this mouse model provides a means of studying the interplay between the bran and PyV and can be used to identify targeted therapies for the treatment of PML.

4.4 Materials and Methods

Mice

Adult (6-12 wks of age) female and male C57BL/6 (B6) mice were purchased from the National Cancer Institute (Frederick, MD). B6.129S2-*Tcra*^{tm1Mom}/J (TCRα$^{-/-}$) mice were purchased from the Jackson Laboratories (Bar Harbor, ME) and bred in house. B6.129S2-*CD8a*^{tm1Mak}/J (CD8α$^{-/-}$) were purchased from the Jackson Laboratories**.** Previous work from our lab has shown that CD8α$^{-/-}$ mice mount a functional D^{b}LT359-restricted response, demonstrating that these mice are not deficient in CD8 T cells (Unpublished data, EL Frost). Mice were bred and housed in accordance with the guidelines of the NIH Guide for the Care and Use of Laboratory Animals and the Institutional Animal Care and Use Committee at the Penn State College of Medicine.

Viruses and Infections

MuPyV.A2 was prepared in baby mouse kidney cells as described [196]. Mice were infected intracerebrally (i.c.) with 3x10^{5} PFU MuPyV.A2 in 30 µL as described [154] or sham infected with 30µL 5% fetal bovine serum (FBS) in media. Mice were infected i.c. with 1.5x10^{7} PFU/mL MuPyV.V296F in 30µL where indicated.

Cell Culture

The N19 oligodendrocyte conditionally immortalized cell line was grown in 10% FBS Hyclone F12-DMEM at 34ºC as described [301]. 48 hours before infection, 5x10^{5} N19 cells were plated onto poly-D-lysine coated 12mm glass coverslips in serum-free Hyclone F12-DMEM to synchronize cell cycle. The cells were infected with 2.5x10^{6} PFU/mL of A2.V296F for 2 hours at 37ºC. After 2 hours, the cells were returned to 10% FBS Hyclone F12-DMEM at 34ºC. 24 hours p.i., the cells were stained with primary antibodies rat anti-VP1 and mouse anti-F4 and secondary antibodies goat anti-rat and goat anti-mouse (Jackson Immunoresearch),

respectively, as published [190]. Slides were imaged on a Leica DM4000 B LED microscope (Leica Microsystems, Buffalo Grove, IL).

Immunofluorescence Microscopy

Mice were perfused with 10mL of 10% heparin in PBS followed by 10mL of 10% NBF 5 days p.i. Brains were post-fixed in 10% NBF overnight. 7μm sections of brain were taken on a microtome by the Comparative Medicine core. FFPE sections were deparaffinized with xylenes and ethanols, underwent antigen retrieval with pH 6.0 10mM sodium citrate buffer at 95ºC, permeabilized with 1% Triton-X in PBS, blocked with 5% BSA in PBS, and stained with the following primary antibodies: goat pAb (polyclonal antibody) to GFAP (Abcam, Cambridge, UK), goat pAb to ZO-1 tight junction protein (Abcam), and rabbit anti-VP1 (Bob Garcea) and the following secondary antibodies: bovine anti-goat and donkey anti-rabbit (Jackson Immunoresearch). Slides were imaged on a Leica DM4000 B LED microscope (Leica Microsystems, Buffalo Grove, IL).

functional MRI

Five MuPyV.V296F inoculated and five sham injected CD8α$^{-/-}$ mice were imaged in a Bruker 7.0 T MRI system 30 days p.i. Animals were anesthetized with 1.5% isoflurane and had their respiration monitored in a heat-controlled environment during imaging. Multi-slice multi-echo T_2 and T_2* images were obtained with nine-echoes and parametric R_2 and R_2* relaxation rate maps were generated. A multi-direction echo planar diffusion sequence with thirty gradient directions was utilized to generate proton fractional anisotropy and diffusivity metrics. Parametric relaxation rate, diffusion, and anatomical images were normalized to a template brain and group based statistical parametric mapping was used to determine significance at a $p < 0.005$ with a 10voxel threshold.

Quantitative PCR

For quantifying viral genome DNA copies, Real-Time® PCR was performed on samples containing 10 ng DNA purified from brain, kidney, and spleen using the Wizard® Genomic DNA Purification Kit (Promega, Madison, WI) as described [200]. Samples were run on an ABI StepOnePlus Real-Time PCR System (ThermoFisher Scientific) and concentrations were calculated based on a standard curve [155].

Histological processing

Mice were perfused with 10mL of 10% heparin in PBS followed by 10mL of 10% NBF. Skulls were post-fixed in 10% NBF overnight and brains excised the next day. 7µm sections of brain were taken on a microtome by the Comparative Medicine core. FFPE sections were stained with LFB-PAS for visualization of myelin fibers and H&E for cell infiltration as described [283]. LFB-PAS-stained sections were digitally imaged on a Keyence BZ-X710 all-in-one fluorescence microscope and stitched together using ImageJ software (National Institutes of Health, Bethesda, MD). Analysis of LFB-stained myelin was performed and analyzed as described [284]. For ventricle size and the white matter tract area, the pixel area of the left and right lateral ventricles or the white matter tract was divided by the total pixel area of the brain section using Adobe Photoshop (San Jose, CA). Ventricle size and corpus callosum area are expressed as a percent of the total brain area.

Statistical Analysis

Experimental data were analyzed on Prism 6.07 (GraphPad, La Jolla, CA) using two-way ANOVA with Tukey or Sidak's multiple comparisons test. Error bars indicate mean $\pm$ SD.

4.5 Figures

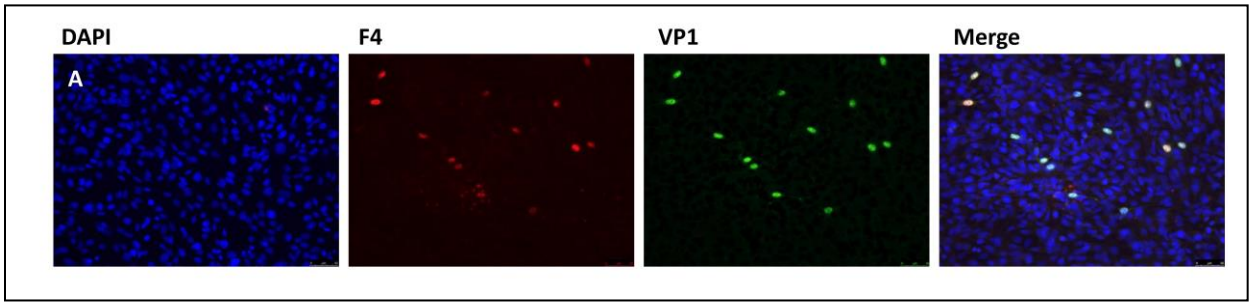

Fig 4-1: MuPyV.V296F infects cells of oligodendrocyte-lineage in culture. (A) N19 cells were serum blocked and infected with MuPyV.V296F. DAPI (blue), F4 (red), and VP1 (green).

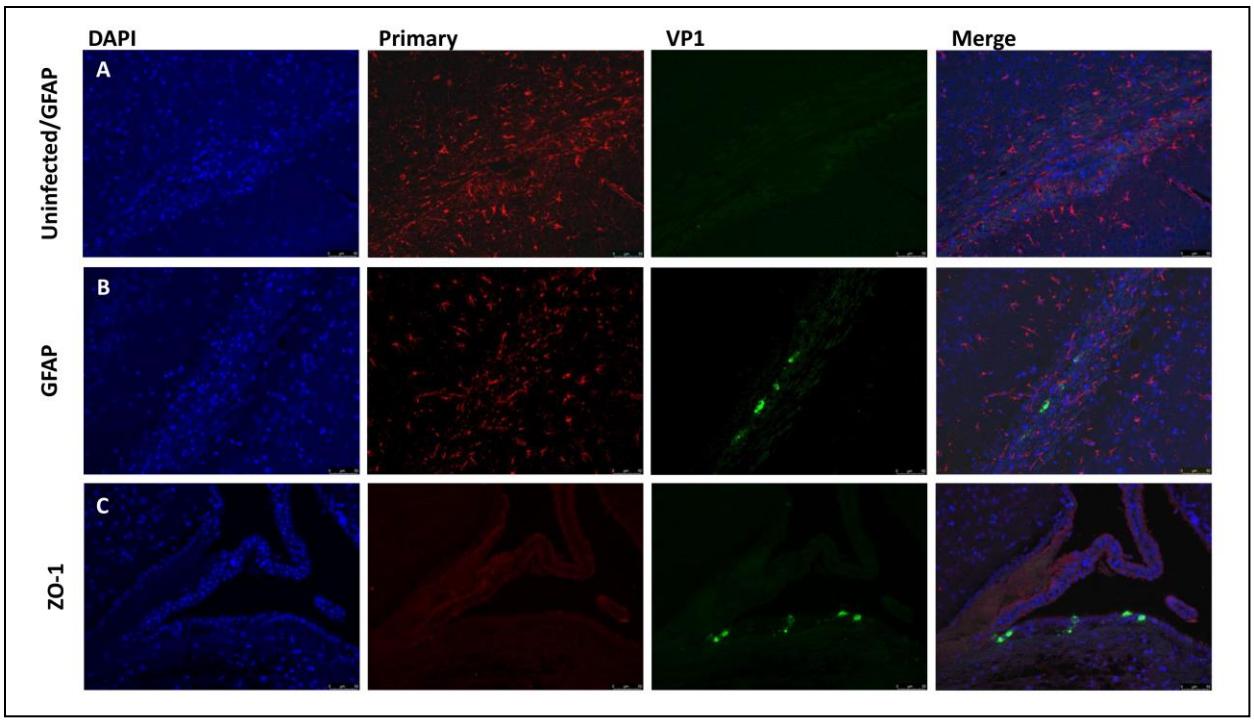

Fig 4-2: MuPyV infects cells in the brain. (A-C) Immunofluorescent staining of MuPyV in TCRα$^{-/-}$ mouse brains 5 days p.i. DAPI (blue), ZO-1 or GFAP (red), and VP1 (green).

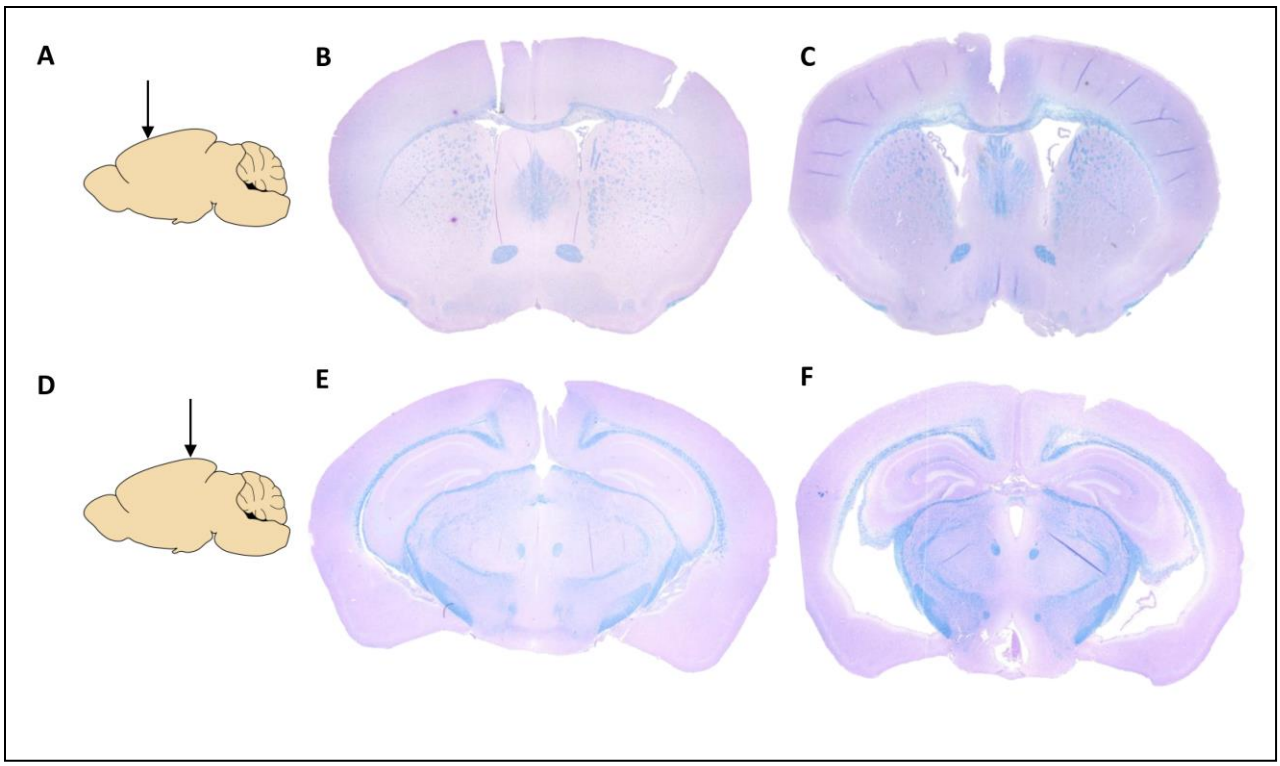

Fig 4-3: Characterization of demyelination following MuPyV inoculation. (A) Approximate location in brain**. (B,C)** Representative LFB-PAS images of sham infected (B) and MuPyV-infected (C) mouse brains at 0.38mm from bregma at 30 days p.i. **(D)** Approximate location in brain. **(E,F)** Representative LFB-PAS images of sham infected (E) and MuPyV-infected (F) mouse brains at -2.70mm from bregma at 30 days p.i.

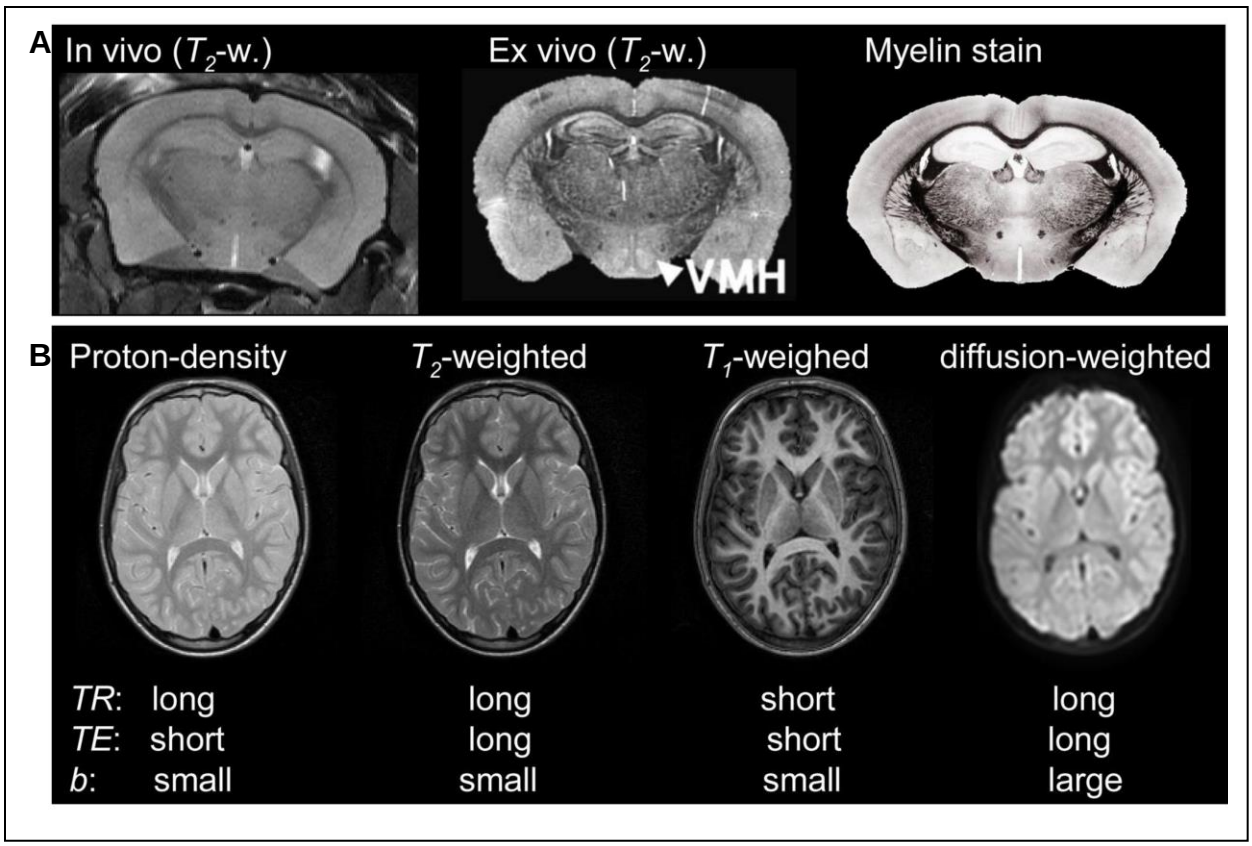

Figure 4-4: Comparison of different types of MRI contrasts. (A) Examples of a(n) conventional MRI (left), ex vivo section (middle), and corresponding histologically stained (right) mouse brain image. **(B)** Examples of human brains analyzed using conventional MRI metrics (proton density, T_2-weighted, and T_1-weighted) versus a DTI image (right) [294].

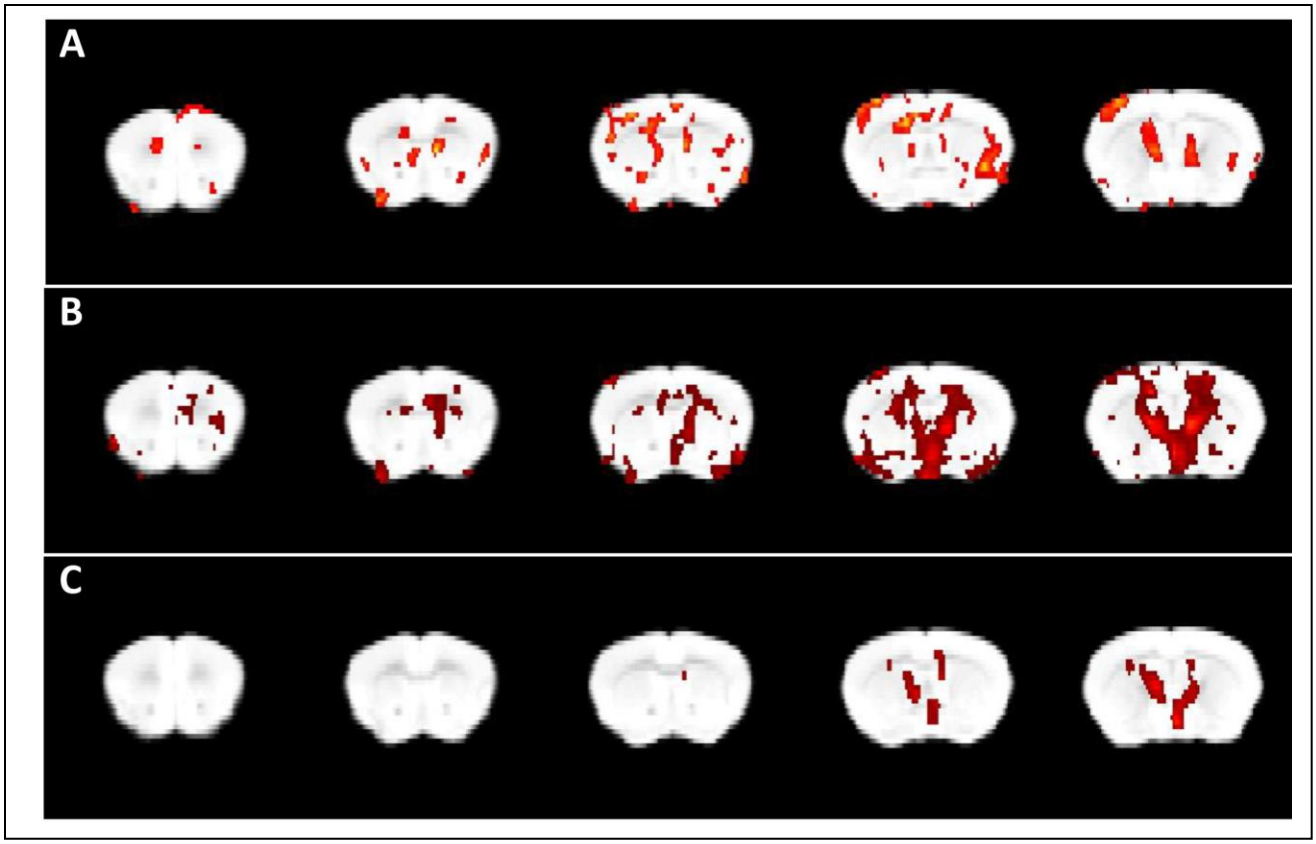

Figure 4-5: Characterization of MuPyV-induced demyelination by DTI. (A) FA images of sham-infected mice overlaid on MuPyV-infected mice. Red indicates significantly increased FA in the sham-infected mice. **(B)** R_2 images of sham-infected mice over MuPyV-infected mice. Red indicates significantly increased R_2 in the sham-infected mice. **(C**) MD images of MuPyV-infected mice over sham-infected mice. Red indicates significantly increased MD in MuPyV-infected mice. n=5 mice per group from 1 independent experiment.

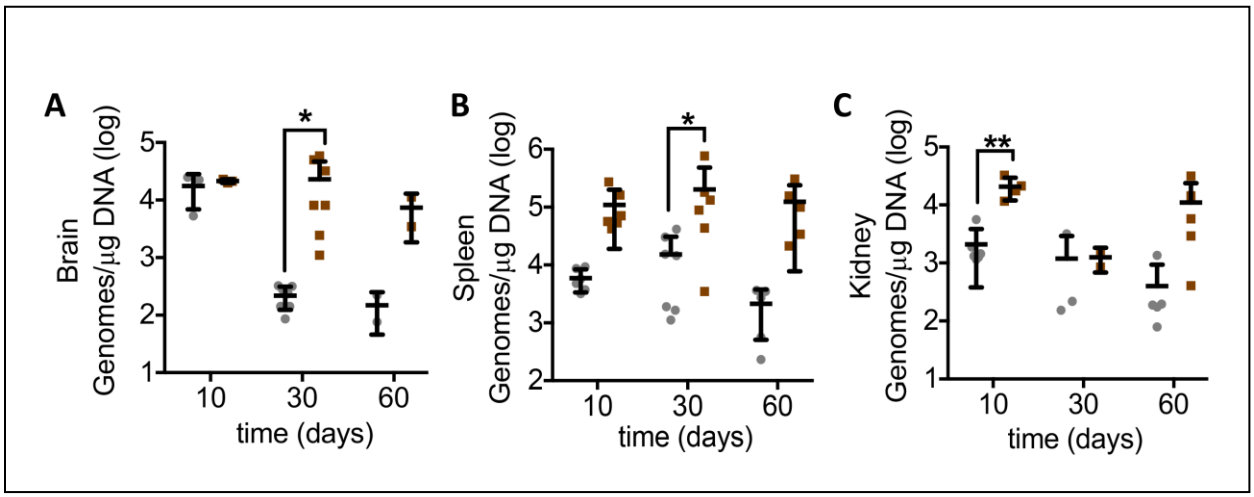

Figure 4-6: MuPyV load in the brains, spleens, and kidneys of WT and TCRα$^{-/-}$ mice during acute and persistent infection. (A-C) Real-time PCR analysis of viral genome copies in brain (A), spleen (B), and kidney (C) at acute (day 10 p.i.) and persistent (days 30 and 60 p.i.) infection. Mean ± SD of 2-7 mice per group from 1-2 independent experiments. *P<0.05, **P<0.01, Two-Way ANOVA

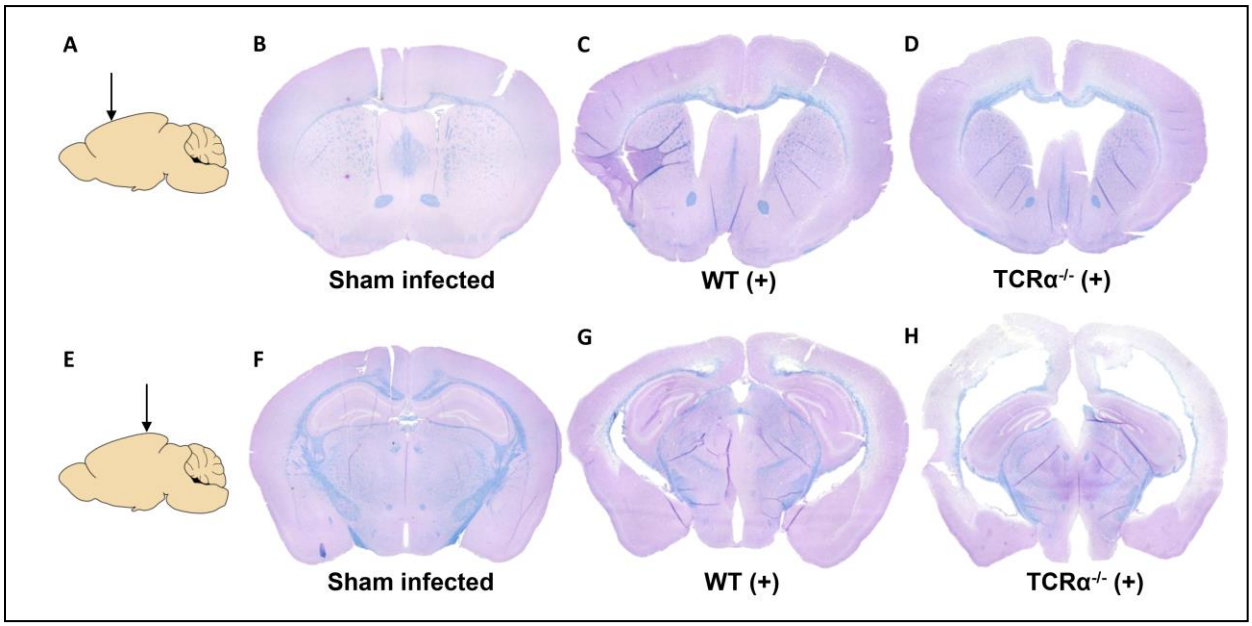

Figure 4-7: Brain integrity in the absence of T cells. (A) Approximate location in brain. **(B-D)** Representative LFB-PAS images of sham infected (B), WT MuPyV-infected (C), and TCRα$^{-/-}$ MuPyV-infected (D) mouse brains at 0.38mm from bregma at 60 days p.i. **(E)** Approximate location in brain. **(F-H**) Representative LFB-PAS images of sham infected (F), WT MuPyV-infected (G), and TCRα$^{-/-}$ MuPyV-infected (H) mouse brains at -2.70mm from bregma at 60 days p.i.

Chapter 5

Discussion

5.1 Overview

The incidence of PML has risen in connection with the increased use of immunomodulatory therapies. However, despite changes in the number of PML cases, the frequency of PML diagnosis among patients receiving immunomodulatory therapies remains relatively low, demonstrating an incomplete understanding of the risk factors predisposing patients to PML. Furthermore, the contribution of the immune system to PML pathogenesis remains poorly defined. In this dissertation, we have discussed three aims that stem from these outstanding questions:

1) Investigate the impact of CD4 T cell deficiency on the magnitude and function of CD8 bT_{RM} cells during persistent MuPyV infection.
2) Elucidate the role of type I, II, and III IFNs on MuPyV infection in the brain.
3) Determine the contribution of T cells and virus to the pathogenesis of MuPyV infection.

5.2 The nature of CD4 T cell help

Naïve CD4 and CD8 T cells receive three signals during priming: stimulation of the TCR by antigen, costimulation via surface receptors such as CD28, and inflammatory cytokines. It is well-documented that the priming of CD8 T cells also requires CD4 T cell help, mostly through CD4 T cell licensing of antigen presenting cells. Licensing of APCs promotes the release of cytokines from and costimulatory receptor expression on APCs, which is required to surpass the higher threshold of activation in naïve CD8 T cells. However, CD4 T cell help is dynamic and is necessary during not only priming but also the effector and memory phases of CD8 T cell differentiation. The continued importance of CD4 T cell help to CD8 T cell responses is underscored by the incidence of PML in HIV/AIDS patients, many of whom may have been previously exposed to JCPyV and should, thus, have memory anti-JCPyV CD8 T cells. In order

to investigate the importance of CD4 T cells to MuPyV control, we used both antibody-mediated depletion of CD4 T cells and mice with genetic deficiencies of CD4 T cells. We found that:

1) CD4 T cells are critical for CD8 bT_{RM} differentiation, as shown by the low expression of CD103 and the dependence of brain unhelped CD8 T cells on circulating CD8 T cells.
2) Unhelped CD8 T cells are functional during acute MuPyV infection in the brain, but fail to control rechallenge.
3) Loss of CD4 T cells causes substantial changes to the transcriptome of CD8 T cells.
4) Acquired CD4 T cell deficiency, modeled by delayed CD4 T cell depletion, also impaired the effector response to reinfection and the differentiation of CD8 bT_{RM}.

Studies investigating the importance of CD4 T cell help to the differentiation of CD8 T_{RM} have overwhelmingly utilized acutely resolving, peripheral viral infections. Similarly, the impact of CD4 T cell deficiency on CD8 bT_{RM} differentiation has also been studied predominately in models of acutely resolving viral infections, and these limited studies have yielded conflicting results as to the role of CD4 T cells in CD8 bT_{RM} differentiation. The study presented in Chapter 2 of this dissertation provides evidence that CD8 bT_{RM} differentiation requires CD4 T cell help before and after CD8 T cells have infiltrated the brain. However, an outstanding question of this study is the nature of CD4 T cell help, which merits further investigation.

We showed that CD4 T cells produced IL-21 upon ex vivo stimulation (**Fig 2-6**). In addition to various CD4 T cells subsets, NK T cells and CD8 T cells are able to produce IL-21 [302]. The IL-21R is expressed on several cell types, including NK cells, CD8 T cells, and CD4 T cells, and signals through the Jak/STAT pathway, predominately involving STAT3 [302]. IL-21 has been shown to have effects on CD8 T cell function and memory development during acute and chronic viral infections. For example, IL-21 promoted development of memory CD8 T cells and the generation of recall responses in CD8 T cells following acute LCMV and vaccinia virus infection [303, 304]. Similarly, during coronavirus infection in the brain, IL-21R deficiency

impaired the effector activity of CD8 T cells and made the normally acute coronavirus infection persistent, despite similar numbers of CD8 T cells in the brain between IL-21-sufficient and -deficient mice [305]. CD4 T cells were found to produce IL-21 during coronavirus infection [306]. IL-21 production is increased during chronic viral infections compared to acute viral infections, and may play a more prominent role in CD8 T cell function during persistent viral infections. Indeed, a trio of reports documented that IL-21, likely produced by CD4 T cells, supports CD8 T cell function during chronic LCMV infection [182, 183, 307]. Additionally, IL-21 also affects CD8 T_{RM} development, as demonstrated by decreased CD103 expression on IL-21-deficient CD8 T cells in the small intestine during lymphopenia-induced homeostatic proliferation [158]. These studies suggest that IL-21 from CD4 T cells may directly contribute to the development of MuPyV-specific CD8 bT_{RM} during persistent viral infection.

In addition to IL-21, CD4 T cells were found to produce TGFβ upon ex vivo stimulation, with the peak of TGFβ production occurring at day 15 p.i. (**Fig 2-6**). TGFβ upregulates the expression of CD103 and negatively regulates T-bet and *Klf2* expression – the downregulation of these factors is required for the differentiation of T_{RM} and the loss of TGFβR reduces the ability of CD8 T cells to become T_{RM} [70, 308-310]. However, not all CD8 T_{RM} require TGFβ, as shown by the development and maintenance of a TGFβR-deficient $CD103^{-}$ T_{RM} population in the gut following *Yersinia pseudotuberculosis* infection [311]. TGFβ is expressed by CD4 T cells and nearly every other cell in the body, including brain-resident cells. Although previous work has shown that WNV-specific CD8 bT_{RM} require TGFβ from regulatory CD4 T cells, the formation of HSV-specific CD8 T_{RM} required infiltration into the skin epithelium, suggesting that local TGFβ production also affects T_{RM} development [157, 195]. In our model, the peak of TGFβ production from CD4 T cells coincides with the upregulation of CD103, but this production was assayed ex vivo following TCR-independent stimulation with PMA/ionomycin, which may not reflect TGFβ production in vivo. Furthermore, helped and unhelped CD8 T cells had similar expression of T-bet, suggesting that TGFβ may not be important for MuPyV-specific CD8 bT_{RM}

development (**Fig 2-2**). These studies and our data leave us with outstanding questions regarding the role of TGFβ in bT_{RM} development: 1) Are CD8 T cells responsive to TGFβ? 2) What cells produce TGFβ in the brain? 3) What is the timeline of CD4 T cell production of TGFβ? Because a complete loss of TGFβR signaling causes embryonic lethality, the studies needed to answer these questions must be completed in mice with conditional knockouts of TGFβR or TGFβ in CD8 T cells and conditional loss of TGFβ production inCD4 T cells, neurons, and glial cells.

5.2.1 Novel targets of CD4 T cell help from RNA Seq

RNA Seq analysis of unhelped CD8 T cells revealed differential expression of Runx3 (**Table 2-1**). The Runx family of transcription factors is composed of three evolutionarily conserved proteins: Runx1, Runx2, and Runx3 [312]. Runx3 expression in CD8 T cells is important for many stages of development. Runx1 and Runx3 expression are critical for *Cd4* silencing during the development of CD8 single positive cells and in mature CD8 T cells, as demonstrated by the development of a T_{FH} phenotype and reduced effector function in mature CD8 T cells with targeted deletion in Runx3 [313-315]. Despite relatively uniform expression of Runx3 in circulating and resident CD8 T cells, Runx3 deficiency resulted in a 2-6 fold loss of splenocytes and a 50-150 fold loss of barrier and non-barrier $CD69^{+}CD103^{+}$ T_{RM} following LCMV Armstrong infection, demonstrating that Runx3 is a central regulator of T_{RM} homeostasis [167]. However, the factor or factors regulating Runx3 expression remain largely unknown. IL-7 signaling was found to be essential for Runx3 upregulation in differentiating CD8 single positive thymocytes, but the effect of IL-7 on Runx3 expression during memory formation is unknown [316]. Runx3 expression was reduced in unhelped memory CD8 T cells primed with neem leaf glycoprotein vaccine as protection against sarcoma tumors, suggesting that CD4 T cells may play a role in Runx3 expression, but the factors produced by CD4 T cells that impact Runx3 expression remain unknown [317]. More studies are needed to understand the regulation of

Runx3. IL-7 is a member of the common γ chain receptor cytokine family, and other members of that family, such as IL-15 and IL-21, have been implicated in the differentiation of T_{RM}, similar to IL-7 itself [158, 195, 318, 319]. Furthermore, IL-7 and its isoforms are tonically made in the brain. Additionally, the seminal study documenting the role of Runx3 in T_{RM} differentiation used an adoptive transfer model of P14 T cell receptor transgenic CD8 T cells, which are uniformly specific for the GP_{33-41} epitope of LCMV [167]. Future studies could focus on the role of Runx3 in persistent viral infections, such as MuPyV, and in a polyclonal CD8 T cell response. Other studies could investigate the cytokines that affect the expression of Runx3, beginning with the common γ chain receptor family.

RNA Seq analyses also revealed differential expression of components of the RhoA and Cell-division cycle 42 (Cdc42) signaling pathways (**Fig 2-12**). RhoA and Cdc42 are members of the Ro GTPase subfamily in the Ras GTPase superfamily [320]. The Ras superfamily has more than 150 members, which are involved in virtually all cellular processes [320]. Deletion of members of the Rho subfamily have shown that Rho GTPases regulate numerous aspects of T cell development [321]. For example, deletion of Rac1 and Rac2, also Rho GTPases, arrests T cell development at the double negative thymocyte stage, whereas Cdc42 deficiency increases the number of double positive thymocytes [322, 323]. Rho GTPases are also important components of downstream signaling cascades from chemokine receptors responsible for the transendothelial migration of T cells into organs. RhoA and Rac1 are important downstream regulators in LFA-1 and VLA-4 signal transduction, which are required for entry into the brain [321]. Furthermore, after TCR engagement, RhoA and Cdc42 localize to the immunological synapse and serve various roles in the regulation of calcium signaling and TCR-induced proliferation, among others [321]. Recently, studies have identified aberrations in Rho GTPases, especially RhoA, as key drivers of CD4 T cell dysfunction in autoimmune disease and cancer. For example, the RhoA pathway is elevated in CD4 T cells isolated from patients with SLE and RA compared to patients without disease, and this change is thought to underlie the increased

differentiation of T_H17 CD4 T cells [324]. Similarly, exome sequencing of patients with angioimmunoblastic T cell lymphoma revealed mutations in RhoA, and similar mutations in mature murine cells caused abnormal CD4 T cell differentiation [325]. Collectively, these studies demonstrate the importance of RhoA to T cell development and homeostasis. However, the role of Rho GTPases on CD8 T cell memory differentiation remains unclear. Our finding that pathways involving two Rho GTPase family members, RhoA and Cdc42, and the regulatory factor Rho-GDI were differentially regulated in unhelped CD8 T cells suggests that CD4 T cells may regulate Rho GTPases in CD8 T cells. It is known that expression of Rho GTPases is susceptible to signaling from numerous cytokines, so future studies could focus on the regulation of Rho GTPases from CD4 T cell-derived cytokines, such as IL-21 [321]. Unfortunately, due to the ubiquitous expression of RhoA and Cdc42, RhoA or Cdc42 KO mice exhibit deficits in heart, vascular, and craniofacial development, in addition to the impact on CD8 T cell development. Thus, conditional knockouts of RhoA and Cdc42 in CD8 T cells specifically should be used to investigate the effect of Rho GTPase family members on CD8 T cell memory differentiation and migration.

5.3 STAT1 signaling in brain resident cells

IFNs program a state of antiviral resistance in infected cells and modulate the immune response to better target infection. The three members of the IFN family signal through disparate receptors, but downstream signaling of type I, II, and III IFNs involve STAT1. The translocation of STAT1 to the nucleus induces the transcription of ISGs. Type I and II IFNs have been shown to impede MuPyV replication in vitro, but their efficiency in the brain has not been tested. In this dissertation, we investigated the role of type I, II, and III IFNs on MuPyV replication in the brain and found that:

1) IFNs are most important for viral control during acute viral infection

2) Global STAT1 deficiency leads to widespread hydrocephalus in the infected mouse brain, and loss of STAT1 in infected cells also contributes to hydrocephalus
3) STAT1 restrains immune cell infiltration and cytotoxic potential of CD8 T cells

These results suggest that STAT1 is a central mediator of neuroinflammation in the brain, but its mechanism remains unknown.

Although STAT1 is considered the canonical IFN transcription factor, it is also involved in the signaling pathways of many other cytokines and growth factors (**Table 5-1**). Brain resident cells rely on the growth factors and cytokines that signal through STAT1 during homeostatic conditions, and they exhibit differential susceptibility to STAT1 activation during inflammatory insult. For example, mice with STAT1 deficiency in astrocytes during *T. gondii* infection have increased brain parasite burden, numbers of cysts in astrocytes, and incidence of astrocyte death, demonstrating that STAT1 in astrocytes promotes anti-parasitic defense [326]. IFNγ from antiviral T cells noncytopathically cleared LCMV infection in microglia via activation of STAT1, raising the possibility that STAT1 induces an antiviral state in microglia, similar to astrocytes [189]. During EAE, however, STAT1-deficient mature oligodendrocytes had reduced apoptosis and the brains of these mice had increased myelination, suggesting that STAT1 activation in oligodendrocytes is harmful [327]. Similarly, STAT1 signaling in OPCs induced cell death and inhibited maturation of OPCs following IFNγ stimulation of cultured OPCs [328]. Neuronal STAT1 signaling and downstream CCL2 expression during CNS infection with attenuated LCMV-Armstrong drove synaptic loss by attracting phagocytes to infected neurons [244]. These results demonstrate that STAT1 is a pleiotropic transcription factor. In our model, the brains of $STAT1^{-/-}$ mice were marked by diffuse hydrocephalus following MuPyV infection (**Fig 3-1 & 2**). Hydrocephalus usually results from aberrant ependyma function, and ependymal cells receive trophic support from many other brain resident cells [267]. Thus, the damage that we see in the brains of MuPyV-infected $STAT1^{-/-}$ mice could therefore be a result of STAT1 deficiency in

ependymal cells and other cells of the brain [329]. Conditional knockout of STAT1 signaling in various brain resident cell subsets is necessary to identify where STAT1 deficiency is most detrimental. Extensive phenotyping has revealed cell-specific markers such as GFAP (astrocytes), NeuN (neuronal nuclei, neurons), PDGFRα (OPCs), Nfix (ependyma), MBP (myelin basic protein, oligodendroyctes), CX3CR1 (fractalkine receptor, microglia), and VEGF 2 (endothelial cells), which provide targets to generate conditional knockouts in specific cells.

5.3.1 Type III IFNs at barrier surfaces of the brain

Barrier surfaces, such as the ependymal lining of the ventricles, the choroid plexus, the cells lining the vasculature of the brain, and the endothelial cells of the BBB, provide important immunological protection against virus infection [122]. These barrier cells, mainly endothelial cells of the BBB, primarily utilize type III IFNs, and recent work has shown that type III IFNs provide noninflammatory, early antiviral protection [330]. Although thereasons for the predominance of type III IFN responsiveness and expression in barrier cells are unknown, it is thought to arise from the high number of peroxisomes in polarized cells [331]. IFNλ is induced by peroxisome-associated mitochondrial antiviral signaling proteins (MAVs) [331]. Similar to other organs, viral infection induces the expression of type III IFNs in the brain, which restrict viral infection through ISG-dependent mechanisms in BBB cells and, uniquely, by increasing endothelial barrier properties [122]. In addition to promoting antiviral defense in barrier organs, IFNλ acts as an immunomodulatory agent on neutrophils by limiting reactive oxygen species production and degranulation following infection of the intestine and during the development of collagen-induced arthritis [125, 332]. IFNλ was also found to affect CD8 T cell responses, but the effect depended on the chronicity of infection [130]. For example, IFNλ reduced CD8 T cell numbers during chronic LCMV infection, but amplified T cell responses during acute LCMV infection [130]. However, despite these studies, the roles of type III IFNs on the immune

response and ependymal cells remains largely unknown. Overall, ependymal cells are largely understudied and they are often discussed similarly to endothelial cells of the brain despite being of different lineages [267]. Thus, future studies should focus on the role of IFNλ in restraining the immune response to MuPyV, particularly given our results of increased neutrophil infiltration in the absence of STAT1. Additional studies should focus on the integrity of the CSF- and blood- brain barriers in the absence of type III IFNs, especially given the characterization of JCPyV infection of barrier cells of the brain [333].

5.4 The role of T cells in brain neuroinflammation and homeostasis

Human PyVs have evolved with their host, conferring strict host specificity. The use of the mouse as our animal mode allowed us to investigate host interactions with a naturally occurring mouse pathogen, MuPyV. Just as in human PyV infection, MuPyV persistsand a strong adaptive immune response, orchestrated mainly by CD8 T cells, confers anti-PyV immunity. Using this MuPyV encephalitis model, we found that:

1) MuPyV shows tropism for astrocytes and ependymal cells.
2) Damage from MuPyV infection is predominately seen in the caudal regions of the brain, but other parts of the brain show changes. The pathology resulting from MuPyV brain infection is evident using histopathological and imaging methods.
3) Brain-infiltrating T cells regulate MuPyV control and are neuroprotective.

These results mimic the role of T cells in other neurodegenerative and inflammatory conditions of the brain.

Under homeostatic conditions, the adaptive immune system has profound effects on cognitive processes [334]. T cell deficiency in the brain, by either genetic deficiency or by blocking T cell trafficking, impaired learning and memory [335, 336]. T cell-derived cytokine release of IL-4, IL-13, and IFNγ was found to mediate the effects of T cells on learning and

memory [121, 336]. Performance of cognitive tasks led to the accumulation of IL-4$^+$ T cells in the meninges, and IL-4 and IL-13 stimulated astrocyte production of brain-derived neurotrophic factor (BDNF) [336, 338]. Recently, direct signaling of IFNγ to receptors on GABAergic cortical interneurons increased inhibitory neurotransmitter release, demonstrating a novel role for T cells in the regulation of neuronal circuits [121]. However, the presence of T cells and their cytokine release is not always neuroprotective. Aberrant T cell function and IL-17 release during maternal immune activation caused fetal cortical malformations and led to long-lasting altered social behaviors [339]. Similarly, the vegetative symptoms of major depression correlate with increased production of IL-1 and IL-6 [340]. T cell-derived cytokines that affect CNS function are not only limited to those discussed here, and the proper balance of these cytokines regulates the homeostatic checkpoint of the CNS and, thus, the entire body.

The recent discovery of lymphatics in the meninges underscores the role of T cells in CNS physiology, but the brain parenchyma is mostly excluded from peripheral immune surveillance under homeostatic conditions [334]. However, the cytokines, chemokines, and integrins released during viral infection of the CNS allow virus-specific effector T cells to bypass the anatomic barriers that separate the immune compartment by modulating the permeability of the BBB and specifically recruiting T cells to the brain parenchyma [137, 341]. These infiltrating T cells, especially CD8 T cells, contribute substantially to virus clearance by cytolytic mechanisms, i.e., perforin and Granzyme-B production, cytokine-dependent pathways, such as IFNγ and TNFα release, and the recruitment of other peripheral immune cells [87, 342, 343]. The ability of T cells to control neurotropic and gliotropic infections is demonstrated by unchecked viremia in mice lacking T cells or their effector molecules [344]. However, the brain is largely intolerant of adaptive immune activity presumptively due to an abundance of terminally differentiated, non-renewable cells [345]. For example, CD8 T cell release of IFNγ to LCMV-infected neurons promoted dendrite and synapse loss, demonstrating the severe, immunopathological consequences of LCMV clearance [346, 347]. In addition to neuronal loss,

demyelination of the CNS is a common pathological feature in mice infected with a variety of viruses, and this demyelination is thought to be mostly immune-mediated [281]. Indeed, CD4 and CD8 T cells responding to CNS infection by JHMV are independently capable of demyelination, as demonstrated by demyelination following depletion of either CD4 or CD8 T cells [281]. Similarly, reconstitution of the immune system during PML promotes the infiltration of immune cells, mostly CD8 T cells, into the CNS. These infiltrating T cells efficiently control JCPyV infection, but promote cell death as a complication of PML called PML-IRIS [50]. Collectively, these studies indicate a fine balance of T cells in the CNS between promoting catastrophic damage and maintaining homeostasis.

Contrary to the role of T cells during PML-IRIS, our results indicated that T cells are protective during MuPyV infection. However, the exact effector mechanisms and T cell subsets that control MuPyV in the brain remain unknown. Although we have previously shown that IFNγ confers anti-PyV immunity in peripheral organs, further studies could identify mechanisms of CNS viral control, as IFNγ was found not to regulate MuPyV replication in the CNS (Chapter 3) [58]. Additionally, as we have already discussed the role of CD4 T cells in MuPyV control in the CNS in this dissertation, future studies of CD8 T cell depletion alone could illuminate the contribution of CD8 T cells to brain MuPyV infection. We have also not pursued any behavioral analyses of MuPyV-infected animals. Thus, future studies could investigate the impact of T cell deficiency on behavior, which may provide a more complete understanding of the neurological sequelae resulting from MuPyV infection. Finally, T cells are critical for the recruitment of innate immune cells into the CNS during viral infection. Future studies could analyze the quality of, the factors responsible for the recruitment of, and the impact of innate immune cell infiltration into the CNS during MuPyV encephalitis.

5.5 Conclusion

In this dissertation, we have explored three central questions with the goal of elucidating the components of host defense against PyV infection of the brain:

1) Are CD4 T cells necessary for the development of CD8 bT_{RM} during persistent MuPyV infection?
2) What is the effect of type I, II, and III IFNs on MuPyV infection in the brain and the immune response?
3) Can we develop a mouse model that mimics PyV-associated encephalitis?

In Chapter 2, we show that CD4 T cells are necessary for the generation of stable and functional CD8 bT_{RM}. In Chapter 3, we found that STAT1 mediates critical anti-PyV control. In Chapter 4, we demonstrate the phenotype of a novel mouse model of PyV-induced encephalitis. Overall, we show that defense against polyomavirus infection is orchestrated at many levels, such as through the interactions of cells in the adaptive immune response and through cytokine pathways, suggesting that therapies to alleviate polyomavirus-associated diseases need to reflect the multifaceted aspects of anti-PyV defense.

The data presented in this dissertation raise several questions regarding host defense against PyV infection in the brain, which merit further discussion. First, can therapies promoting CD4 T cell function, instead of the entire immune response, improve PML prognosis? Similarly, can reconstituting CD4 T cells promote CD8 T_{RM} responses in JCPyV infected individuals? Given the absence of pathology in mice deficient in IFNs, how is STAT1 inhibiting pathology in MuPyV-infected mice? Additionally, is the antiviral mechanism employed against JCPyV dependent on the cell type infected? Finally, there are many outstanding questions regarding PyV infection in the brain. This work indicates that ependymal cells and astrocytes are the predominant cell type infected by MuPyV in the brain. Thus, how does the infection of these cell

types affect demyelination and development of pathology? Additionally, could therapies that promote an antiviral state in these cells decrease the incidence of PML in at risk populations?

Due to the increasing use of immunomodulatory therapies, PML poses a significant and increasing health risk. Understanding of PyV pathogenesis in the brain and the contribution of the immune response to PyV defense is vital to better assess risk of PML in patients receiving immunosuppressive regiments and to decrease the morbidity and mortality of PML.

Family name	Members that Use STAT1
Interferon family	Type I, II, and III IFNs
Receptor Tyrosine Kinases	EGF, platelet derived growth factor, stem cell factor, macrophage colony stimulating factor, fibroblast growth factor, brain-derived neurotrophic factor, VEGF, hepatocyte growth factor
Homodimeric Hormone Receptors	Growth hormone, thrombopoietin, erythropoietin, prolactin
Common beta chain receptor family	IL-3, granulocyte macrophage colony-stimulating factor
Common gamma chain receptor family	IL-2, IL-4, IL-7, IL-9, IL-13, IL-15, IL-21
IL-6 family	IL-6, IL-11, ciliary neurotrophic factor, leukemia inhibitory factor, granulocyte-colony stimulating factor
IL-10 family	IL-10, IL-22, IL-24,
IL-12 family	IL-12, IL-23, IL-27, IL-35
G Protein-Coupled Receptors	Angiotensin, serotonin, coagulation factor II, catecholamines, CXCL12, CCL12, CCL5, CCL15

Table 5-1: Signaling pathways involving STAT1. Table representing the families and members of that family that use STAT1 in their downstream signaling.

References

1. Louveau A, Smirnov I, Keyes TJ, Eccles JD, Rouhani SJ, Peske JD, et al. Structural and functional features of central nervous system lymphatic vessels. Nature. 2015;523(7560):337-41. Epub 2015/06/01. doi: 10.1038/nature14432. PubMed PMID: 26030524; PubMed Central PMCID: PMCPMC4506234.
2. Nayak D, Zinselmeyer BH, Corps KN, McGavern DB. In vivo dynamics of innate immune sentinels in the CNS. Intravital. 2012;1(2):95-106. doi: 10.4161/intv.22823. PubMed PMID: 24078900; PubMed Central PMCID: PMCPMC3784260.
3. Nayak D, Roth TL, McGavern DB. Microglia development and function. Annu Rev Immunol. 2014;32:367-402. Epub 2014/01/22. doi: 10.1146/annurev-immunol-032713-120240. PubMed PMID: 24471431; PubMed Central PMCID: PMCPMC5001846.
4. Ransohoff RM, Brown MA. Innate immunity in the central nervous system. J Clin Invest. 2012;122(4):1164-71. Epub 2012/04/02. doi: 10.1172/JCI58644. PubMed PMID: 22466658; PubMed Central PMCID: PMCPMC3314450.
5. Trang T, Beggs S, Salter MW. Brain-derived neurotrophic factor from microglia: a molecular substrate for neuropathic pain. Neuron Glia Biol. 2011;7(1):99-108. Epub 2012/05/22. doi: 10.1017/S1740925X12000087. PubMed PMID: 22613083; PubMed Central PMCID: PMCPMC3748035.
6. Nakajima K, Honda S, Tohyama Y, Imai Y, Kohsaka S, Kurihara T. Neurotrophin secretion from cultured microglia. J Neurosci Res. 2001;65(4):322-31. doi: 10.1002/jnr.1157. PubMed PMID: 11494368.
7. Eroglu C, Barres BA. Regulation of synaptic connectivity by glia. Nature. 2010;468(7321):223-31. doi: 10.1038/nature09612. PubMed PMID: 21068831; PubMed Central PMCID: PMCPMC4431554.
8. Attwell D, Buchan AM, Charpak S, Lauritzen M, Macvicar BA, Newman EA. Glial and neuronal control of brain blood flow. Nature. 2010;468(7321):232-43. doi: 10.1038/nature09613. PubMed PMID: 21068832; PubMed Central PMCID: PMCPMC3206737.
9. McKimmie CS, Graham GJ. Astrocytes modulate the chemokine network in a pathogen-specific manner. Biochem Biophys Res Commun. 2010;394(4):1006-11. Epub 2010/03/21. doi: 10.1016/j.bbrc.2010.03.111. PubMed PMID: 20331977.
10. Yuan J, Liu W, Zhu H, Chen Y, Zhang X, Li L, et al. Curcumin inhibits glial scar formation by suppressing astrocyte-induced inflammation and fibrosis in vitro and in vivo. Brain Res. 2017;1655:90-103. Epub 2016/11/16. doi: 10.1016/j.brainres.2016.11.002. PubMed PMID: 27865778.
11. Mayhan WG. Regulation of blood-brain barrier permeability. Microcirculation. 2001;8(2):89-104. PubMed PMID: 11379794.
12. Abbott NJ, Patabendige AA, Dolman DE, Yusof SR, Begley DJ. Structure and function of the blood-brain barrier. Neurobiol Dis. 2010;37(1):13-25. Epub 2009/08/05. doi: 10.1016/j.nbd.2009.07.030. PubMed PMID: 19664713.
13. Soung A, Klein RS. Viral Encephalitis and Neurologic Diseases: Focus on Astrocytes. Trends Mol Med. 2018;24(11):950-62. Epub 2018/10/09. doi: 10.1016/j.molmed.2018.09.001. PubMed PMID: 30314877.
14. Miller KD, Schnell MJ, Rall GF. Keeping it in check: chronic viral infection and antiviral immunity in the brain. Nat Rev Neurosci. 2016;17(12):766-76. Epub 2016/11/04. doi: 10.1038/nrn.2016.140. PubMed PMID: 27811921; PubMed Central PMCID: PMCPMC5477650.
15. Kinchington PR, Leger AJ, Guedon JM, Hendricks RL. Herpes simplex virus and varicella zoster virus, the house guests who never leave. Herpesviridae. 2012;3(1):5. Epub 2012/06/12. doi: 10.1186/2042-4280-3-5. PubMed PMID: 22691604; PubMed Central PMCID: PMCPMC3541251.
16. Parra B, Hinton DR, Marten NW, Bergmann CC, Lin MT, Yang CS, et al. IFN-gamma is required for viral clearance from central nervous system oligodendroglia. J Immunol. 1999;162(3):1641-7. PubMed PMID: 9973424.

17. Klein RS, Hunter CA. Protective and Pathological Immunity during Central Nervous System Infections. Immunity. 2017;46(6):891-909. doi: 10.1016/j.immuni.2017.06.012. PubMed PMID: 28636958; PubMed Central PMCID: PMCPMC5662000.
18. Wakim LM, Woodward-Davis A, Bevan MJ. Memory T cells persisting within the brain after local infection show functional adaptations to their tissue of residence. Proc Natl Acad Sci U S A. 2010;107(42):17872-9. Epub 2010/10/05. doi: 10.1073/pnas.1010201107. PubMed PMID: 20923878; PubMed Central PMCID: PMCPMC2964240.
19. Haley SA, Atwood WJ. Progressive Multifocal Leukoencephalopathy: Endemic Viruses and Lethal Brain Disease. Annu Rev Virol. 2017;4(1):349-67. Epub 2017/06/21. doi: 10.1146/annurev-virology-101416-041439. PubMed PMID: 28637388.
20. Imperiale MJ, Jiang M. Polyomavirus Persistence. Annu Rev Virol. 2016;3(1):517-32. Epub 2016/08/03. doi: 10.1146/annurev-virology-110615-042226. PubMed PMID: 27501263.
21. Cook L. Polyomaviruses. Microbiol Spectr. 2016;4(4). doi: 10.1128/microbiolspec.DMIH2-0010-2015. PubMed PMID: 27726799.
22. Kamminga S, van der Meijden E, Feltkamp MCW, Zaaijer HL. Seroprevalence of fourteen human polyomaviruses determined in blood donors. PLoS One. 2018;13(10):e0206273. Epub 2018/10/23. doi: 10.1371/journal.pone.0206273. PubMed PMID: 30352098.
23. ASTROM KE, MANCALL EL, RICHARDSON EP. Progressive multifocal leuko-encephalopathy; a hitherto unrecognized complication of chronic lymphatic leukaemia and Hodgkin's disease. Brain. 1958;81(1):93-111. PubMed PMID: 13523006.
24. RICHARDSON EP. Progressive multifocal leukoencephalopathy. N Engl J Med. 1961;265:815-23. doi: 10.1056/NEJM196110262651701. PubMed PMID: 14038684.
25. Padgett BL, Walker DL, ZuRhein GM, Hodach AE, Chou SM. JC Papovavirus in progressive multifocal leukoencephalopathy. J Infect Dis. 1976;133(6):686-90. PubMed PMID: 778304.
26. Kondo Y, Windrem MS, Zou L, Chandler-Militello D, Schanz SJ, Auvergne RM, et al. Human glial chimeric mice reveal astrocytic dependence of JC virus infection. J Clin Invest. 2014;124(12):5323-36. Epub 2014/11/17. doi: 10.1172/JCI76629. PubMed PMID: 25401469; PubMed Central PMCID: PMCPMC4348956.
27. Tan CS, Koralnik IJ. Progressive multifocal leukoencephalopathy and other disorders caused by JC virus: clinical features and pathogenesis. Lancet Neurol. 2010;9(4):425-37. doi: 10.1016/S1474-4422(10)70040-5. PubMed PMID: 20298966; PubMed Central PMCID: PMCPMC2880524.
28. Koralnik IJ, Wüthrich C, Dang X, Rottnek M, Gurtman A, Simpson D, et al. JC virus granule cell neuronopathy: A novel clinical syndrome distinct from progressive multifocal leukoencephalopathy. Ann Neurol. 2005;57(4):576-80. doi: 10.1002/ana.20431. PubMed PMID: 15786466.
29. Wüthrich C, Dang X, Westmoreland S, McKay J, Maheshwari A, Anderson MP, et al. Fulminant JC virus encephalopathy with productive infection of cortical pyramidal neurons. Ann Neurol. 2009;65(6):742-8. doi: 10.1002/ana.21619. PubMed PMID: 19557867; PubMed Central PMCID: PMCPMC2865689.
30. Miskin DP, Koralnik IJ. Novel syndromes associated with JC virus infection of neurons and meningeal cells: no longer a gray area. Curr Opin Neurol. 2015;28(3):288-94. doi: 10.1097/WCO.0000000000000201. PubMed PMID: 25887767; PubMed Central PMCID: PMCPMC4414882.
31. Jelcic I, Kempf C, Largey F, Planas R, Schippling S, Budka H, et al. Mechanisms of immune escape in central nervous system infection with neurotropic JC virus variant. Ann Neurol. 2016;79(3):404-18. Epub 2016/02/13. doi: 10.1002/ana.24574. PubMed PMID: 26874214.
32. Dang X, Vidal JE, Oliveira AC, Simpson DM, Morgello S, Hecht JH, et al. JC virus granule cell neuronopathy is associated with VP1 C terminus mutants. J Gen Virol. 2012;93(Pt 1):175-83. Epub

2011/09/21. doi: 10.1099/vir.0.037440-0. PubMed PMID: 21940415; PubMed Central PMCID: PMCPMC3352331.
33. Berger JR, Pall L, Lanska D, Whiteman M. Progressive multifocal leukoencephalopathy in patients with HIV infection. J Neurovirol. 1998;4(1):59-68. doi: 10.3109/13550289809113482. PubMed PMID: 9531012.
34. Selik RM, Karon JM, Ward JW. Effect of the human immunodeficiency virus epidemic on mortality from opportunistic infections in the United States in 1993. J Infect Dis. 1997;176(3):632-6. PubMed PMID: 9291308.
35. Christensen KL, Holman RC, Hammett TA, Belay ED, Schonberger LB. Progressive multifocal leukoencephalopathy deaths in the USA, 1979-2005. Neuroepidemiology. 2010;35(3):178-84. Epub 2010/07/24. doi: 10.1159/000311014. PubMed PMID: 20664291.
36. Casado JL, Corral I, García J, Martinez-San Millán J, Navas E, Moreno A, et al. Continued declining incidence and improved survival of progressive multifocal leukoencephalopathy in HIV/AIDS patients in the current era. Eur J Clin Microbiol Infect Dis. 2014;33(2):179-87. Epub 2013/08/16. doi: 10.1007/s10096-013-1941-6. PubMed PMID: 23948752.
37. Ho PR, Koendgen H, Campbell N, Haddock B, Richman S, Chang I. Risk of natalizumab-associated progressive multifocal leukoencephalopathy in patients with multiple sclerosis: a retrospective analysis of data from four clinical studies. Lancet Neurol. 2017;16(11):925-33. Epub 2017/09/29. doi: 10.1016/S1474-4422(17)30282-X. PubMed PMID: 28969984.
38. Patera AC, Butler SL, Cinque P, Clifford DB, Elston R, Garcea RL, et al. 2nd International Conference on Progressive Multifocal Leukoencephalopathy (PML) 2015: JCV virology, progressive multifocal leukoencephalopathy pathogenesis, diagnosis and risk stratification, and new approaches to prevention and treatment. J Neurovirol. 2015;21(6):702-5. doi: 10.1007/s13365-015-0392-5. PubMed PMID: 26501778.
39. Jelcic I, Faigle W, Sospedra M, Martin R. Immunology of progressive multifocal leukoencephalopathy. J Neurovirol. 2015;21(6):614-22. Epub 2015/03/05. doi: 10.1007/s13365-014-0294-y. PubMed PMID: 25740538.
40. Molloy ES, Calabrese LH. Progressive multifocal leukoencephalopathy: a national estimate of frequency in systemic lupus erythematosus and other rheumatic diseases. Arthritis Rheum. 2009;60(12):3761-5. doi: 10.1002/art.24966. PubMed PMID: 19950261.
41. Du Pasquier RA, Clark KW, Smith PS, Joseph JT, Mazullo JM, De Girolami U, et al. JCV-specific cellular immune response correlates with a favorable clinical outcome in HIV-infected individuals with progressive multifocal leukoencephalopathy. J Neurovirol. 2001;7(4):318-22. doi: 10.1080/13550280152537175. PubMed PMID: 11517410.
42. Du Pasquier RA, Kuroda MJ, Zheng Y, Jean-Jacques J, Letvin NL, Koralnik IJ. A prospective study demonstrates an association between JC virus-specific cytotoxic T lymphocytes and the early control of progressive multifocal leukoencephalopathy. Brain. 2004;127(Pt 9):1970-8. Epub 2004/06/23. doi: 10.1093/brain/awh215. PubMed PMID: 15215217.
43. Koralnik IJ, Du Pasquier RA, Letvin NL. JC virus-specific cytotoxic T lymphocytes in individuals with progressive multifocal leukoencephalopathy. J Virol. 2001;75(7):3483-7. doi: 10.1128/JVI.75.7.3483-3487.2001. PubMed PMID: 11238876; PubMed Central PMCID: PMCPMC114143.
44. Muftuoglu M, Olson A, Marin D, Ahmed S, Mulanovich V, Tummala S, et al. Allogeneic BK Virus-Specific T Cells for Progressive Multifocal Leukoencephalopathy. N Engl J Med. 2018;379(15):1443-51. doi: 10.1056/NEJMoa1801540. PubMed PMID: 30304652.
45. Spadaro M, Caldano M, Marnetto F, Lugaresi A, Bertolotto A. Natalizumab treatment reduces L-selectin (CD62L) in CD4+ T cells. J Neuroinflammation. 2015;12:146. Epub 2015/08/12. doi: 10.1186/s12974-015-0365-x. PubMed PMID: 26259673; PubMed Central PMCID: PMCPMC4532246.

46. Schneider-Hohendorf T, Philipp K, Husstedt IW, Wiendl H, Schwab N. Specific loss of cellular L-selectin on CD4(+) T cells is associated with progressive multifocal leukoencephalopathy development during HIV infection. AIDS. 2014;28(5):793-5. doi: 10.1097/QAD.0000000000000201. PubMed PMID: 24445368.
47. Dubois E, Ruschil C, Bischof F. Low frequencies of central memory CD4 T cells in progressive multifocal leukoencephalopathy. Neurol Neuroimmunol Neuroinflamm. 2015;2(6):e177. Epub 2015/10/29. doi: 10.1212/NXI.0000000000000177. PubMed PMID: 26568972; PubMed Central PMCID: PMCPMC4630684.
48. Scarpazza C, Prosperini L, De Rossi N, Moiola L, Sormani MP, Gerevini S, et al. To do or not to do? plasma exchange and timing of steroid administration in progressive multifocal leukoencephalopathy. Ann Neurol. 2017;82(5):697-705. Epub 2017/10/31. doi: 10.1002/ana.25070. PubMed PMID: 29023856.
49. Martin-Blondel G, Bauer J, Cuvinciuc V, Uro-Coste E, Debard A, Massip P, et al. In situ evidence of JC virus control by CD8+ T cells in PML-IRIS during HIV infection. Neurology. 2013;81(11):964-70. Epub 2013/08/09. doi: 10.1212/WNL.0b013e3182a43e6d. PubMed PMID: 23935178.
50. Bauer J, Gold R, Adams O, Lassmann H. Progressive multifocal leukoencephalopathy and immune reconstitution inflammatory syndrome (IRIS). Acta Neuropathol. 2015;130(6):751-64. Epub 2015/09/01. doi: 10.1007/s00401-015-1471-7. PubMed PMID: 26323992.
51. Kleinschmidt-DeMasters BK, Miravalle A, Schowinsky J, Corboy J, Vollmer T. Update on PML and PML-IRIS occurring in multiple sclerosis patients treated with natalizumab. J Neuropathol Exp Neurol. 2012;71(7):604-17. doi: 10.1097/NEN.0b013e31825caf2c. PubMed PMID: 22710964.
52. Riddell LA, Pinching AJ, Hill S, Ng TT, Arbe E, Lapham GP, et al. A phase III study of recombinant human interferon gamma to prevent opportunistic infections in advanced HIV disease. AIDS Res Hum Retroviruses. 2001;17(9):789-97. doi: 10.1089/088922201750251981. PubMed PMID: 11429120.
53. Co JK, Verma S, Gurjav U, Sumibcay L, Nerurkar VR. Interferon- alpha and - beta restrict polyomavirus JC replication in primary human fetal glial cells: implications for progressive multifocal leukoencephalopathy therapy. J Infect Dis. 2007;196(5):712-8. Epub 2007/07/20. doi: 10.1086/520518. PubMed PMID: 17674314; PubMed Central PMCID: PMCPMC2661426.
54. Verma S, Ziegler K, Ananthula P, Co JK, Frisque RJ, Yanagihara R, et al. JC virus induces altered patterns of cellular gene expression: interferon-inducible genes as major transcriptional targets. Virology. 2006;345(2):457-67. Epub 2005/11/17. doi: 10.1016/j.virol.2005.10.012. PubMed PMID: 16297951.
55. De-Simone FI, Sariyer R, Otalora YL, Yarandi S, Craigie M, Gordon J, et al. IFN-Gamma Inhibits JC Virus Replication in Glial Cells by Suppressing T-Antigen Expression. PLoS One. 2015;10(6):e0129694. Epub 2015/06/10. doi: 10.1371/journal.pone.0129694. PubMed PMID: 26061652; PubMed Central PMCID: PMCPMC4465661.
56. Zerbe CS, Marciano BE, Katial RK, Santos CB, Adamo N, Hsu AP, et al. Progressive Multifocal Leukoencephalopathy in Primary Immune Deficiencies: Stat1 Gain of Function and Review of the Literature. Clin Infect Dis. 2016;62(8):986-94. Epub 2016/01/06. doi: 10.1093/cid/civ1220. PubMed PMID: 26743090; PubMed Central PMCID: PMCPMC4803104.
57. Windrem MS, Schanz SJ, Guo M, Tian GF, Washco V, Stanwood N, et al. Neonatal chimerization with human glial progenitor cells can both remyelinate and rescue the otherwise lethally hypomyelinated shiverer mouse. Cell Stem Cell. 2008;2(6):553-65. doi: 10.1016/j.stem.2008.03.020. PubMed PMID: 18522848; PubMed Central PMCID: PMCPMC3358921.
58. Wilson JJ, Lin E, Pack CD, Frost EL, Hadley A, Swimm AI, et al. Gamma interferon controls mouse polyomavirus infection in vivo. J Virol. 2011;85(19):10126-34. Epub 2011/07/20. doi: 10.1128/JVI.00761-11. PubMed PMID: 21775464; PubMed Central PMCID: PMCPMC3196421.

59. Byers AM, Hadley A, Lukacher AE. Protection against polyoma virus-induced tumors is perforin-independent. Virology. 2007;358(2):485-92. Epub 2006/09/28. doi: 10.1016/j.virol.2006.08.044. PubMed PMID: 17011010; PubMed Central PMCID: PMCPMC2861337.
60. Laidlaw BJ, Craft JE, Kaech SM. The multifaceted role of CD4(+) T cells in CD8(+) T cell memory. Nat Rev Immunol. 2016;16(2):102-11. Epub 2016/01/19. doi: 10.1038/nri.2015.10. PubMed PMID: 26781939; PubMed Central PMCID: PMCPMC4860014.
61. Novy P, Quigley M, Huang X, Yang Y. CD4 T cells are required for CD8 T cell survival during both primary and memory recall responses. J Immunol. 2007;179(12):8243-51. PubMed PMID: 18056368.
62. Sun JC, Williams MA, Bevan MJ. CD4+ T cells are required for the maintenance, not programming, of memory CD8+ T cells after acute infection. Nat Immunol. 2004;5(9):927-33. Epub 2004/08/08. doi: 10.1038/ni1105. PubMed PMID: 15300249; PubMed Central PMCID: PMCPMC2776074.
63. Grakoui A, Shoukry NH, Woollard DJ, Han JH, Hanson HL, Ghrayeb J, et al. HCV persistence and immune evasion in the absence of memory T cell help. Science. 2003;302(5645):659-62. doi: 10.1126/science.1088774. PubMed PMID: 14576438.
64. Intlekofer AM, Takemoto N, Kao C, Banerjee A, Schambach F, Northrop JK, et al. Requirement for T-bet in the aberrant differentiation of unhelped memory CD8+ T cells. J Exp Med. 2007;204(9):2015-21. Epub 2007/08/13. doi: 10.1084/jem.20070841. PubMed PMID: 17698591; PubMed Central PMCID: PMCPMC2118697.
65. Belz GT, Wodarz D, Diaz G, Nowak MA, Doherty PC. Compromised influenza virus-specific CD8(+)-T-cell memory in CD4(+)-T-cell-deficient mice. J Virol. 2002;76(23):12388-93. PubMed PMID: 12414983; PubMed Central PMCID: PMCPMC136883.
66. Williams M, Bevan M. Effector and memory CTL differentiation. Annual Review of Immunology. 2007;25:171-92. doi: 10.1146/annurev.immunol.25.022106.141548. PubMed PMID: WOS:000246437100007.
67. Sallusto F, Geginat J, Lanzavecchia A. Central memory and effector memory T cell subsets: Function, generation, and maintenance. Annual Review of Immunology. 2004;22:745-63. doi: 10.1146/annurev.immunol.22.012703.104702. PubMed PMID: WOS:000221601500025.
68. Jameson S, Masopust D. Understanding Subset Diversity in T Cell Memory. Immunity. 2018;48(2):214-26. doi: 10.1016/j.immuni.2018.02.010. PubMed PMID: WOS:000425507800009.
69. Masopust D, Vezys V, Marzo A, Lefrancois L. Preferential localization of effector memory cells in nonlymphoid tissue. Science. 2001;291(5512):2413-7. doi: 10.1126/science.1058867. PubMed PMID: WOS:000167618700057.
70. Mackay LK, Kallies A. Transcriptional Regulation of Tissue-Resident Lymphocytes. Trends Immunol. 2017;38(2):94-103. Epub 2016/12/09. doi: 10.1016/j.it.2016.11.004. PubMed PMID: 27939451.
71. Schenkel JM, Masopust D. Tissue-resident memory T cells. Immunity. 2014;41(6):886-97. Epub 2014/12/06. doi: 10.1016/j.immuni.2014.12.007. PubMed PMID: 25526304; PubMed Central PMCID: PMCPMC4276131.
72. Pan Y, Tian T, Park CO, Lofftus SY, Mei S, Liu X, et al. Survival of tissue-resident memory T cells requires exogenous lipid uptake and metabolism. Nature. 2017;543(7644):252-6. Epub 2017/02/20. doi: 10.1038/nature21379. PubMed PMID: 28219080; PubMed Central PMCID: PMCPMC5509051.
73. Rosato PC, Beura LK, Masopust D. Tissue resident memory T cells and viral immunity. Curr Opin Virol. 2017;22:44-50. Epub 2016/12/14. doi: 10.1016/j.coviro.2016.11.011. PubMed PMID: 27987416; PubMed Central PMCID: PMCPMC5346042.
74. Shwetank, Abdelsamed HA, Frost EL, Schmitz HM, Mockus TE, Youngblood BA, et al. Maintenance of PD-1 on brain-resident memory CD8 T cells is antigen independent. Immunol Cell Biol.

2017;95(10):953-9. Epub 2017/08/22. doi: 10.1038/icb.2017.62. PubMed PMID: 28829048; PubMed Central PMCID: PMCPMC5698165.
75. Landrith TA, Sureshchandra S, Rivera A, Jang JC, Rais M, Nair MG, et al. CD103. Front Immunol. 2017;8:335. Epub 2017/03/29. doi: 10.3389/fimmu.2017.00335. PubMed PMID: 28424687; PubMed Central PMCID: PMCPMC5372813.
76. Wakim LM, Woodward-Davis A, Liu R, Hu Y, Villadangos J, Smyth G, et al. The molecular signature of tissue resident memory CD8 T cells isolated from the brain. J Immunol. 2012;189(7):3462-71. Epub 2012/08/24. doi: 10.4049/jimmunol.1201305. PubMed PMID: 22922816; PubMed Central PMCID: PMCPMC3884813.
77. Mackay LK, Minnich M, Kragten NA, Liao Y, Nota B, Seillet C, et al. Hobit and Blimp1 instruct a universal transcriptional program of tissue residency in lymphocytes. Science. 2016;352(6284):459-63. doi: 10.1126/science.aad2035. PubMed PMID: 27102484.
78. Pearce EL, Poffenberger MC, Chang CH, Jones RG. Fueling immunity: insights into metabolism and lymphocyte function. Science. 2013;342(6155):1242454. doi: 10.1126/science.1242454. PubMed PMID: 24115444; PubMed Central PMCID: PMCPMC4486656.
79. Caldeira-Dantas S, Furmanak T, Smith C, Quinn M, Teos L, Ertel A, et al. The Chemokine Receptor CXCR3 Promotes CD8(+) T Cell Accumulation in Uninfected Salivary Glands but Is Not Necessary after Murine Cytomegalovirus Infection. Journal of Immunology. 2018;200(3):1133-45. doi: 10.4049/jimmunol.1701272. PubMed PMID: WOS:000423124400025.
80. Beura L, Mitchell J, Thompson E, Schenkel J, Mohammed J, Wijeyesinghe S, et al. Intravital mucosal imaging of CD8(+) resident memory T cells shows tissue-autonomous recall responses that amplify secondary memory. Nature Immunology. 2018;19(2):173-+. doi: 10.1038/s41590-017-0029-3. PubMed PMID: WOS:000423435200017.
81. Harris T, Banigan E, Christian D, Konradt C, Wojno E, Norose K, et al. Generalized Levy walks and the role of chemokines in migration of effector CD8(+) T cells. Nature. 2012;486(7404):545-U145. doi: 10.1038/nature11098. PubMed PMID: WOS:000305760600046.
82. Ariotti S, Hogenbirk M, Dijkgraaf F, Visser L, Hoekstra M, Song J, et al. Skin-resident memory CD8(+) T cells trigger a state of tissue-wide pathogen alert. Science. 2014;346(6205):101-5. doi: 10.1126/science.1254803. PubMed PMID: WOS:000342446900060.
83. Bergsbaken T, Bevan MJ, Fink PJ. Local Inflammatory Cues Regulate Differentiation and Persistence of CD8. Cell Rep. 2017;19(1):114-24. doi: 10.1016/j.celrep.2017.03.031. PubMed PMID: 28380351; PubMed Central PMCID: PMCPMC5444811.
84. Steinbach K, Vincenti I, Kreutzfeldt M, Page N, Muschaweckh A, Wagner I, et al. Brain-resident memory T cells represent an autonomous cytotoxic barrier to viral infection. J Exp Med. 2016;213(8):1571-87. Epub 2016/07/04. doi: 10.1084/jem.20151916. PubMed PMID: 27377586; PubMed Central PMCID: PMCPMC4986533.
85. Masopust D, Vezys V, Wherry E, Barber D, Ahmed R. Cutting edge: Gut microenvironment promotes differentiation of a unique memory CD8 T cell population. Journal of Immunology. 2006;176(4):2079-83. doi: 10.4049/jimmunol.176.4.2079. PubMed PMID: WOS:000235180900008.
86. Iijima N, Linehan M, Zamora M, Butkus D, Dunn R, Kehry M, et al. Dendritic cells and B cells maximize mucosal Th1 memory response to herpes simplex virus. Journal of Experimental Medicine. 2008;205(13):3041-52. doi: 10.1084/jem.20082039. PubMed PMID: WOS:000266428700011.
87. Schenkel J, Fraser K, Vezys V, Masopust D. Sensing and alarm function of resident memory CD8(+) T cells. Nature Immunology. 2013;14(5):509-+. doi: 10.1038/ni.2568. PubMed PMID: WOS:000317732100016.
88. Romagnoli PA, Fu HH, Qiu Z, Khairallah C, Pham QM, Puddington L, et al. Differentiation of distinct long-lived memory CD4 T cells in intestinal tissues after oral Listeria monocytogenes infection.

Mucosal Immunol. 2017;10(2):520-30. Epub 2016/07/27. doi: 10.1038/mi.2016.66. PubMed PMID: 27461178; PubMed Central PMCID: PMCPMC5272904.
89. Gray JI, Westerhof LM, MacLeod MKL. The roles of resident, central and effector memory CD4 T-cells in protective immunity following infection or vaccination. Immunology. 2018. Epub 2018/03/23. doi: 10.1111/imm.12929. PubMed PMID: 29570776; PubMed Central PMCID: PMCPMC6050220.
90. Iijima N, Iwasaki A. T cell memory. A local macrophage chemokine network sustains protective tissue-resident memory CD4 T cells. Science. 2014;346(6205):93-8. Epub 2014/08/28. doi: 10.1126/science.1257530. PubMed PMID: 25170048; PubMed Central PMCID: PMCPMC4254703.
91. Collins N, Jiang X, Zaid A, Macleod BL, Li J, Park CO, et al. Skin CD4(+) memory T cells exhibit combined cluster-mediated retention and equilibration with the circulation. Nat Commun. 2016;7:11514. Epub 2016/05/10. doi: 10.1038/ncomms11514. PubMed PMID: 27160938; PubMed Central PMCID: PMCPMC4866325.
92. Owens T, Khorooshi R, Wlodarczyk A, Asgari N. Interferons in the central nervous system: a few instruments play many tunes. Glia. 2014;62(3):339-55. PubMed PMID: 24588027.
93. Schneider WM, Chevillotte MD, Rice CM. Interferon-stimulated genes: a complex web of host defenses. Annu Rev Immunol. 2014;32:513-45. Epub 2014/02/06. doi: 10.1146/annurev-immunol-032713-120231. PubMed PMID: 24555472; PubMed Central PMCID: PMCPMC4313732.
94. Blank T, Prinz M. Type I interferon pathway in CNS homeostasis and neurological disorders. Glia. 2017;65(9):1397-406. Epub 2017/05/18. doi: 10.1002/glia.23154. PubMed PMID: 28519900.
95. Costello DA, Lynch MA. Toll-like receptor 3 activation modulates hippocampal network excitability, via glial production of interferon-β. Hippocampus. 2013;23(8):696-707. Epub 2013/06/03. doi: 10.1002/hipo.22129. PubMed PMID: 23554175.
96. Kallfass C, Ackerman A, Lienenklaus S, Weiss S, Heimrich B, Staeheli P. Visualizing production of beta interferon by astrocytes and microglia in brain of La Crosse virus-infected mice. J Virol. 2012;86(20):11223-30. Epub 2012/08/08. doi: 10.1128/JVI.01093-12. PubMed PMID: 22875966; PubMed Central PMCID: PMCPMC3457137.
97. Hosmane S, Tegenge MA, Rajbhandari L, Uapinyoying P, Ganesh Kumar N, Thakor N, et al. Toll/interleukin-1 receptor domain-containing adapter inducing interferon-β mediates microglial phagocytosis of degenerating axons. J Neurosci. 2012;32(22):7745-57. doi: 10.1523/JNEUROSCI.0203-12.2012. PubMed PMID: 22649252; PubMed Central PMCID: PMCPMC3398425.
98. Tedeschi B, Barrett JN, Keane RW. Astrocytes produce interferon that enhances the expression of H-2 antigens on a subpopulation of brain cells. J Cell Biol. 1986;102(6):2244-53. PubMed PMID: 2423537; PubMed Central PMCID: PMCPMC2114253.
99. Yamada T, Horisberger MA, Kawaguchi N, Moroo I, Toyoda T. Immunohistochemistry using antibodies to alpha-interferon and its induced protein, MxA, in Alzheimer's and Parkinson's disease brain tissues. Neurosci Lett. 1994;181(1-2):61-4. PubMed PMID: 7898772.
100. Chopy D, Detje CN, Lafage M, Kalinke U, Lafon M. The type I interferon response bridles rabies virus infection and reduces pathogenicity. J Neurovirol. 2011;17(4):353-67. Epub 2011/07/30. doi: 10.1007/s13365-011-0041-6. PubMed PMID: 21805057.
101. Detje CN, Meyer T, Schmidt H, Kreuz D, Rose JK, Bechmann I, et al. Local type I IFN receptor signaling protects against virus spread within the central nervous system. J Immunol. 2009;182(4):2297-304. doi: 10.4049/jimmunol.0800596. PubMed PMID: 19201884.
102. Dionne KR, Galvin JM, Schittone SA, Clarke P, Tyler KL. Type I interferon signaling limits reoviral tropism within the brain and prevents lethal systemic infection. J Neurovirol. 2011;17(4):314-26. Epub 2011/06/14. doi: 10.1007/s13365-011-0038-1. PubMed PMID: 21671121; PubMed Central PMCID: PMCPMC3163031.

103. Kapil P, Butchi NB, Stohlman SA, Bergmann CC. Oligodendroglia are limited in type I interferon induction and responsiveness in vivo. Glia. 2012;60(10):1555-66. Epub 2012/06/26. doi: 10.1002/glia.22375. PubMed PMID: 22736486; PubMed Central PMCID: PMCPMC3422432.
104. Daniels BP, Jujjavarapu H, Durrant DM, Williams JL, Green RR, White JP, et al. Regional astrocyte IFN signaling restricts pathogenesis during neurotropic viral infection. J Clin Invest. 2017;127(3):843-56. Epub 2017/01/30. doi: 10.1172/JCI88720. PubMed PMID: 28134626; PubMed Central PMCID: PMCPMC5330728.
105. Sorgeloos F, Kreit M, Hermant P, Lardinois C, Michiels T. Antiviral type I and type III interferon responses in the central nervous system. Viruses. 2013;5(3):834-57. Epub 2013/03/15. doi: 10.3390/v5030834. PubMed PMID: 23503326; PubMed Central PMCID: PMCPMC3705299.
106. Crouse J, Kalinke U, Oxenius A. Regulation of antiviral T cell responses by type I interferons. Nat Rev Immunol. 2015;15(4):231-42. Epub 2015/03/20. doi: 10.1038/nri3806. PubMed PMID: 25790790.
107. Teijaro JR, Ng C, Lee AM, Sullivan BM, Sheehan KC, Welch M, et al. Persistent LCMV infection is controlled by blockade of type I interferon signaling. Science. 2013;340(6129):207-11. doi: 10.1126/science.1235214. PubMed PMID: 23580529; PubMed Central PMCID: PMCPMC3640797.
108. Wilson EB, Yamada DH, Elsaesser H, Herskovitz J, Deng J, Cheng G, et al. Blockade of chronic type I interferon signaling to control persistent LCMV infection. Science. 2013;340(6129):202-7. doi: 10.1126/science.1235208. PubMed PMID: 23580528; PubMed Central PMCID: PMCPMC3704950.
109. Farrar MA, Schreiber RD. The molecular cell biology of interferon-gamma and its receptor. Annu Rev Immunol. 1993;11:571-611. doi: 10.1146/annurev.iy.11.040193.003035. PubMed PMID: 8476573.
110. Goodbourn S, Didcock L, Randall RE. Interferons: cell signalling, immune modulation, antiviral response and virus countermeasures. J Gen Virol. 2000;81(Pt 10):2341-64. doi: 10.1099/0022-1317-81-10-2341. PubMed PMID: 10993923.
111. Monteiro S, Roque S, Marques F, Correia-Neves M, Cerqueira JJ. Brain interference: Revisiting the role of IFNγ in the central nervous system. Prog Neurobiol. 2017;156:149-63. Epub 2017/05/18. doi: 10.1016/j.pneurobio.2017.05.003. PubMed PMID: 28528956.
112. Barcia C, Ros CM, Annese V, Gómez A, Ros-Bernal F, Aguado-Llera D, et al. IFN-γ signaling, with the synergistic contribution of TNF-α, mediates cell specific microglial and astroglial activation in experimental models of Parkinson's disease. Cell Death Dis. 2012;3:e379. Epub 2012/08/23. doi: 10.1038/cddis.2012.123. PubMed PMID: 22914327; PubMed Central PMCID: PMCPMC3434670.
113. Browne TC, McQuillan K, McManus RM, O'Reilly JA, Mills KH, Lynch MA. IFN-γ Production by amyloid β-specific Th1 cells promotes microglial activation and increases plaque burden in a mouse model of Alzheimer's disease. J Immunol. 2013;190(5):2241-51. Epub 2013/01/30. doi: 10.4049/jimmunol.1200947. PubMed PMID: 23365075.
114. Hunt NH, Ball HJ, Hansen AM, Khaw LT, Guo J, Bakmiwewa S, et al. Cerebral malaria: gamma-interferon redux. Front Cell Infect Microbiol. 2014;4:113. Epub 2014/08/15. doi: 10.3389/fcimb.2014.00113. PubMed PMID: 25177551; PubMed Central PMCID: PMCPMC4133756.
115. Too LK, Ball HJ, McGregor IS, Hunt NH. The pro-inflammatory cytokine interferon-gamma is an important driver of neuropathology and behavioural sequelae in experimental pneumococcal meningitis. Brain Behav Immun. 2014;40:252-68. Epub 2014/03/07. doi: 10.1016/j.bbi.2014.02.020. PubMed PMID: 24607660.
116. Moody LR, Herbst AJ, Aiken JM. Upregulation of interferon-gamma-induced genes during prion infection. J Toxicol Environ Health A. 2011;74(2-4):146-53. doi: 10.1080/15287394.2011.529064. PubMed PMID: 21218343; PubMed Central PMCID: PMCPMC4621959.
117. Remy MM, Sahin M, Flatz L, Regen T, Xu L, Kreutzfeldt M, et al. Interferon-γ-Driven iNOS: A Molecular Pathway to Terminal Shock in Arenavirus Hemorrhagic Fever. Cell Host Microbe. 2017;22(3):354-65.e5. Epub 2017/08/17. doi: 10.1016/j.chom.2017.07.008. PubMed PMID: 28826838.

118. Deczkowska A, Baruch K, Schwartz M. Type I/II Interferon Balance in the Regulation of Brain Physiology and Pathology. Trends Immunol. 2016;37(3):181-92. Epub 2016/02/11. doi: 10.1016/j.it.2016.01.006. PubMed PMID: 26877243.
119. Yau B, Mitchell AJ, Too LK, Ball HJ, Hunt NH. Interferon-γ-Induced Nitric Oxide Synthase-2 Contributes to Blood/Brain Barrier Dysfunction and Acute Mortality in Experimental Streptococcus pneumoniae Meningitis. J Interferon Cytokine Res. 2016;36(2):86-99. Epub 2015/09/29. doi: 10.1089/jir.2015.0078. PubMed PMID: 26418460.
120. Arolt V, Rothermundt M, Wandinger KP, Kirchner H. Decreased in vitro production of interferon-gamma and interleukin-2 in whole blood of patients with schizophrenia during treatment. Mol Psychiatry. 2000;5(2):150-8. PubMed PMID: 10822342.
121. Filiano AJ, Xu Y, Tustison NJ, Marsh RL, Baker W, Smirnov I, et al. Unexpected role of interferon-γ in regulating neuronal connectivity and social behaviour. Nature. 2016;535(7612):425-9. Epub 2016/07/13. doi: 10.1038/nature18626. PubMed PMID: 27409813; PubMed Central PMCID: PMCPMC4961620.
122. Wells AI, Coyne CB. Type III Interferons in Antiviral Defenses at Barrier Surfaces. Trends Immunol. 2018;39(10):848-58. Epub 2018/09/12. doi: 10.1016/j.it.2018.08.008. PubMed PMID: 30219309; PubMed Central PMCID: PMCPMC6179363.
123. Mendoza JL, Schneider WM, Hoffmann HH, Vercauteren K, Jude KM, Xiong A, et al. The IFN-λ-IFN-λR1-IL-10Rβ Complex Reveals Structural Features Underlying Type III IFN Functional Plasticity. Immunity. 2017;46(3):379-92. doi: 10.1016/j.immuni.2017.02.017. PubMed PMID: 28329704; PubMed Central PMCID: PMCPMC5510750.
124. Sommereyns C, Paul S, Staeheli P, Michiels T. IFN-lambda (IFN-lambda) is expressed in a tissue-dependent fashion and primarily acts on epithelial cells in vivo. PLoS Pathog. 2008;4(3):e1000017. Epub 2008/03/14. doi: 10.1371/journal.ppat.1000017. PubMed PMID: 18369468; PubMed Central PMCID: PMCPMC2265414.
125. Blazek K, Eames HL, Weiss M, Byrne AJ, Perocheau D, Pease JE, et al. IFN-λ resolves inflammation via suppression of neutrophil infiltration and IL-1β production. J Exp Med. 2015;212(6):845-53. Epub 2015/05/04. doi: 10.1084/jem.20140995. PubMed PMID: 25941255; PubMed Central PMCID: PMCPMC4451128.
126. de Weerd NA, Nguyen T. The interferons and their receptors--distribution and regulation. Immunol Cell Biol. 2012;90(5):483-91. Epub 2012/03/13. doi: 10.1038/icb.2012.9. PubMed PMID: 22410872.
127. Bolen CR, Ding S, Robek MD, Kleinstein SH. Dynamic expression profiling of type I and type III interferon-stimulated hepatocytes reveals a stable hierarchy of gene expression. Hepatology. 2014;59(4):1262-72. Epub 2014/02/18. doi: 10.1002/hep.26657. PubMed PMID: 23929627; PubMed Central PMCID: PMCPMC3938553.
128. Lazear HM, Daniels BP, Pinto AK, Huang AC, Vick SC, Doyle SE, et al. Interferon-λ restricts West Nile virus neuroinvasion by tightening the blood-brain barrier. Sci Transl Med. 2015;7(284):284ra59. doi: 10.1126/scitranslmed.aaa4304. PubMed PMID: 25904743; PubMed Central PMCID: PMCPMC4435724.
129. Lazear HM, Nice TJ, Diamond MS. Interferon-λ: Immune Functions at Barrier Surfaces and Beyond. Immunity. 2015;43(1):15-28. doi: 10.1016/j.immuni.2015.07.001. PubMed PMID: 26200010; PubMed Central PMCID: PMCPMC4527169.
130. Misumi I, Whitmire JK. IFN-λ exerts opposing effects on T cell responses depending on the chronicity of the virus infection. J Immunol. 2014;192(8):3596-606. Epub 2014/03/19. doi: 10.4049/jimmunol.1301705. PubMed PMID: 24646741; PubMed Central PMCID: PMCPMC4157331.
131. Ivashkiv LB, Hu X. Signaling by STATs. Arthritis Res Ther. 2004;6(4):159-68. Epub 2004/06/21. doi: 10.1186/ar1197. PubMed PMID: 15225360; PubMed Central PMCID: PMCPMC464899.

132. Ivashkiv LB. Cytokines and STATs: how can signals achieve specificity? Immunity. 1995;3(1):1-4. PubMed PMID: 7621070.
133. Pasieka TJ, Lu B, Leib DA. Enhanced pathogenesis of an attenuated herpes simplex virus for mice lacking Stat1. J Virol. 2008;82(12):6052-5. Epub 2008/04/09. doi: 10.1128/JVI.00297-08. PubMed PMID: 18400863; PubMed Central PMCID: PMCPMC2395151.
134. Durbin JE, Fernandez-Sesma A, Lee CK, Rao TD, Frey AB, Moran TM, et al. Type I IFN modulates innate and specific antiviral immunity. J Immunol. 2000;164(8):4220-8. PubMed PMID: 10754318.
135. Park SL, Zaid A, Hor JL, Christo SN, Prier JE, Davies B, et al. Local proliferation maintains a stable pool of tissue-resident memory T cells after antiviral recall responses. Nat Immunol. 2018;19(2):183-91. Epub 2018/01/08. doi: 10.1038/s41590-017-0027-5. PubMed PMID: 29311695.
136. Beura LK, Wijeyesinghe S, Thompson EA, Macchietto MG, Rosato PC, Pierson MJ, et al. T Cells in Nonlymphoid Tissues Give Rise to Lymph-Node-Resident Memory T Cells. Immunity. 2018;48(2):327-38.e5. doi: 10.1016/j.immuni.2018.01.015. PubMed PMID: 29466758; PubMed Central PMCID: PMCPMC5828517.
137. Korn T, Kallies A. T cell responses in the central nervous system. Nat Rev Immunol. 2017;17(3):179-94. Epub 2017/01/31. doi: 10.1038/nri.2016.144. PubMed PMID: 28138136.
138. Elsner C, Dörries K. Evidence of human polyomavirus BK and JC infection in normal brain tissue. Virology. 1992;191(1):72-80. PubMed PMID: 1329338.
139. Kean JM, Rao S, Wang M, Garcea RL. Seroepidemiology of human polyomaviruses. PLoS Pathog. 2009;5(3):e1000363. Epub 2009/03/27. doi: 10.1371/journal.ppat.1000363. PubMed PMID: 19325891; PubMed Central PMCID: PMCPMC2655709.
140. Frost EL, Lukacher AE. The importance of mouse models to define immunovirologic determinants of progressive multifocal leukoencephalopathy. Front Immunol. 2014;5:646. Epub 2015/01/05. doi: 10.3389/fimmu.2014.00646. PubMed PMID: 25601860; PubMed Central PMCID: PMCPMC4283601.
141. Fuse S, Tsai CY, Molloy MJ, Allie SR, Zhang W, Yagita H, et al. Recall responses by helpless memory CD8+ T cells are restricted by the up-regulation of PD-1. J Immunol. 2009;182(7):4244-54. doi: 10.4049/jimmunol.0802041. PubMed PMID: 19299723; PubMed Central PMCID: PMCPMC2713929.
142. Provine NM, Larocca RA, Aid M, Penaloza-MacMaster P, Badamchi-Zadeh A, Borducchi EN, et al. Immediate Dysfunction of Vaccine-Elicited CD8+ T Cells Primed in the Absence of CD4+ T Cells. J Immunol. 2016;197(5):1809-22. Epub 2016/07/22. doi: 10.4049/jimmunol.1600591. PubMed PMID: 27448585; PubMed Central PMCID: PMCPMC4991249.
143. Sitati EM, Diamond MS. CD4+ T-cell responses are required for clearance of West Nile virus from the central nervous system. J Virol. 2006;80(24):12060-9. Epub 2006/10/11. doi: 10.1128/JVI.01650-06. PubMed PMID: 17035323; PubMed Central PMCID: PMCPMC1676257.
144. Stohlman SA, Bergmann CC, Lin MT, Cua DJ, Hinton DR. CTL effector function within the central nervous system requires CD4+ T cells. J Immunol. 1998;160(6):2896-904. PubMed PMID: 9510193.
145. Phares TW, Stohlman SA, Hinton DR, Bergmann CC. Enhanced CD8 T-cell anti-viral function and clinical disease in B7-H1-deficient mice requires CD4 T cells during encephalomyelitis. J Neuroinflammation. 2012;9:269. Epub 2012/12/14. doi: 10.1186/1742-2094-9-269. PubMed PMID: 23237504; PubMed Central PMCID: PMCPMC3545890.
146. Hwang M, Phares TW, Hinton DR, Stohlman SA, Bergmann CC, Min B. Distinct CD4 T-cell effects on primary versus recall CD8 T-cell responses during viral encephalomyelitis. Immunology. 2015;144(3):374-86. doi: 10.1111/imm.12378. PubMed PMID: 25187405; PubMed Central PMCID: PMCPMC4557674.
147. Weidinger G, Czub S, Neumeister C, Harriott P, ter Meulen V, Niewiesk S. Role of CD4(+) and CD8(+) T cells in the prevention of measles virus-induced encephalitis in mice. J Gen Virol. 2000;81(Pt 11):2707-13. doi: 10.1099/0022-1317-81-11-2707. PubMed PMID: 11038383.

148. Tishon A, Lewicki H, Andaya A, McGavern D, Martin L, Oldstone MB. CD4 T cell control primary measles virus infection of the CNS: regulation is dependent on combined activity with either CD8 T cells or with B cells: CD4, CD8 or B cells alone are ineffective. Virology. 2006;347(1):234-45. Epub 2006/03/10. doi: 10.1016/j.virol.2006.01.050. PubMed PMID: 16529787.
149. Velupillai P, Yoshizawa I, Dey DC, Nahill SR, Carroll JP, Bronson RT, et al. Wild-derived inbred mice have a novel basis of susceptibility to polyomavirus-induced tumors. J Virol. 1999;73(12):10079-85. PubMed PMID: 10559322; PubMed Central PMCID: PMCPMC113059.
150. Drake DR, Moser JM, Hadley A, Altman JD, Maliszewski C, Butz E, et al. Polyomavirus-infected dendritic cells induce antiviral CD8(+) T lymphocytes. J Virol. 2000;74(9):4093-101. PubMed PMID: 10756021; PubMed Central PMCID: PMCPMC111923.
151. Dawe CJ, Freund R, Mandel G, Ballmer-Hofer K, Talmage DA, Benjamin TL. Variations in polyoma virus genotype in relation to tumor induction in mice. Characterization of wild type strains with widely differing tumor profiles. Am J Pathol. 1987;127(2):243-61. PubMed PMID: 2437801; PubMed Central PMCID: PMCPMC1899751.
152. Dubensky TW, Freund R, Dawe CJ, Benjamin TL. Polyomavirus replication in mice: influences of VP1 type and route of inoculation. J Virol. 1991;65(1):342-9. PubMed PMID: 1845895; PubMed Central PMCID: PMCPMC240523.
153. Albrecht JA, Dong Y, Wang J, Breeden C, Farris AB, Lukacher AE, et al. Adaptive immunity rather than viral cytopathology mediates polyomavirus-associated nephropathy in mice. Am J Transplant. 2012;12(6):1419-28. Epub 2012/03/15. doi: 10.1111/j.1600-6143.2012.04005.x. PubMed PMID: 22420885; PubMed Central PMCID: PMCPMC3365603.
154. Frost EL, Kersh AE, Evavold BD, Lukacher AE. Cutting Edge: Resident Memory CD8 T Cells Express High-Affinity TCRs. J Immunol. 2015;195(8):3520-4. Epub 2015/09/14. doi: 10.4049/jimmunol.1501521. PubMed PMID: 26371252; PubMed Central PMCID: PMCPMC4592826.
155. Maru S, Jin G, Schell TD, Lukacher AE. TCR stimulation strength is inversely associated with establishment of functional brain-resident memory CD8 T cells during persistent viral infection. PLoS Pathog. 2017;13(4):e1006318. Epub 2017/04/14. doi: 10.1371/journal.ppat.1006318. PubMed PMID: 28410427; PubMed Central PMCID: PMCPMC5406018.
156. Nayar R, Enos M, Prince A, Shin H, Hemmers S, Jiang JK, et al. TCR signaling via Tec kinase ITK and interferon regulatory factor 4 (IRF4) regulates CD8+ T-cell differentiation. Proc Natl Acad Sci U S A. 2012;109(41):E2794-802. Epub 2012/09/24. doi: 10.1073/pnas.1205742109. PubMed PMID: 23011795; PubMed Central PMCID: PMCPMC3478592.
157. Graham JB, Da Costa A, Lund JM. Regulatory T cells shape the resident memory T cell response to virus infection in the tissues. J Immunol. 2014;192(2):683-90. Epub 2013/12/11. doi: 10.4049/jimmunol.1202153. PubMed PMID: 24337378; PubMed Central PMCID: PMCPMC3894741.
158. Tian Y, Cox MA, Kahan SM, Ingram JT, Bakshi RK, Zajac AJ. A Context-Dependent Role for IL-21 in Modulating the Differentiation, Distribution, and Abundance of Effector and Memory CD8 T Cell Subsets. J Immunol. 2016;196(5):2153-66. Epub 2016/01/29. doi: 10.4049/jimmunol.1401236. PubMed PMID: 26826252; PubMed Central PMCID: PMCPMC4761492.
159. Andrews NP, Pack CD, Vezys V, Barber GN, Lukacher AE. Early virus-associated bystander events affect the fitness of the CD8 T cell response to persistent virus infection. J Immunol. 2007;178(11):7267-75. PubMed PMID: 17513776.
160. Simon ID, van Rooijen N, Rose JK. Vesicular stomatitis virus genomic RNA persists in vivo in the absence of viral replication. J Virol. 2010;84(7):3280-6. Epub 2009/12/23. doi: 10.1128/JVI.02052-09. PubMed PMID: 20032173; PubMed Central PMCID: PMCPMC2838132.
161. Shedlock DJ, Shen H. Requirement for CD4 T cell help in generating functional CD8 T cell memory. Science. 2003;300(5617):337-9. doi: 10.1126/science.1082305. PubMed PMID: 12690201.

162. Kemball CC, Pack CD, Guay HM, Li ZN, Steinhauer DA, Szomolanyi-Tsuda E, et al. The antiviral CD8+ T cell response is differentially dependent on CD4+ T cell help over the course of persistent infection. J Immunol. 2007;179(2):1113-21. PubMed PMID: 17617604.
163. Szomolanyi-Tsuda E, Seedhom MO, Carroll MC, Garcea RL. T cell-independent and T cell-dependent immunoglobulin G responses to polyomavirus infection are impaired in complement receptor 2-deficient mice. Virology. 2006;352(1):52-60. Epub 2006/06/02. doi: 10.1016/j.virol.2006.04.018. PubMed PMID: 16733062; PubMed Central PMCID: PMCPMC4714765.
164. Lee BO, Rangel-Moreno J, Moyron-Quiroz JE, Hartson L, Makris M, Sprague F, et al. CD4 T cell-independent antibody response promotes resolution of primary influenza infection and helps to prevent reinfection. J Immunol. 2005;175(9):5827-38. PubMed PMID: 16237075.
165. Swimm AI, Bornmann W, Jiang M, Imperiale MJ, Lukacher AE, Kalman D. Abl family tyrosine kinases regulate sialylated ganglioside receptors for polyomavirus. J Virol. 2010;84(9):4243-51. Epub 2010/02/24. doi: 10.1128/JVI.00129-10. PubMed PMID: 20181697; PubMed Central PMCID: PMCPMC2863717.
166. Manresa-Arraut A, Johansen FF, Brakebusch C, Issazadeh-Navikas S, Hasseldam H. RhoA Drives T-Cell Activation and Encephalitogenic Potential in an Animal Model of Multiple Sclerosis. Front Immunol. 2018;9:1235. Epub 2018/05/31. doi: 10.3389/fimmu.2018.01235. PubMed PMID: 29904389; PubMed Central PMCID: PMCPMC5990621.
167. Milner JJ, Toma C, Yu B, Zhang K, Omilusik K, Phan AT, et al. Runx3 programs CD8+ T cell residency in non-lymphoid tissues and tumours. Nature. 2017. Epub 2017/12/06. doi: 10.1038/nature24993. PubMed PMID: 29211713.
168. Srivastava N, Sudan R, Kerr WG. Role of inositol poly-phosphatases and their targets in T cell biology. Front Immunol. 2013;4:288. Epub 2013/09/23. doi: 10.3389/fimmu.2013.00288. PubMed PMID: 24069021; PubMed Central PMCID: PMCPMC3779868.
169. Wentink MWJ, Mueller YM, Dalm VASH, Driessen GJ, van Hagen PM, van Montfrans JM, et al. Exhaustion of the CD8. Front Immunol. 2018;9:446. Epub 2018/03/07. doi: 10.3389/fimmu.2018.00446. PubMed PMID: 29563914; PubMed Central PMCID: PMCPMC5845988.
170. Yu F, Hao Y, Zhao H, Xiao J, Han N, Zhang Y, et al. Distinct Mitochondrial Disturbance in CD4+T and CD8+T Cells From HIV-Infected Patients. J Acquir Immune Defic Syndr. 2017;74(2):206-12. doi: 10.1097/QAI.0000000000001175. PubMed PMID: 27608061.
171. Gorelik L, Reid C, Testa M, Brickelmaier M, Bossolasco S, Pazzi A, et al. Progressive multifocal leukoencephalopathy (PML) development is associated with mutations in JC virus capsid protein VP1 that change its receptor specificity. J Infect Dis. 2011;204(1):103-14. doi: 10.1093/infdis/jir198. PubMed PMID: 21628664; PubMed Central PMCID: PMCPMC3307153.
172. Ray U, Cinque P, Gerevini S, Longo V, Lazzarin A, Schippling S, et al. JC polyomavirus mutants escape antibody-mediated neutralization. Sci Transl Med. 2015;7(306):306ra151. Epub 2015/09/23. doi: 10.1126/scitranslmed.aab1720. PubMed PMID: 26400912.
173. Jelcic I, Combaluzier B, Faigle W, Senn L, Reinhart BJ, Ströh L, et al. Broadly neutralizing human monoclonal JC polyomavirus VP1-specific antibodies as candidate therapeutics for progressive multifocal leukoencephalopathy. Sci Transl Med. 2015;7(306):306ra150. Epub 2015/09/23. doi: 10.1126/scitranslmed.aac8691. PubMed PMID: 26400911; PubMed Central PMCID: PMCPMC4820754.
174. Assetta B, Atwood WJ. The biology of JC polyomavirus. Biol Chem. 2017;398(8):839-55. doi: 10.1515/hsz-2016-0345. PubMed PMID: 28493815.
175. Zonios DI, Falloon J, Bennett JE, Shaw PA, Chaitt D, Baseler MW, et al. Idiopathic CD4+ lymphocytopenia: natural history and prognostic factors. Blood. 2008;112(2):287-94. Epub 2008/05/02. doi: 10.1182/blood-2007-12-127878. PubMed PMID: 18456875; PubMed Central PMCID: PMCPMC2442741.

176. Balduzzi A, Lucchini G, Hirsch HH, Basso S, Cioni M, Rovelli A, et al. Polyomavirus JC-targeted T-cell therapy for progressive multiple leukoencephalopathy in a hematopoietic cell transplantation recipient. Bone Marrow Transplant. 2011;46(7):987-92. Epub 2010/10/04. doi: 10.1038/bmt.2010.221. PubMed PMID: 20921942.
177. Wherry EJ, Kurachi M. Molecular and cellular insights into T cell exhaustion. Nat Rev Immunol. 2015;15(8):486-99. doi: 10.1038/nri3862. PubMed PMID: 26205583; PubMed Central PMCID: PMCPMC4889009.
178. Fuller MJ, Khanolkar A, Tebo AE, Zajac AJ. Maintenance, loss, and resurgence of T cell responses during acute, protracted, and chronic viral infections. J Immunol. 2004;172(7):4204-14. PubMed PMID: 15034033.
179. Blackburn SD, Crawford A, Shin H, Polley A, Freeman GJ, Wherry EJ. Tissue-specific differences in PD-1 and PD-L1 expression during chronic viral infection: implications for CD8 T-cell exhaustion. J Virol. 2010;84(4):2078-89. Epub 2009/12/02. doi: 10.1128/JVI.01579-09. PubMed PMID: 19955307; PubMed Central PMCID: PMCPMC2812396.
180. Frank GM, Lepisto AJ, Freeman ML, Sheridan BS, Cherpes TL, Hendricks RL. Early CD4(+) T cell help prevents partial CD8(+) T cell exhaustion and promotes maintenance of Herpes Simplex Virus 1 latency. J Immunol. 2010;184(1):277-86. Epub 2009/11/30. doi: 10.4049/jimmunol.0902373. PubMed PMID: 19949087; PubMed Central PMCID: PMCPMC3298035.
181. Rougerie P, Delon J. Rho GTPases: masters of T lymphocyte migration and activation. Immunol Lett. 2012;142(1-2):1-13. Epub 2011/12/21. doi: 10.1016/j.imlet.2011.12.003. PubMed PMID: 22207038.
182. Yi JS, Du M, Zajac AJ. A vital role for interleukin-21 in the control of a chronic viral infection. Science. 2009;324(5934):1572-6. Epub 2009/05/14. doi: 10.1126/science.1175194. PubMed PMID: 19443735; PubMed Central PMCID: PMCPMC2736049.
183. Elsaesser H, Sauer K, Brooks DG. IL-21 is required to control chronic viral infection. Science. 2009;324(5934):1569-72. Epub 2009/05/07. doi: 10.1126/science.1174182. PubMed PMID: 19423777; PubMed Central PMCID: PMCPMC2830017.
184. Bachmann MF, Wolint P, Walton S, Schwarz K, Oxenius A. Differential role of IL-2R signaling for CD8+ T cell responses in acute and chronic viral infections. Eur J Immunol. 2007;37(6):1502-12. doi: 10.1002/eji.200637023. PubMed PMID: 17492805.
185. Brooks DG, Walsh KB, Elsaesser H, Oldstone MB. IL-10 directly suppresses CD4 but not CD8 T cell effector and memory responses following acute viral infection. Proc Natl Acad Sci U S A. 2010;107(7):3018-23. Epub 2010/01/26. doi: 10.1073/pnas.0914500107. PubMed PMID: 20133700; PubMed Central PMCID: PMCPMC2840337.
186. Vezys V, Masopust D, Kemball CC, Barber DL, O'Mara LA, Larsen CP, et al. Continuous recruitment of naive T cells contributes to heterogeneity of antiviral CD8 T cells during persistent infection. J Exp Med. 2006;203(10):2263-9. Epub 2006/09/11. doi: 10.1084/jem.20060995. PubMed PMID: 16966427; PubMed Central PMCID: PMCPMC2118117.
187. Lin E, Kemball CC, Hadley A, Wilson JJ, Hofstetter AR, Pack CD, et al. Heterogeneity among viral antigen-specific CD4+ T cells and their de novo recruitment during persistent polyomavirus infection. J Immunol. 2010;185(3):1692-700. Epub 2010/07/09. doi: 10.4049/jimmunol.0904210. PubMed PMID: 20622115; PubMed Central PMCID: PMCPMC3642206.
188. Zhao J, Perlman S. De novo recruitment of antigen-experienced and naive T cells contributes to the long-term maintenance of antiviral T cell populations in the persistently infected central nervous system. J Immunol. 2009;183(8):5163-70. Epub 2009/09/28. doi: 10.4049/jimmunol.0902164. PubMed PMID: 19786545; PubMed Central PMCID: PMCPMC2811315.
189. Herz J, Johnson KR, McGavern DB. Therapeutic antiviral T cells noncytopathically clear persistently infected microglia after conversion into antigen-presenting cells. J Exp Med.

2015;212(8):1153-69. Epub 2015/06/29. doi: 10.1084/jem.20142047. PubMed PMID: 26122661; PubMed Central PMCID: PMCPMC4516789.
190. Qin Q, Shwetank, Frost EL, Maru S, Lukacher AE. Type I Interferons Regulate the Magnitude and Functionality of Mouse Polyomavirus-Specific CD8 T Cells in a Virus Strain-Dependent Manner. J Virol. 2016;90(10):5187-99. Epub 2016/04/29. doi: 10.1128/JVI.00199-16. PubMed PMID: 26984726; PubMed Central PMCID: PMCPMC4859723.
191. Abend JR, Low JA, Imperiale MJ. Inhibitory effect of gamma interferon on BK virus gene expression and replication. J Virol. 2007;81(1):272-9. Epub 2006/10/11. doi: 10.1128/JVI.01571-06. PubMed PMID: 17035315; PubMed Central PMCID: PMCPMC1797268.
192. Palazzo E, Yahia SA. Progressive multifocal leukoencephalopathy in autoimmune diseases. Joint Bone Spine. 2012;79(4):351-5. Epub 2012/01/26. doi: 10.1016/j.jbspin.2011.11.002. PubMed PMID: 22281228.
193. Molloy ES, Calabrese LH. Progressive multifocal leukoencephalopathy associated with immunosuppressive therapy in rheumatic diseases: evolving role of biologic therapies. Arthritis Rheum. 2012;64(9):3043-51. doi: 10.1002/art.34468. PubMed PMID: 22422012.
194. Casey KA, Fraser KA, Schenkel JM, Moran A, Abt MC, Beura LK, et al. Antigen-independent differentiation and maintenance of effector-like resident memory T cells in tissues. J Immunol. 2012;188(10):4866-75. Epub 2012/04/13. doi: 10.4049/jimmunol.1200402. PubMed PMID: 22504644; PubMed Central PMCID: PMCPMC3345065.
195. Mackay LK, Rahimpour A, Ma JZ, Collins N, Stock AT, Hafon ML, et al. The developmental pathway for CD103(+)CD8+ tissue-resident memory T cells of skin. Nat Immunol. 2013;14(12):1294-301. Epub 2013/10/27. doi: 10.1038/ni.2744. PubMed PMID: 24162776.
196. Lukacher AE, Wilson CS. Resistance to polyoma virus-induced tumors correlates with CTL recognition of an immunodominant H-2Dk-restricted epitope in the middle T protein. J Immunol. 1998;160(4):1724-34. PubMed PMID: 9469430.
197. Anderson KG, Mayer-Barber K, Sung H, Beura L, James BR, Taylor JJ, et al. Intravascular staining for discrimination of vascular and tissue leukocytes. Nat Protoc. 2014;9(1):209-22. Epub 2014/01/02. doi: 10.1038/nprot.2014.005. PubMed PMID: 24385150; PubMed Central PMCID: PMCPMC4428344.
198. Kemball CC, Lee ED, Szomolanyi-Tsuda E, Pearson TC, Larsen CP, Lukacher AE. Costimulation requirements for antiviral CD8+ T cells differ for acute and persistent phases of polyoma virus infection. J Immunol. 2006;176(3):1814-24. PubMed PMID: 16424212.
199. Maru S, Jin G, Desai D, Amin S, Shwetank, Lauver MD, et al. Inhibition of Retrograde Transport Limits Polyomavirus Infection. mSphere. 2017;2(6). Epub 2017/11/15. doi: 10.1128/mSphereDirect.00494-17. PubMed PMID: 29152583; PubMed Central PMCID: PMCPMC5687923.
200. Wilson JJ, Pack CD, Lin E, Frost EL, Albrecht JA, Hadley A, et al. CD8 T cells recruited early in mouse polyomavirus infection undergo exhaustion. J Immunol. 2012;188(9):4340-8. Epub 2012/03/23. doi: 10.4049/jimmunol.1103727. PubMed PMID: 22447978; PubMed Central PMCID: PMCPMC3331907.
201. Hein J, Schellenberg U, Bein G, Hackstein H. Quantification of murine IFN-gamma mRNA and protein expression: impact of real-time kinetic RT-PCR using SYBR green I dye. Scand J Immunol. 2001;54(3):285-91. PubMed PMID: 11555392.
202. Savarin C, Bergmann CC, Hinton DR, Stohlman SA. Differential Regulation of Self-reactive CD4. Front Immunol. 2016;7:370. Epub 2016/09/21. doi: 10.3389/fimmu.2016.00370. PubMed PMID: 27708643; PubMed Central PMCID: PMCPMC5030268.
203. Livak KJ, Schmittgen TD. Analysis of relative gene expression data using real-time quantitative PCR and the 2(-Delta Delta C(T)) Method. Methods. 2001;25(4):402-8. doi: 10.1006/meth.2001.1262. PubMed PMID: 11846609.

204. Sullivan DE, Ferris M, Nguyen H, Abboud E, Brody AR. TNF-alpha induces TGF-beta1 expression in lung fibroblasts at the transcriptional level via AP-1 activation. J Cell Mol Med. 2009;13(8B):1866-76. doi: 10.1111/j.1582-4934.2009.00647.x. PubMed PMID: 20141610; PubMed Central PMCID: PMCPMC2855747.
205. Dobin A, Davis CA, Schlesinger F, Drenkow J, Zaleski C, Jha S, et al. STAR: ultrafast universal RNA-seq aligner. Bioinformatics. 2013;29(1):15-21. Epub 2012/10/25. doi: 10.1093/bioinformatics/bts635. PubMed PMID: 23104886; PubMed Central PMCID: PMCPMC3530905.
206. Li B, Dewey CN. RSEM: accurate transcript quantification from RNA-Seq data with or without a reference genome. BMC Bioinformatics. 2011;12:323. Epub 2011/08/04. doi: 10.1186/1471-2105-12-323. PubMed PMID: 21816040; PubMed Central PMCID: PMCPMC3163565.
207. Varet H, Brillet-Guéguen L, Coppée JY, Dillies MA. SARTools: A DESeq2- and EdgeR-Based R Pipeline for Comprehensive Differential Analysis of RNA-Seq Data. PLoS One. 2016;11(6):e0157022. Epub 2016/06/09. doi: 10.1371/journal.pone.0157022. PubMed PMID: 27280887; PubMed Central PMCID: PMCPMC4900645.
208. Samuel CE. Antiviral actions of interferons. Clin Microbiol Rev. 2001;14(4):778-809, table of contents. doi: 10.1128/CMR.14.4.778-809.2001. PubMed PMID: 11585785; PubMed Central PMCID: PMCPMC89003.
209. Katze MG, He Y, Gale M. Viruses and interferon: a fight for supremacy. Nat Rev Immunol. 2002;2(9):675-87. doi: 10.1038/nri888. PubMed PMID: 12209136.
210. Brierley MM, Fish EN. Review: IFN-alpha/beta receptor interactions to biologic outcomes: understanding the circuitry. J Interferon Cytokine Res. 2002;22(8):835-45. doi: 10.1089/107999002760274845. PubMed PMID: 12396722.
211. Kawai T, Akira S. Innate immune recognition of viral infection. Nat Immunol. 2006;7(2):131-7. doi: 10.1038/ni1303. PubMed PMID: 16424890.
212. Platanias LC. Mechanisms of type-I- and type-II-interferon-mediated signalling. Nat Rev Immunol. 2005;5(5):375-86. doi: 10.1038/nri1604. PubMed PMID: 15864272.
213. Kotenko SV, Gallagher G, Baurin VV, Lewis-Antes A, Shen M, Shah NK, et al. IFN-lambdas mediate antiviral protection through a distinct class II cytokine receptor complex. Nat Immunol. 2003;4(1):69-77. Epub 2002/12/16. doi: 10.1038/ni875. PubMed PMID: 12483210.
214. Lasfar A, Zloza A, Silk AW, Lee LY, Cohen-Solal KA. Interferon Lambda: Toward a Dual Role in Cancer. J Interferon Cytokine Res. 2018. Epub 2018/07/18. doi: 10.1089/jir.2018.0046. PubMed PMID: 30020822.
215. O'Donnell LA, Henkins KM, Kulkarni A, Matullo CM, Balachandran S, Pattisapu AK, et al. Interferon gamma induces protective non-canonical signaling pathways in primary neurons. J Neurochem. 2015;135(2):309-22. Epub 2015/08/31. doi: 10.1111/jnc.13250. PubMed PMID: 26190522; PubMed Central PMCID: PMCPMC4809142.
216. Chesler DA, Reiss CS. The role of IFN-gamma in immune responses to viral infections of the central nervous system. Cytokine Growth Factor Rev. 2002;13(6):441-54. PubMed PMID: 12401479.
217. Ferenczy MW, Marshall LJ, Nelson CD, Atwood WJ, Nath A, Khalili K, et al. Molecular biology, epidemiology, and pathogenesis of progressive multifocal leukoencephalopathy, the JC virus-induced demyelinating disease of the human brain. Clin Microbiol Rev. 2012;25(3):471-506. doi: 10.1128/CMR.05031-11. PubMed PMID: 22763635; PubMed Central PMCID: PMCPMC3416490.
218. Assetta B, De Cecco M, O'Hara B, Atwood WJ. JC Polyomavirus Infection of Primary Human Renal Epithelial Cells Is Controlled by a Type I IFN-Induced Response. MBio. 2016;7(4). Epub 2016/07/05. doi: 10.1128/mBio.00903-16. PubMed PMID: 27381292; PubMed Central PMCID: PMCPMC4958256.
219. Whitman L, Zhou H, Perlman S, Lane TE. IFN-gamma-mediated suppression of coronavirus replication in glial-committed progenitor cells. Virology. 2009;384(1):209-15. Epub 2008/12/06. doi: 10.1016/j.virol.2008.10.036. PubMed PMID: 19059617; PubMed Central PMCID: PMCPMC2779567.

220. Aguilar-Valenzuela R, Netland J, Seo YJ, Bevan MJ, Grakoui A, Suthar MS. Dynamics of Tissue-Specific CD8. J Virol. 2018;92(10). Epub 2018/04/27. doi: 10.1128/JVI.00014-18. PubMed PMID: 29514902; PubMed Central PMCID: PMCPMC5923067.
221. Stubblefield Park SR, Widness M, Levine AD, Patterson CE. T cell-, interleukin-12-, and gamma interferon-driven viral clearance in measles virus-infected brain tissue. J Virol. 2011;85(7):3664-76. Epub 2011/01/26. doi: 10.1128/JVI.01496-10. PubMed PMID: 21270150; PubMed Central PMCID: PMCPMC3067849.
222. Zhang SY, Boisson-Dupuis S, Chapgier A, Yang K, Bustamante J, Puel A, et al. Inborn errors of interferon (IFN)-mediated immunity in humans: insights into the respective roles of IFN-alpha/beta, IFN-gamma, and IFN-lambda in host defense. Immunol Rev. 2008;226:29-40. doi: 10.1111/j.1600-065X.2008.00698.x. PubMed PMID: 19161414.
223. VALENTE G, OZMEN L, NOVELLI F, GEUNA M, PALESTRO G, FORNI G, et al. DISTRIBUTION OF INTERFERON-GAMMA RECEPTOR IN HUMAN TISSUES. European Journal of Immunology. 1992;22(9):2403-12. doi: 10.1002/eji.1830220933. PubMed PMID: WOS:A1992JN49000032.
224. Daniels B, Holman D, Cruz-Orengo L, Jujjavarapu H, Durrant D, Klein R. Viral Pathogen-Associated Molecular Patterns Regulate Blood-Brain Barrier Integrity via Competing Innate Cytokine Signals. Mbio. 2014;5(5). doi: 10.1128/mBio.01476-14. PubMed PMID: WOS:000345459000013.
225. Blanchette M, Daneman R. Formation and maintenance of the BBB. Mechanisms of Development. 2015;138:8-16. doi: 10.1016/j.mod.2015.07.007. PubMed PMID: WOS:000365324200003.
226. Gelb S, Stock AD, Anzi S, Putterman C, Ben-Zvi A. Mechanisms of neuropsychiatric lupus: The relative roles of the blood-cerebrospinal fluid barrier versus blood-brain barrier. J Autoimmun. 2018;91:34-44. Epub 2018/04/04. doi: 10.1016/j.jaut.2018.03.001. PubMed PMID: 29627289; PubMed Central PMCID: PMCPMC5994369.
227. Grebenciucova E, Berger JR. Progressive Multifocal Leukoencephalopathy. Neurol Clin. 2018;36(4):739-50. doi: 10.1016/j.ncl.2018.06.002. PubMed PMID: 30366552.
228. Rumble JM, Huber AK, Krishnamoorthy G, Srinivasan A, Giles DA, Zhang X, et al. Neutrophil-related factors as biomarkers in EAE and MS. J Exp Med. 2015;212(1):23-35. Epub 2015/01/05. doi: 10.1084/jem.20141015. PubMed PMID: 25559893; PubMed Central PMCID: PMCPMC4291533.
229. Lawrence T, Natoli G. Transcriptional regulation of macrophage polarization: enabling diversity with identity. Nat Rev Immunol. 2011;11(11):750-61. Epub 2011/10/25. doi: 10.1038/nri3088. PubMed PMID: 22025054.
230. Boisvert M, Shoukry NH. Type III Interferons in Hepatitis C Virus Infection. Front Immunol. 2016;7:628. Epub 2016/12/23. doi: 10.3389/fimmu.2016.00628. PubMed PMID: 28066437; PubMed Central PMCID: PMCPMC5179541.
231. Teige I, Liu Y, Issazadeh-Navikas S. IFN-beta inhibits T cell activation capacity of central nervous system APCs. J Immunol. 2006;177(6):3542-53. PubMed PMID: 16951313.
232. Ivashkiv L. IFN gamma: signalling, epigenetics and roles in immunity, metabolism, disease and cancer immunotherapy. Nature Reviews Immunology. 2018;18(9):545-58. doi: 10.1038/s41577-018-0029-z. PubMed PMID: WOS:000442900900009.
233. Schoenborn JR, Wilson CB. Regulation of interferon-gamma during innate and adaptive immune responses. Adv Immunol. 2007;96:41-101. doi: 10.1016/S0065-2776(07)96002-2. PubMed PMID: 17981204.
234. Deblandre GA, Leo O, Huez GA, Wathelet MG. CD69 is expressed on Daudi cells in response to interferon-alpha. Cytokine. 1992;4(1):36-43. PubMed PMID: 1617156.
235. Ziegler SF, Levin SD, Johnson L, Copeland NG, Gilbert DJ, Jenkins NA, et al. The mouse CD69 gene. Structure, expression, and mapping to the NK gene complex. J Immunol. 1994;152(3):1228-36. PubMed PMID: 8301128.

236. Skon CN, Lee JY, Anderson KG, Masopust D, Hogquist KA, Jameson SC. Transcriptional downregulation of S1pr1 is required for the establishment of resident memory CD8+ T cells. Nat Immunol. 2013;14(12):1285-93. Epub 2013/10/27. doi: 10.1038/ni.2745. PubMed PMID: 24162775; PubMed Central PMCID: PMCPMC3844557.
237. Shiow LR, Rosen DB, Brdicková N, Xu Y, An J, Lanier LL, et al. CD69 acts downstream of interferon-alpha/beta to inhibit S1P1 and lymphocyte egress from lymphoid organs. Nature. 2006;440(7083):540-4. Epub 2006/03/08. doi: 10.1038/nature04606. PubMed PMID: 16525420.
238. Joshi NS, Cui W, Chandele A, Lee HK, Urso DR, Hagman J, et al. Inflammation directs memory precursor and short-lived effector CD8(+) T cell fates via the graded expression of T-bet transcription factor. Immunity. 2007;27(2):281-95. doi: 10.1016/j.immuni.2007.07.010. PubMed PMID: 17723218; PubMed Central PMCID: PMCPMC2034442.
239. Kaech SM, Tan JT, Wherry EJ, Konieczny BT, Surh CD, Ahmed R. Selective expression of the interleukin 7 receptor identifies effector CD8 T cells that give rise to long-lived memory cells. Nat Immunol. 2003;4(12):1191-8. Epub 2003/11/16. doi: 10.1038/ni1009. PubMed PMID: 14625547.
240. Giroux M, Schmidt M, Descoteaux A. IFN-gamma-Induced MHC class II expression: Transactivation of class II transactivator promoter IV by IFN regulatory factor-1 is regulated by protein kinase C-alpha. Journal of Immunology. 2003;171(8):4187-94. doi: 10.4049/jimmunol.171.8.4187. PubMed PMID: WOS:000185866100035.
241. Sadzak I, Schiff M, Gattermeier I, Glinitzer R, Sauer I, Saalmüller A, et al. Recruitment of Stat1 to chromatin is required for interferon-induced serine phosphorylation of Stat1 transactivation domain. Proc Natl Acad Sci U S A. 2008;105(26):8944-9. Epub 2008/06/23. doi: 10.1073/pnas.0801794105. PubMed PMID: 18574148; PubMed Central PMCID: PMCPMC2435588.
242. Putz EM, Gotthardt D, Hoermann G, Csiszar A, Wirth S, Berger A, et al. CDK8-mediated STAT1-S727 phosphorylation restrains NK cell cytotoxicity and tumor surveillance. Cell Rep. 2013;4(3):437-44. Epub 2013/08/08. doi: 10.1016/j.celrep.2013.07.012. PubMed PMID: 23933255; PubMed Central PMCID: PMCPMC3748339.
243. Tenoever BR, Ng SL, Chua MA, McWhirter SM, García-Sastre A, Maniatis T. Multiple functions of the IKK-related kinase IKKepsilon in interferon-mediated antiviral immunity. Science. 2007;315(5816):1274-8. doi: 10.1126/science.1136567. PubMed PMID: 17332413.
244. Di Liberto G, Pantelyushin S, Kreutzfeldt M, Page N, Musardo S, Coras R, et al. Neurons under T Cell Attack Coordinate Phagocyte-Mediated Synaptic Stripping. Cell. 2018;175(2):458-71.e19. Epub 2018/08/30. doi: 10.1016/j.cell.2018.07.049. PubMed PMID: 30173917.
245. Ashouri J, Weiss A. Endogenous Nur77 Is a Specific Indicator of Antigen Receptor Signaling in Human T and B Cells. Arthritis & Rheumatology. 2016;68. PubMed PMID: WOS:000417143405055.
246. Monteiro S, Ferreira F, Pinto V, Roque S, Morais M, de Sa-Calcada D, et al. Absence of IFN gamma promotes hippocampal plasticity and enhances cognitive performance. Translational Psychiatry. 2016;6. doi: 10.1038/tp.2015.194. PubMed PMID: WOS:000368549500007.
247. McNab F, Mayer-Barber K, Sher A, Wack A, O'Garra A. Type I interferons in infectious disease. Nat Rev Immunol. 2015;15(2):87-103. doi: 10.1038/nri3787. PubMed PMID: 25614319.
248. McMaster SR, Gabbard JD, Koutsonanos DG, Compans RW, Tripp RA, Tompkins SM, et al. Memory T cells generated by prior exposure to influenza cross react with the novel H7N9 influenza virus and confer protective heterosubtypic immunity. PLoS One. 2015;10(2):e0115725. Epub 2015/02/11. doi: 10.1371/journal.pone.0115725. PubMed PMID: 25671696; PubMed Central PMCID: PMCPMC4324938.
249. Hu Z, Molloy MJ, Usherwood EJ. CD4(+) T-cell dependence of primary CD8(+) T-cell response against vaccinia virus depends upon route of infection and viral dose. Cell Mol Immunol. 2016;13(1):82-93. Epub 2014/12/29. doi: 10.1038/cmi.2014.128. PubMed PMID: 25544501; PubMed Central PMCID: PMCPMC4711678.

250. Schindler C, Plumlee C. Inteferons pen the JAK-STAT pathway. Semin Cell Dev Biol. 2008;19(4):311-8. Epub 2008/08/26. doi: 10.1016/j.semcdb.2008.08.010. PubMed PMID: 18765289; PubMed Central PMCID: PMCPMC2741134.
251. Ruff-Jamison S, Chen K, Cohen S. Induction by EGF and interferon-gamma of tyrosine phosphorylated DNA binding proteins in mouse liver nuclei. Science. 1993;261(5129):1733-6. PubMed PMID: 8378774.
252. Weis N, Weigert A, von Knethen A, Brüne B. Heme oxygenase-1 contributes to an alternative macrophage activation profile induced by apoptotic cell supernatants. Mol Biol Cell. 2009;20(5):1280-8. Epub 2009/01/07. doi: 10.1091/mbc.e08-10-1005. PubMed PMID: 19129475; PubMed Central PMCID: PMCPMC2649271.
253. Meyer DJ, Campbell GS, Cochran BH, Argetsinger LS, Larner AC, Finbloom DS, et al. Growth hormone induces a DNA binding factor related to the interferon-stimulated 91-kDa transcription factor. J Biol Chem. 1994;269(7):4701-4. PubMed PMID: 7508925.
254. Nagata Y, Todokoro K. Interleukin 3 activates not only JAK2 and STAT5, but also Tyk2, STAT1, and STAT3. Biochem Biophys Res Commun. 1996;221(3):785-9. doi: 10.1006/bbrc.1996.0674. PubMed PMID: 8630039.
255. Brizzi MF, Aronica MG, Rosso A, Bagnara GP, Yarden Y, Pegoraro L. Granulocyte-macrophage colony-stimulating factor stimulates JAK2 signaling pathway and rapidly activates p93fes, STAT1 p91, and STAT3 p92 in polymorphonuclear leukocytes. J Biol Chem. 1996;271(7):3562-7. PubMed PMID: 8631962.
256. Zeng YX, Takahashi H, Shibata M, Hirokawa K. JAK3 Janus kinase is involved in interleukin 7 signal pathway. FEBS Lett. 1994;353(3):289-93. PubMed PMID: 7957877.
257. Frank DA, Robertson MJ, Bonni A, Ritz J, Greenberg ME. Interleukin 2 signaling involves the phosphorylation of Stat proteins. Proc Natl Acad Sci U S A. 1995;92(17):7779-83. PubMed PMID: 7544001; PubMed Central PMCID: PMCPMC41229.
258. Larner AC, David M, Feldman GM, Igarashi K, Hackett RH, Webb DS, et al. Tyrosine phosphorylation of DNA binding proteins by multiple cytokines. Science. 1993;261(5129):1730-3. PubMed PMID: 8378773.
259. Li X, Kumar A, Zhang F, Lee C, Tang Z. Complicated life, complicated VEGF-B. Trends Mol Med. 2012;18(2):119-27. Epub 2011/12/15. doi: 10.1016/j.molmed.2011.11.006. PubMed PMID: 22178229.
260. Vinukonda G, Hu F, Mehdizadeh R, Dohare P, Kidwai A, Juneja A, et al. Epidermal growth factor preserves myelin and promotes astrogliosis after intraventricular hemorrhage. Glia. 2016;64(11):1987-2004. Epub 2016/07/29. doi: 10.1002/glia.23037. PubMed PMID: 27472419; PubMed Central PMCID: PMCPMC5026581.
261. Yang J, Cheng X, Qi J, Xie B, Zhao X, Zheng K, et al. EGF Enhances Oligodendrogenesis from Glial Progenitor Cells. Front Mol Neurosci. 2017;10:106. Epub 2017/04/11. doi: 10.3389/fnmol.2017.00106. PubMed PMID: 28442994; PubMed Central PMCID: PMCPMC5387051.
262. Aguirre A, Dupree JL, Mangin JM, Gallo V. A functional role for EGFR signaling in myelination and remyelination. Nat Neurosci. 2007;10(8):990-1002. Epub 2007/07/08. doi: 10.1038/nn1938. PubMed PMID: 17618276.
263. Greenberg DA, Jin K. Vascular endothelial growth factors (VEGFs) and stroke. Cell Mol Life Sci. 2013;70(10):1753-61. Epub 2013/03/12. doi: 10.1007/s00018-013-1282-8. PubMed PMID: 23475070; PubMed Central PMCID: PMCPMC3634892.
264. Craigie M, Cicalese S, Sariyer I. Neuroimmune Regulation of JC Virus by Intracellular and Extracellular Agnoprotein. Journal of Neuroimmune Pharmacology. 2018;13(2):126-42. doi: 10.1007/s11481-017-9770-5. PubMed PMID: WOS:000431210500002.
265. Ramesh G, MacLean AG, Philipp MT. Cytokines and chemokines at the crossroads of neuroinflammation, neurodegeneration, and neuropathic pain. Mediators Inflamm. 2013;2013:480739.

Epub 2013/08/12. doi: 10.1155/2013/480739. PubMed PMID: 23997430; PubMed Central PMCID: PMCPMC3753746.
266. Wolf S, Boddeke H, Kettenmann H, Julius D. Microglia in Physiology and Disease. Annual Review of Physiology, Vol 79. 2017;79:619-43. doi: 10.1146/annurev-physiol-022516-034406. PubMed PMID: WOS:000396049000027.
267. Jiménez AJ, Domínguez-Pinos MD, Guerra MM, Fernández-Llebrez P, Pérez-Fígares JM. Structure and function of the ependymal barrier and diseases associated with ependyma disruption. Tissue Barriers. 2014;2:e28426. Epub 2014/03/19. doi: 10.4161/tisb.28426. PubMed PMID: 25045600; PubMed Central PMCID: PMCPMC4091052.
268. Del Bigio MR. Ependymal cells: biology and pathology. Acta Neuropathol. 2010;119(1):55-73. Epub 2009/12/19. doi: 10.1007/s00401-009-0624-y. PubMed PMID: 20024659.
269. Xing YL, Röth PT, Stratton JA, Chuang BH, Danne J, Ellis SL, et al. Adult neural precursor cells from the subventricular zone contribute significantly to oligodendrocyte regeneration and remyelination. J Neurosci. 2014;34(42):14128-46. doi: 10.1523/JNEUROSCI.3491-13.2014. PubMed PMID: 25319708.
270. Kernbauer E, Maier V, Stoiber D, Strobl B, Schneckenleithner C, Sexl V, et al. Conditional Stat1 ablation reveals the importance of interferon signaling for immunity to Listeria monocytogenes infection. PLoS Pathog. 2012;8(6):e1002763. Epub 2012/06/14. doi: 10.1371/journal.ppat.1002763. PubMed PMID: 22719255; PubMed Central PMCID: PMCPMC3375314.
271. Leopold Wager CM, Hole CR, Wozniak KL, Olszewski MA, Mueller M, Wormley FL. STAT1 signaling within macrophages is required for antifungal activity against Cryptococcus neoformans. Infect Immun. 2015;83(12):4513-27. Epub 2015/09/08. doi: 10.1128/IAI.00935-15. PubMed PMID: 26351277; PubMed Central PMCID: PMCPMC4645398.
272. Leopold Wager CM, Hole CR, Wozniak KL, Olszewski MA, Wormley FL. STAT1 signaling is essential for protection against Cryptococcus neoformans infection in mice. J Immunol. 2014;193(8):4060-71. Epub 2014/09/08. doi: 10.4049/jimmunol.1400318. PubMed PMID: 25200956; PubMed Central PMCID: PMCPMC4185263.
273. Hofer MJ, Li W, Manders P, Terry R, Lim SL, King NJ, et al. Mice deficient in STAT1 but not STAT2 or IRF9 develop a lethal CD4+ T-cell-mediated disease following infection with lymphocytic choriomeningitis virus. J Virol. 2012;86(12):6932-46. Epub 2012/04/11. doi: 10.1128/JVI.07147-11. PubMed PMID: 22496215; PubMed Central PMCID: PMCPMC3393544.
274. Choi KS, Scorpio DG, Dumler JS. Stat1 negatively regulates immune-mediated injury with Anaplasma phagocytophilum infection. J Immunol. 2014;193(10):5088-98. Epub 2014/10/10. doi: 10.4049/jimmunol.1401381. PubMed PMID: 25305312; PubMed Central PMCID: PMCPMC4225178.
275. Quigley M, Huang X, Yang Y. STAT1 signaling in CD8 T cells is required for their clonal expansion and memory formation following viral infection in vivo. J Immunol. 2008;180(4):2158-64. PubMed PMID: 18250422.
276. Novy P, Huang X, Leonard W, Yang Y. Intrinsic IL-21 Signaling Is Critical for CD8 T Cell Survival and Memory Formation in Response to Vaccinia Viral Infection. Journal of Immunology. 2011;186(5):2729-38. doi: 10.4049/jimmunol.1003009. PubMed PMID: WOS:000287356900008.
277. Strengell M, Matikainen S, Siren J, Lehtonen A, Foster D, Julkunen I, et al. IL-21 in synergy with IL-15 or IL-18 enhances IFN-gamma production in human NK and T cells. Journal of Immunology. 2003;170(11):5464-9. doi: 10.4049/jimmunol.170.11.5464. PubMed PMID: WOS:000183055000017.
278. Liu L, Belkadi A, Darnall L, Hu T, Drescher C, Cotleur AC, et al. CXCR2-positive neutrophils are essential for cuprizone-induced demyelination: relevance to multiple sclerosis. Nat Neurosci. 2010;13(3):319-26. Epub 2010/02/14. doi: 10.1038/nn.2491. PubMed PMID: 20154684; PubMed Central PMCID: PMCPMC2827651.

279. Aubé B, Lévesque SA, Paré A, Chamma É, Kébir H, Gorina R, et al. Neutrophils mediate blood-spinal cord barrier disruption in demyelinating neuroinflammatory diseases. J Immunol. 2014;193(5):2438-54. Epub 2014/07/21. doi: 10.4049/jimmunol.1400401. PubMed PMID: 25049355.
280. Howe CL, Lafrance-Corey RG, Sundsbak RS, Sauer BM, Lafrance SJ, Buenz EJ, et al. Hippocampal protection in mice with an attenuated inflammatory monocyte response to acute CNS picornavirus infection. Sci Rep. 2012;2:545. Epub 2012/07/30. doi: 10.1038/srep00545. PubMed PMID: 22848791; PubMed Central PMCID: PMCPMC3408132.
281. Wu GF, Dandekar AA, Pewe L, Perlman S. CD4 and CD8 T cells have redundant but not identical roles in virus-induced demyelination. J Immunol. 2000;165(4):2278-86. PubMed PMID: 10925317.
282. Grist JJ, Marro B, Lane TE. Neutrophils and viral-induced neurologic disease. Clin Immunol. 2018;189:52-6. Epub 2016/06/08. doi: 10.1016/j.clim.2016.05.009. PubMed PMID: 27288312; PubMed Central PMCID: PMCPMC5145788.
283. Sheehan D, Hrapchack B. The practice and theory of histotechnology. 2 ed. Columbus, OH: Batelle Press; 1980.
284. Swartz EM, Holmes GM. Gastric vagal motoneuron function is maintained following experimental spinal cord injury. Neurogastroenterol Motil. 2014;26(12):1717-29. Epub 2014/10/15. doi: 10.1111/nmo.12452. PubMed PMID: 25316513; PubMed Central PMCID: PMCPMC4245370.
285. Bayliss J, Karasoulos T, McLean CA. Frequency and large T (LT) sequence of JC polyomavirus DNA in oligodendrocytes, astrocytes and granular cells in non-PML brain. Brain Pathol. 2012;22(3):329-36. Epub 2011/10/27. doi: 10.1111/j.1750-3639.2011.00538.x. PubMed PMID: 21951346.
286. Koralnik IJ. Progressive multifocal leukoencephalopathy revisited: Has the disease outgrown its name? Ann Neurol. 2006;60(2):162-73. doi: 10.1002/ana.20933. PubMed PMID: 16862584.
287. García-Suárez J, de Miguel D, Krsnik I, Bañas H, Arribas I, Burgaleta C. Changes in the natural history of progressive multifocal leukoencephalopathy in HIV-negative lymphoproliferative disorders: impact of novel therapies. Am J Hematol. 2005;80(4):271-81. doi: 10.1002/ajh.20492. PubMed PMID: 16315252.
288. Jackson A. JC Virus Infection: An Expanding Spectrum of Neurological Disorders. Canadian Journal of Neurological Sciences. 2018;45(4):365-6. doi: 10.1017/cjn.2018.32. PubMed PMID: WOS:000440313600001.
289. O'Hara B, Gee G, Atwood W, Haley S. Susceptibility of Primary Human Choroid Plexus Epithelial Cells and Meningeal Cells to Infection by JC Virus. Journal of Virology. 2018;92(8). doi: 10.1128/JVI.00105-18. PubMed PMID: WOS:000428538800003.
290. Schwab N, Schneider-Hohendorf T, Melzer N, Cutter G, Wiendl H. Natalizumab-associated PML: Challenges with incidence, resulting risk, and risk stratification. Neurology. 2017;88(12):1197-205. Epub 2017/02/22. doi: 10.1212/WNL.0000000000003739. PubMed PMID: 28228564.
291. Wattjes MP, Wijburg MT, van Eijk J, Frequin S, Uitdehaag BMJ, Barkhof F, et al. Inflammatory natalizumab-associated PML: baseline characteristics, lesion evolution and relation with PML-IRIS. J Neurol Neurosurg Psychiatry. 2018;89(5):535-41. Epub 2017/11/15. doi: 10.1136/jnnp-2017-316886. PubMed PMID: 29142146.
292. Himedan M, Camelo-Piragua S, Mills EA, Gupta A, Aburashed R, Mao-Draayer Y. Pathologic Findings of Chronic PML-IRIS in a Patient with Prolonged PML Survival Following Natalizumab Treatment. J Investig Med High Impact Case Rep. 2017;5(3):2324709617734248. Epub 2017/09/27. doi: 10.1177/2324709617734248. PubMed PMID: 28989935; PubMed Central PMCID: PMCPMC5624358.
293. Igra MS, Paling D, Wattjes MP, Connolly DJA, Hoggard N. Multiple sclerosis update: use of MRI for early diagnosis, disease monitoring and assessment of treatment related complications. Br J Radiol. 2017;90(1074):20160721. Epub 2017/04/26. doi: 10.1259/bjr.20160721. PubMed PMID: 28362522; PubMed Central PMCID: PMCPMC5602172.

294. Mori S, Zhang J. Principles of diffusion tensor imaging and its applications to basic neuroscience research. Neuron. 2006;51(5):527-39. doi: 10.1016/j.neuron.2006.08.012. PubMed PMID: 16950152.
295. Zeisel A, Muñoz-Manchado AB, Codeluppi S, Lönnerberg P, La Manno G, Juréus A, et al. Brain structure. Cell types in the mouse cortex and hippocampus revealed by single-cell RNA-seq. Science. 2015;347(6226):1138-42. Epub 2015/02/19. doi: 10.1126/science.aaa1934. PubMed PMID: 25700174.
296. Dulken BW, Leeman DS, Boutet SC, Hebestreit K, Brunet A. Single-Cell Transcriptomic Analysis Defines Heterogeneity and Transcriptional Dynamics in the Adult Neural Stem Cell Lineage. Cell Rep. 2017;18(3):777-90. doi: 10.1016/j.celrep.2016.12.060. PubMed PMID: 28099854; PubMed Central PMCID: PMCPMC5269583.
297. Gokce O, Stanley GM, Treutlein B, Neff NF, Camp JG, Malenka RC, et al. Cellular Taxonomy of the Mouse Striatum as Revealed by Single-Cell RNA-Seq. Cell Rep. 2016;16(4):1126-37. Epub 2016/07/14. doi: 10.1016/j.celrep.2016.06.059. PubMed PMID: 27425622; PubMed Central PMCID: PMCPMC5004635.
298. Cho H, Proll S, Szretter K, Katze M, Gale M, Diamond M. Differential innate immune response programs in neuronal subtypes determine susceptibility to infection in the brain by positive-stranded RNA viruses. Nature Medicine. 2013;19(4):458-+. doi: 10.1038/nm.3108. PubMed PMID: WOS:000317109100031.
299. Zhang Y, Barres B. Astrocyte heterogeneity: an underappreciated topic in neurobiology. Current Opinion in Neurobiology. 2010;20(5):588-94. doi: 10.1016/j.conb.2010.06.005. PubMed PMID: WOS:000283481100010.
300. Klein R, Lin E, Zhang B, Luster A, Tollett J, Samuel M, et al. Neuronal CXCL10 directs CD8(+) T-cell recruitment and control of West Nile virus encephalitis. Journal of Virology. 2005;79(17):11457-66. doi: 10.1128/JVI.79.17.11457-11466.2005. PubMed PMID: WOS:000231303900060.
301. Paez PM, Spreuer V, Handley V, Feng JM, Campagnoni C, Campagnoni AT. Increased expression of golli myelin basic proteins enhances calcium influx into oligodendroglial cells. J Neurosci. 2007;27(46):12690-9. doi: 10.1523/JNEUROSCI.2381-07.2007. PubMed PMID: 18003849.
302. Tian Y, Zajac AJ. IL-21 and T Cell Differentiation: Consider the Context. Trends Immunol. 2016;37(8):557-68. Epub 2016/07/04. doi: 10.1016/j.it.2016.06.001. PubMed PMID: 27389961; PubMed Central PMCID: PMCPMC4969098.
303. Barker BR, Gladstone MN, Gillard GO, Panas MW, Letvin NL. Critical role for IL-21 in both primary and memory anti-viral CD8+ T-cell responses. Eur J Immunol. 2010;40(11):3085-96. Epub 2010/10/27. doi: 10.1002/eji.200939939. PubMed PMID: 21061439; PubMed Central PMCID: PMCPMC3119210.
304. Cui W, Liu Y, Weinstein JS, Craft J, Kaech SM. An interleukin-21-interleukin-10-STAT3 pathway is critical for functional maturation of memory CD8+ T cells. Immunity. 2011;35(5):792-805. doi: 10.1016/j.immuni.2011.09.017. PubMed PMID: 22118527; PubMed Central PMCID: PMCPMC3431922.
305. Phares TW, DiSano KD, Hinton DR, Hwang M, Zajac AJ, Stohlman SA, et al. IL-21 optimizes T cell and humoral responses in the central nervous system during viral encephalitis. J Neuroimmunol. 2013;263(1-2):43-54. Epub 2013/08/06. doi: 10.1016/j.jneuroim.2013.07.019. PubMed PMID: 23992866; PubMed Central PMCID: PMCPMC3796038.
306. Phares TW, Stohlman SA, Hwang M, Min B, Hinton DR, Bergmann CC. CD4 T cells promote CD8 T cell immunity at the priming and effector site during viral encephalitis. J Virol. 2012;86(5):2416-27. Epub 2011/12/28. doi: 10.1128/JVI.06797-11. PubMed PMID: 22205741; PubMed Central PMCID: PMCPMC3302259.
307. Fröhlich A, Marsland BJ, Sonderegger I, Kurrer M, Hodge MR, Harris NL, et al. IL-21 receptor signaling is integral to the development of Th2 effector responses in vivo. Blood. 2007;109(5):2023-31. Epub 2006/10/31. doi: 10.1182/blood-2006-05-021600. PubMed PMID: 17077330.

308. Mackay LK, Wynne-Jones E, Freestone D, Pellicci DG, Mielke LA, Newman DM, et al. T-box Transcription Factors Combine with the Cytokines TGF-β and IL-15 to Control Tissue-Resident Memory T Cell Fate. Immunity. 2015;43(6):1101-11. doi: 10.1016/j.immuni.2015.11.008. PubMed PMID: 26682984.
309. Laidlaw BJ, Zhang N, Marshall HD, Staron MM, Guan T, Hu Y, et al. CD4+ T cell help guides formation of CD103+ lung-resident memory CD8+ T cells during influenza viral infection. Immunity. 2014;41(4):633-45. Epub 2014/10/09. doi: 10.1016/j.immuni.2014.09.007. PubMed PMID: 25308332; PubMed Central PMCID: PMCPMC4324721.
310. Zhang N, Bevan MJ. Transforming growth factor-β signaling controls the formation and maintenance of gut-resident memory T cells by regulating migration and retention. Immunity. 2013;39(4):687-96. Epub 2013/09/26. doi: 10.1016/j.immuni.2013.08.019. PubMed PMID: 24076049; PubMed Central PMCID: PMCPMC3805703.
311. Bergsbaken T, Bevan MJ. Proinflammatory microenvironments within the intestine regulate the differentiation of tissue-resident CD8$^+$ T cells responding to infection. Nat Immunol. 2015;16(4):406-14. Epub 2015/02/23. doi: 10.1038/ni.3108. PubMed PMID: 25706747; PubMed Central PMCID: PMCPMC4368475.
312. Issuree PD, Ng CP, Littman DR. Heritable Gene Regulation in the CD4:CD8 T Cell Lineage Choice. Front Immunol. 2017;8:291. Epub 2017/03/22. doi: 10.3389/fimmu.2017.00291. PubMed PMID: 28382035; PubMed Central PMCID: PMCPMC5360760.
313. Cruz-Guilloty F, Pipkin ME, Djuretic IM, Levanon D, Lotem J, Lichtenheld MG, et al. Runx3 and T-box proteins cooperate to establish the transcriptional program of effector CTLs. J Exp Med. 2009;206(1):51-9. Epub 2009/01/12. doi: 10.1084/jem.20081242. PubMed PMID: 19139168; PubMed Central PMCID: PMCPMC2626671.
314. Shan Q, Zeng Z, Xing S, Li F, Hartwig SM, Gullicksrud JA, et al. The transcription factor Runx3 guards cytotoxic CD8. Nat Immunol. 2017;18(8):931-9. Epub 2017/06/12. doi: 10.1038/ni.3773. PubMed PMID: 28604718; PubMed Central PMCID: PMCPMC5564218.
315. Taniuchi I. CD4 Helper and CD8 Cytotoxic T Cell Differentiation. Annu Rev Immunol. 2018;36:579-601. doi: 10.1146/annurev-immunol-042617-053411. PubMed PMID: 29677476.
316. Park JH, Adoro S, Guinter T, Erman B, Alag AS, Catalfamo M, et al. Signaling by intrathymic cytokines, not T cell antigen receptors, specifies CD8 lineage choice and promotes the differentiation of cytotoxic-lineage T cells. Nat Immunol. 2010;11(3):257-64. Epub 2010/01/31. doi: 10.1038/ni.1840. PubMed PMID: 20118929; PubMed Central PMCID: PMCPMC3555225.
317. Ghosh S, Sarkar M, Ghosh T, Guha I, Bhuniya A, Biswas J, et al. Absence of CD4(+) T cell help generates corrupt CD8(+) effector T cells in sarcoma-bearing Swiss mice treated with NLGP vaccine. Immunol Lett. 2016;175:31-9. Epub 2016/05/10. doi: 10.1016/j.imlet.2016.05.004. PubMed PMID: 27178306.
318. Lin JX, Leonard WJ. The Common Cytokine Receptor γ Chain Family of Cytokines. Cold Spring Harb Perspect Biol. 2018;10(9). Epub 2018/09/04. doi: 10.1101/cshperspect.a028449. PubMed PMID: 29038115.
319. Adachi T, Kobayashi T, Sugihara E, Yamada T, Ikuta K, Pittaluga S, et al. Hair follicle-derived IL-7 and IL-15 mediate skin-resident memory T cell homeostasis and lymphoma. Nature Medicine. 2015;21(11):1272-9. doi: 10.1038/nm.3962. PubMed PMID: WOS:000364621200011.
320. Goitre L, Trapani E, Trabalzini L, Retta SF. The Ras superfamily of small GTPases: the unlocked secrets. Methods Mol Biol. 2014;1120:1-18. doi: 10.1007/978-1-62703-791-4_1. PubMed PMID: 24470015.
321. Saoudi A, Kassem S, Dejean A, Gaud G. Rho-GTPases as key regulators of T lymphocyte biology. Small GTPases. 2014;5. Epub 2014/05/08. doi: 10.4161/sgtp.28208. PubMed PMID: 24825161; PubMed Central PMCID: PMCPMC4160340.

322. Guo F, Cancelas JA, Hildeman D, Williams DA, Zheng Y. Rac GTPase isoforms Rac1 and Rac2 play a redundant and crucial role in T-cell development. Blood. 2008;112(5):1767-75. Epub 2008/06/25. doi: 10.1182/blood-2008-01-132068. PubMed PMID: 18579797; PubMed Central PMCID: PMCPMC2518885.
323. Smits K, Iannucci V, Stove V, Van Hauwe P, Naessens E, Meuwissen PJ, et al. Rho GTPase Cdc42 is essential for human T-cell development. Haematologica. 2010;95(3):367-75. doi: 10.3324/haematol.2009.006890. PubMed PMID: 20207844; PubMed Central PMCID: PMCPMC2833065.
324. Rozo C, Chinenov Y, Maharaj RK, Gupta S, Leuenberger L, Kirou KA, et al. Targeting the RhoA-ROCK pathway to reverse T-cell dysfunction in SLE. Ann Rheum Dis. 2017;76(4):740-7. Epub 2016/11/09. doi: 10.1136/annrheumdis-2016-209850. PubMed PMID: 28283529; PubMed Central PMCID: PMCPMC5839171.
325. Zang S, Li J, Yang H, Zeng H, Han W, Zhang J, et al. Mutations in 5-methylcytosine oxidase TET2 and RhoA cooperatively disrupt T cell homeostasis. J Clin Invest. 2017;127(8):2998-3012. Epub 2017/07/10. doi: 10.1172/JCI92026. PubMed PMID: 28691928; PubMed Central PMCID: PMCPMC5531410.
326. Hidano S, Randall LM, Dawson L, Dietrich HK, Konradt C, Klover PJ, et al. STAT1 Signaling in Astrocytes Is Essential for Control of Infection in the Central Nervous System. MBio. 2016;7(6). Epub 2016/11/08. doi: 10.1128/mBio.01881-16. PubMed PMID: 27834206; PubMed Central PMCID: PMCPMC5101356.
327. Lin W, Lin Y. Interferon-γ inhibits central nervous system myelination through both STAT1-dependent and STAT1-independent pathways. J Neurosci Res. 2010;88(12):2569-77. doi: 10.1002/jnr.22425. PubMed PMID: 20648647; PubMed Central PMCID: PMCPMC2911948.
328. Wang Y, Ren Z, Tao D, Tilwalli S, Goswami R, Balabanov R. STAT1/IRF-1 signaling pathway mediates the injurious effect of interferon-gamma on oligodendrocyte progenitor cells. Glia. 2010;58(2):195-208. doi: 10.1002/glia.20912. PubMed PMID: 19606498.
329. Lecca D, Ceruti S, Fumagalli M, Abbracchio MP. Purinergic trophic signalling in glial cells: functional effects and modulation of cell proliferation, differentiation, and death. Purinergic Signal. 2012;8(3):539-57. Epub 2012/04/12. doi: 10.1007/s11302-012-9310-y. PubMed PMID: 22528683; PubMed Central PMCID: PMCPMC3360088.
330. Galani I, Triantafyllia V, Eleminiadou E, Koltsida O, Stavropoulos A, Manioudaki M, et al. Interferon-lambda Mediates Non-redundant Front-Line Antiviral Protection against Influenza Virus Infection without Compromising Host Fitness. Immunity. 2017;46(5):875-+. doi: 10.1016/j.immuni.2017.04.025. PubMed PMID: WOS:000401316300021.
331. Kotenko S, Durbin J. Contribution of type III interferons to antiviral immunity: location, location, location. Journal of Biological Chemistry. 2017;292(18):7295-303. doi: 10.1074/jbc.R117.777102. PubMed PMID: WOS:000400761300002.
332. Broggi A, Tan Y, Granucci F, Zanoni I. IFN-lambda suppresses intestinal inflammation by non-translational regulation of neutrophil function. Nature Immunology. 2017;18(10):1084-+. doi: 10.1038/ni.3821. PubMed PMID: WOS:000411134000013.
333. Chapagain ML, Verma S, Mercier F, Yanagihara R, Nerurkar VR. Polyomavirus JC infects human brain microvascular endothelial cells independent of serotonin receptor 2A. Virology. 2007;364(1):55-63. Epub 2007/03/30. doi: 10.1016/j.virol.2007.02.018. PubMed PMID: 17399760; PubMed Central PMCID: PMCPMC2034208.
334. Norris GT, Kipnis J. Immune cells and CNS physiology: Microglia and beyond. J Exp Med. 2019;216(1):60-70. Epub 2018/11/30. doi: 10.1084/jem.20180199. PubMed PMID: 30504438; PubMed Central PMCID: PMCPMC6314530.
335. Kipnis J, Cohen H, Cardon M, Ziv Y, Schwartz M. T cell deficiency leads to cognitive dysfunction: implications for therapeutic vaccination for schizophrenia and other psychiatric conditions. Proc Natl

Acad Sci U S A. 2004;101(21):8180-5. Epub 2004/05/12. doi: 10.1073/pnas.0402268101. PubMed PMID: 15141078; PubMed Central PMCID: PMCPMC419577.
336. Derecki NC, Cardani AN, Yang CH, Quinnies KM, Crihfield A, Lynch KR, et al. Regulation of learning and memory by meningeal immunity: a key role for IL-4. J Exp Med. 2010;207(5):1067-80. Epub 2010/05/03. doi: 10.1084/jem.20091419. PubMed PMID: 20439540; PubMed Central PMCID: PMCPMC2867291.
337. Tanabe S, Yamashita T. B-1a lymphocytes promote oligodendrogenesis during brain development. Nat Neurosci. 2018;21(4):506-16. Epub 2018/03/05. doi: 10.1038/s41593-018-0106-4. PubMed PMID: 29507409.
338. Brombacher TM, Nono JK, De Gouveia KS, Makena N, Darby M, Womersley J, et al. IL-13-Mediated Regulation of Learning and Memory. J Immunol. 2017;198(7):2681-8. Epub 2017/02/15. doi: 10.4049/jimmunol.1601546. PubMed PMID: 28202615.
339. Choi GB, Yim YS, Wong H, Kim S, Kim H, Kim SV, et al. The maternal interleukin-17a pathway in mice promotes autism-like phenotypes in offspring. Science. 2016;351(6276):933-9. Epub 2016/01/28. doi: 10.1126/science.aad0314. PubMed PMID: 26822608; PubMed Central PMCID: PMCPMC4782964.
340. Miller AH, Haroon E, Raison CL, Felger JC. Cytokine targets in the brain: impact on neurotransmitters and neurocircuits. Depress Anxiety. 2013;30(4):297-306. Epub 2013/03/06. doi: 10.1002/da.22084. PubMed PMID: 23468190; PubMed Central PMCID: PMCPMC4141874.
341. Osipova ED, Semyachkina-Glushkovskaya OV, Morgun AV, Pisareva NV, Malinovskaya NA, Boitsova EB, et al. Gliotransmitters and cytokines in the control of blood-brain barrier permeability. Rev Neurosci. 2018;29(5):567-91. doi: 10.1515/revneuro-2017-0092. PubMed PMID: 29306934.
342. Kägi D, Ledermann B, Bürki K, Zinkernagel RM, Hengartner H. Molecular mechanisms of lymphocyte-mediated cytotoxicity and their role in immunological protection and pathogenesis in vivo. Annu Rev Immunol. 1996;14:207-32. doi: 10.1146/annurev.immunol.14.1.207. PubMed PMID: 8717513.
343. Guidotti LG, Chisari FV. Noncytolytic control of viral infections by the innate and adaptive immune response. Annu Rev Immunol. 2001;19:65-91. doi: 10.1146/annurev.immunol.19.1.65. PubMed PMID: 11244031.
344. Griffin DE. Immune responses to RNA-virus infections of the CNS. Nat Rev Immunol. 2003;3(6):493-502. doi: 10.1038/nri1105. PubMed PMID: 12776209.
345. Russo MV, McGavern DB. Immune Surveillance of the CNS following Infection and Injury. Trends Immunol. 2015;36(10):637-50. doi: 10.1016/j.it.2015.08.002. PubMed PMID: 26431941; PubMed Central PMCID: PMCPMC4592776.
346. Cole GA, Nathanson N, Prendergast RA. Requirement for theta-bearing cells in lymphocytic choriomeningitis virus-induced central nervous system disease. Nature. 1972;238(5363):335-7. PubMed PMID: 4561841.
347. Kreutzfeldt M, Bergthaler A, Fernandez M, Brück W, Steinbach K, Vorm M, et al. Neuroprotective intervention by interferon-γ blockade prevents CD8+ T cell-mediated dendrite and synapse loss. J Exp Med. 2013;210(10):2087-103. Epub 2013/09/02. doi: 10.1084/jem.20122143. PubMed PMID: 23999498; PubMed Central PMCID: PMCPMC3782053.

VITA

Taryn Mockus

EDUCATION

2009-2013	University of Rochester Rochester, NY Scholarships: Bausch and Lomb Honorary Science Scholarship B.S. Neuroscience *cum laude* with minors in American Sign Language and Psychology
2013-present	Pennsylvania State University College of Medicine Hershey, PA PhD candidate in the Neuroscience graduate program Department of Microbiology and Immunology Mentor: Aron Lukacher MD, PhD

HONORS AND AWARDS

2013	*"Fund for Excellence in Graduate Recruitment Award"* at the Pennsylvania State University (State College, PA)
2015	*"Graduate Women in Science Award"* from the Kappa Rho Chapter of Graduate Women in Science at the College of Medicine (Hershey, PA)
2016	*"AAI Poster Trainee Award"* at the AAI Annual Meeting (Seattle, WA)
2016-2018	*"Judy S. Finkelstein Memorial Research Award"* from the Judy S. Finkelstein Memorial Research Fund at the College of Medicine
2018	"*Graduate Student Excellence in Mentoring Award"* at the Pennsylvania State University (State College, PA)
2018	"*FASEB Conference travel award"* from the FASEB SRC team (Bethesda, MD)

PEER REVIEWED PUBLICATIONS

1. Marker DF, Puccini JM, **Mockus TE**, Barbieri J, Lu S, Gelbard HA. (2012) LRRK2 kinase inhibition prevents pathological microglial phagocytosis in response to HIV-1 Tat protein. *Journal of neuroinflammation*. 9:261-261.
2. Shwetank, Abdelsamed HA, Frost EL, Schmitz HM, **Mockus TE**, Youngblood BA, Lukacher AE. (2017) Maintenance of PD1 on brain resident cells is antigen independent. *Immunology Cell Biology*.
3. **Mockus TE**, Shwetank, Lauver MD, Ren HM, Netherby CS, Salameh T, Kawasawa YI, Yue F, Broach JR, Lukacher AE. (2018) CD4 T cells control the development and maintenance of brain-resident CD8 T cells during polyomavirus infection. *PLOS Pathogens.*
4. Shwetank, Frost EL, **Mockus TE**, Ren HM, Lauver MD, Netherby CS, Toprak M, and Lukacher AE. (2019) PD-1 regulates tissue-resident memory CD8 T cells during polyomavirus encephalitis. *Submitted to Frontiers in Immunology*